PRINTING AND CHARACTERIZATION OF INKS FOR PAPER-BASED BIOSENSORS

PRINTING AND CHARACTERIZATION OF INKS FOR PAPER-BASED BIOSENSORS

By

JINGYUN WANG, B.Eng., M.A.Sc

A Thesis

Submitted to the School of Graduate Studies

in Partial Fulfillment of the Requirements

for the Degree

Doctor of Philosophy

McMaster University

DOCTOR OF PHILOSOPHY (2014)   McMaster University

(Chemical Engineering)   Hamilton, Ontario

TITLE: Printing and Characterization of Inks for Paper-
                based Biosensors

AUTHOR: Jingyun Wang
                B.Eng. (Donghua University)
                M.A.Sc (McMaster University)

SUPERVISORS: Professor Robert H. Pelton
                Professor John D. Brennan

NUMBER OF PAGES: vii, 79

Abstract

This thesis describes solutions to many of the challenges in the development of paper-based biosensors. Coupling techniques in analytical biochemistry with knowledge of paper science and technology, advances are described in the areas of: the influence of paper surface chemistry on bioactivity; optimizing bioactive ink formulation; the printing of paper supported microfluidic channels; and, the characterization of complex sensors based on printed sol-gel material layers.

The stability of paper-immobilized antibodies under various conditions was first studied using both untreated filter paper and PAE-treated paper. Antibody stability decreased with increasing temperature and relative humidity. Paper treated with PAE had no significant influence on antibody stability under the experimental conditions. The experimental result was also encapsulated in an empirical equation to predict the impact of printing and coating operations on antibody activity.

The influence of paper sizing agent (AKD) on the adsorption and inactivation of antibody was also investigated. The preliminary study showed that the small amount of AKD improved the antibody adsorption on paper and also did not interfere antibody activity. Therefore, packaging papers containing sizing agents can be used as a substrate for antibody immobilization.

Two strategies to fabricate hydrophobic barriers were developed, based on sol-gel derived MSQ material. The first method is based on ink-jet printing a highly basic solution onto MSQ-impregnated filter paper to re-exposing the cellulose and producing a hydrophilic patterned region. The second method is direct ink-jet printing of MSQ onto paper to outline the hydrophobic walls bordering the hydrophilic channels. The resistance of the barriers to surfactants and organic solvents was tested. The functionality of MSQ-based devices was further demonstrated by using a colorimetric assay for *E. coli* detection.

Multiple-stage inkjet printing of sol-gel based bioink onto porous filter paper for enzyme immobilization was characterized by various methods. Confocal microscope and SEM/TEM images confirmed the formation of sol-gel and enzyme composite material on the paper fibers without cracking. The protease assay proved that the entrapment of enzyme molecules improved with the increasing amount of the sol-gel derived material printed on paper. The top layer of sol-gel ink was found to play a major role in protection against enzyme proteolysis, while the bottom layer of sol-gel ink was found to be necessary to prevent the potential inhibition of enzyme by the cationic polymer.

Acknowledgements

First of all, I would like to express my most sincere gratitude to my supervisors, Dr. Robert H. Pelton and Dr. John D. Brennan, for their precious guidance, numerous suggestion and constant support throughout my research work. Their great motivation, vital encouragement, endless support, and insightful guidance inspired me all the time during the PhD journey. Having two well-known professors as my supervisors brought me more than the usual privilege in wisdom and knowledge from both scientific and engineering world. I truly appreciate the opportunities they provided me in attending several conferences and delivering their skills in paper writing and presentation to me.

I would like to thank my supervisory committee members, Dr. Carlos Filipe and Dr. Fred Capretta. They have provided me valuable suggestion and tremendous help on experimental designs and scientific writing. Their positive attitude and enthusiasm motivated me through the ups and downs of my research. Dr. Raja Ghosh and Dr. Chris Hall are also acknowledged for their advice on the antibody work. Dr. Glynis de Silveira, Ms. Marcia Reid and Ms. Marine Timeleck are thanked for SEM, TEM and confocal microscopy support.

I also would also like to acknowledge all the current and previous group members from both Dr. Pelton and Dr. Brennan' groups for their encouragement and support. I appreciate the valuable discussion and instrument training from Dr. Zuohe Wang, Zhen Hu, Sana Jahanshahi, Dr. Yuguo Cui, Dr. Quan Wen, Dr. Dan Zhang, Dr. Songtao Yang, Dr. Xinghua Sun, Dr. Yang Chen, Dr. Xiaojiao Shang, Dr. Danielle Covelli and Ms. Dawn White. I thank Dr. Hanjiang Dong, Dr. Maria Rowena N. Monton, Dr. Zakir Hossain, Dr. Clemence Sicard, Anne Marie Smith, Carmen Carrasquilla, Christy Hui, Meghan McFadden and Erica Forsberg for sharing their silica sol-gel and bioanalytical chemistry knowledge. Moreover, I am also thankful for several undergraduate students, Xi Zhang, Devon Bowie, Jacqueline Sim, Jaclyn Obermeyer, Hiba Bouji and Brian Yiu, for their hard work and contributions.

I would like to thank my lab manager Mr. Doug Keller, administrator Ms. Sally Watson, Ms. Kathy Goodram, Ms. Lynn Falkiner, Ms. Nanci Cole, Ms. Melissa Vasi, Ms. Cathie Roberts, Mr. Paul Gatt, Ms. Justyna Derkach and Mr. Dan Wright for their administrative assistant and technical support.

I acknowledge SENTINEL bioactive paper network and Chemical Engineering Department at McMaster University for research funding support.

Last but not least I am forever grateful to all my family members, specially my parents and my partner Kor Zheng Mah for their unconditional love, relentless support and constant encouragement.

TABLE OF CONTENTS

Abbreviation

AChE	acetylcholinesterase
AKD	alkyl ketene dimer
ATCh	acetylthiocholine iodide
CPRG	chlorophenol red-β-D-galactopyranoside
CTAB	hexadecyltrimethylammonium bromide
DMSO	dimethyl sulfoxide
DTNB	5,5′-dithiobis-(2-nitrobenzoic acid)
E.coli	Escherichia coli
EDS	energy dispersive spectroscopy
ELISA	enzyme-linked immunosorbent assay
FITC	fluorescein-5(6)-isothiocyanate
HRP	horseradish peroxidase
HSA	human serum albumin
IgG	immunoglobulin G
MSQ	methylsilsesquioxane
MTMS	methyltrimethoxysilane
PAE	polyamide-epichlorohydrin
R6G	rhodamine 6G
SDS	sodium dodecyl sulfate
SEM	scanning electron microscopy
SS	sodium silicate
TEM	transmission electron microscopy
β-GAL	β-galactosidase

Chapter 1 Introduction

In recent years, there has been a tremendous interest in the development of paper-based biosensors for point-of-care diagnostics and on-site environmental monitoring. The ultimate goal of biosensor development is low-cost, simple, sensitive, and reliable tools to detect diseases, toxins, and pathogens without sophisticated instrumentation.[1-3] Compared with other widely used material (e.g. plastic and porous nitrocellulose), paper offers more advantages. Paper is inexpensive, biodegradable, biomolecule friendly, and easy to modify its surface characteristics, through various printing and coating techniques.[2]

The initial development of paper-supported biosensor is based on the invention of paper chromatography by Martin and Syne[4] who both won 1952's Nobel Prize in Chemistry. In 1957, Free et al. [5] reported the urine glucose testing method using papers as the support. Then in the 1980s, paper dipsticks became commercially available for diabetes, pregnancy, and infectious disease tests.[6-7] In the past decade, several research networks and laboratories have been actively working in this area for the purpose of developing bioactive paper and expanding the concept to wider applications. Today, significant progress in this area has already been achieved. **Figure 1** shows a few examples of paper-based sensor applications in detecting the presence of glucose,[8] DNA enzyme[9], and pesticides[10], by simply observing the color change or development.

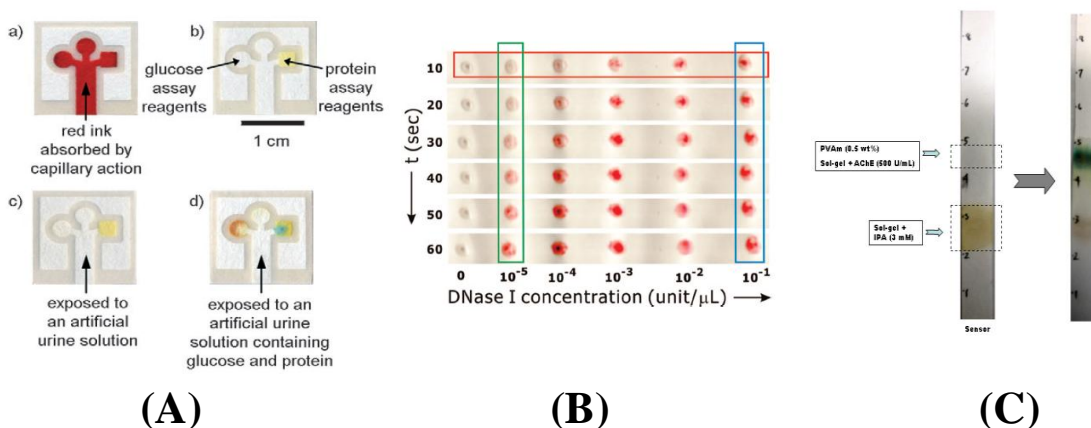**(A)**   **(B)**   **(C)**

Figure 1: Detection of glucose (A, adapted from Martinez et al. [8]), DNA enzyme (B, adapted from Zhao et al. [9]) and pesticide (C, adapted from Hossain et al.[10]) on papers.

This chapter will first present a literature review of this work, followed by the specific objectives and an outline of the thesis.

1.1   Literature Review

In order to engineer a functioning paper-based biosensor, three basic and critical components are required, a paper support surface, biorecognition agent, and reporters. The biorecognition agent should be immobilized on the paper surface while retaining its

functionality to react with the target and produce the signals. The following sections will subsequently discuss these three components.

1.1.1 Fundamental Properties of Paper

1.1.1.1 Paper Surface Chemistry

Since the start of the major invention, paper has been a part of the necessary materials in people's daily life, as a multi-purpose medium for wrapping, packaging, cleaning, writing, and printing. It is mainly composed of cellulose, which is mostly derived from wood fibers. Cellulose is a polysaccharide with repeating units of $C_6H_{10}O_5$ and has polymerization degree of 1000 to 50000. Besides cellulose, wood fibers also contain hemicelluloses and lignin. Hemicelluloses are heteropolymers, containing xylose, galactose, and arabinose with a degree of polymerization of about 150 ± 30.[11]

In the paper-making process, several different additives are added to the cellulose to impart or improve specific paper attributes. For instance, pure cellulosic paper has very weak strength when wet. This is because water molecules can break the hydrogen bonding between the fibers, resulting in the loss of 90% of its original strength. As such, it is useful to add some additives, commonly known as wet-strength resin, to help retain part of paper strength when wet. [12] Wet-strength resins are positively charged and chemically reactive, which facilitate resin absorption onto the negatively charged fibers and subsequent formation of network with the fibers. This network can enhance the contact of fibers and prevent fibers from falling apart, especially when the paper is wet.

Polyamide-epichlorohydrin (PAE) is one of the commercial wet-strength resins added in paper-making process. It is a water-soluble, cationic polymer, which is utilized in neutral conditions to strengthen tissue, paper towel, liquid packaging board, laminating, filter, and fine papers. [12] PAE is typically synthesized by the reaction between polyamideamine and epichlorohydrin to form polymer chains with four-membered 3-hydroxy-azetidinium groups (AZR) upon heating at 60 -70°C.[13] The reaction between PAE and cellulose is shown in **Figure 2**. The azetidinium group of PAE does not only react with carboxyl group of cellulose fibers, but also with amine group of the other PAE chains. As a result, both reactions contribute to the formation of crosslinking network, which reinforce stable wet strength in paper.[14]
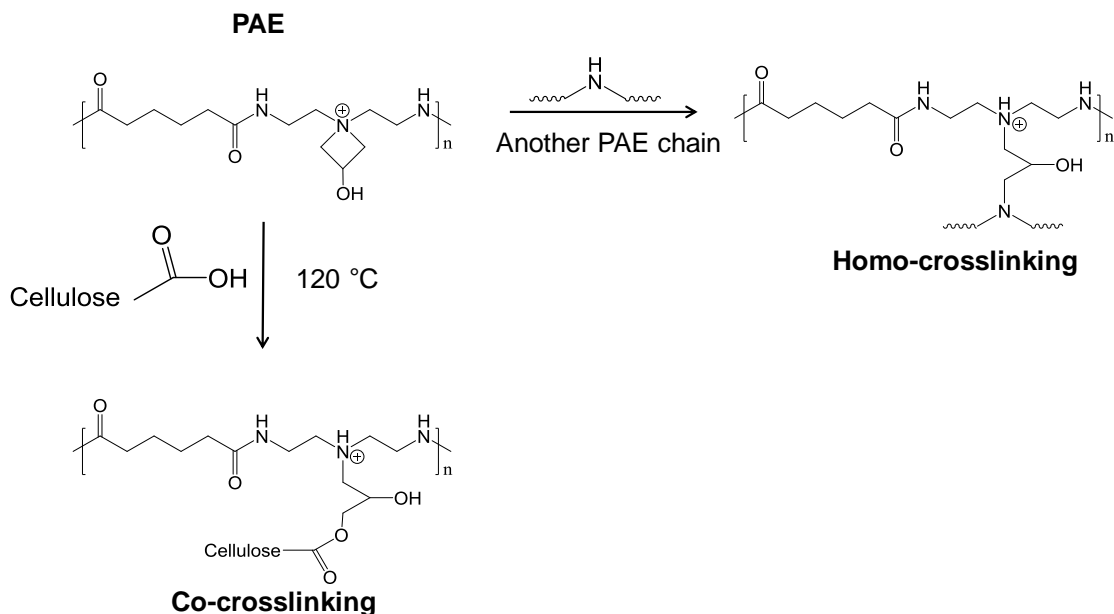
Figure 2: The reaction between the PAE and cellulose for paper wet-strength improvement (adapted from Wang. et al.[15])

Besides wet-strength resins, sizing agents are the other additives, commonly added in paper-making process to inhibit liquid penetration (e.g. water) on paper by making the paper surface relatively hydrophobic. In general, there are two types of sizing agent, based on reaction conditions, used in paper-making process: 1) Rosin sizing in acidic pH condition and 2) sizing in neutral or alkaline pH condition with alkyl succinic anhydride (ASA) or alkyl ketene dimer (AKD). Presently, most paper-making industries have steered towards the use of neutral sizing agents, instead of acidic ones. The main benefit of using neutral sizing agents is combining the addition of sizing agent and common fillers, such as calcium carbonate, into single step, without the need to change the pH condition in paper-making process. Furthermore, a neutral paper making environment helps prolong the life and operation of the papermachine, without being subjected to corrosion.[16] AKD and ASA are both synthetic sizing agents, which can form covalent linkages with cellulose fibers and increase the paper dry weight by additional 0.04-0.2%.[17] Compared with ASA, AKD is more commonly used because of its low reactivity and high stability characteristics. Additionally, AKD emulsions can be stored for long period of time without breakdown, while ASA emulsions need to be prepared right before use, due to rapid hydrolysis.[16] AKD sizing agent is generally prepared from dimerization of long chain fatty acid chlorides. The strained lactone ring of AKD can either react with the hydroxyl group of cellulose to form a β-keto ester, or be hydrolyzed by the water to form a ketone, which is unable to react with cellulose, as shown in **Figure 3**.[18]
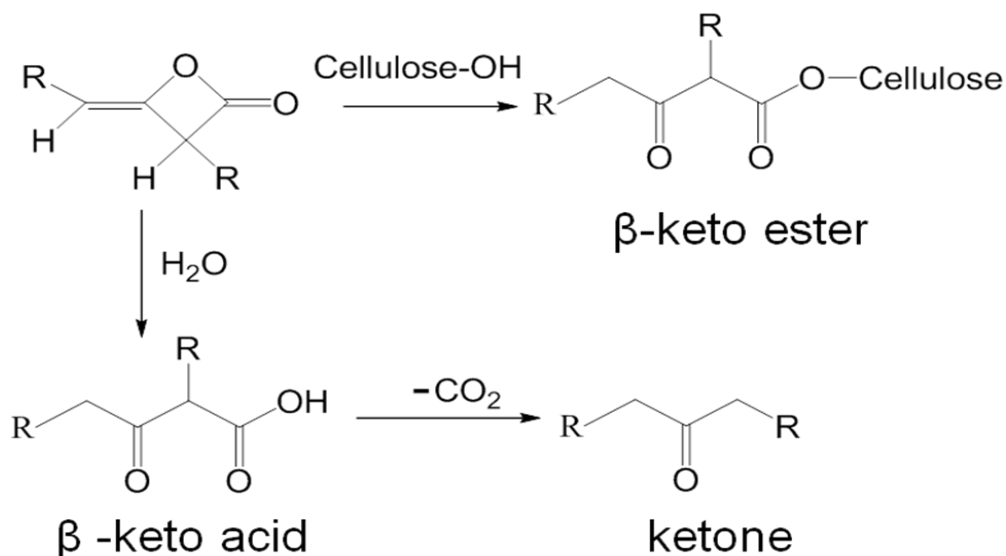
3

Figure 3: Reaction between AKD and cellulose fibers (adapted from Lindström. et al.[18]).

The surface chemistry of paper can be characterized by several spectroscopic methods, including Raman Spectroscopy, X-ray Photoelectron Spectroscopy, and Fourier Transform Infrared Spectroscopy (FT-IR Spectroscopy).

1.1.1.2 Paper Physical Properties

Paper is a three dimensional network of cellulose fibers, which are hollow tubes with approximately 1.5 mm length and 20 μm width. The thickness, basis weight, porosity, and specific surface area are some of the important physical properties of papers. These factors affect the printing, coating, and immobilization of reagents onto paper and ultimately the responsiveness of a paper-based biosensor.[2]

Filter paper has been widely used in developing paper-based biosensor or paper-based microfluidics due to its large porosity and specific surface area. For example, Whatman #1 filter paper is most commonly used as biosensor and microfluidic substrate, primarily, because of its large pore volume fraction which can support fast lateral flow. Also, due to its porous nature, Whatman #1 filter paper can absorb more biomolecules (9.5 mg per g of paper) than nonporous pure cellulose substrate, such as glassine paper (0.004 mg per g of paper).[2] The properties of Whatman #1 filter paper, glassine paper and copy paper were compared and summarized in **Table 1**.

Table 1: Typical properties of Whatman #1 filter paper, glassine paper and common copy paper.

	Whatman #1 Paper[19]	ECHO® Standard Glassine Paper[20]	Copy Paper[21]
Component	Pure cellulose	Pure cellulose	Cellulose and filler
Basis weight (g/m^2)	88	25-90	~80
Tensile Strength(N/15mm)	39.1	27-82	44-49
Apparent	White	Translucent	White
Particle Retention Liquid (μm)	~10μm	N/A	N/A
Application	Filtering	Packaging or wrapping of foodstuffs	Office Printing

The hydrophobicity of the paper surface is another important property, particularly for paper-based microfluidics. To direct the liquid flow on paper, the paper can be patterned into hydrophilic flow channels separated by hydrophobic walls. Such patterns can prevent the spreading of liquid on the paper, give strong signals on certain spots, and allow running multiple reactions simultaneously along a single strip of paper. A variety of pattern fabricating techniques on paper have been reported in literature, including photolithography[22], various printing methods[23-26], chemical treatment[27], plasma etching[28] and laser treatment[29].

1.1.2 The Biorecognition Agent

The most common recognition agents utilized in paper-based biosensors are enzymes,[10, 30-31] antibodies,[15, 32] DNA/RNA,[9, 32] and bacteriophage.[33] Enzymes are used widely as biorecognition agent, owing to their biocatalytic function with their specific substrate. Similarly, antibodies also exhibit high specific recognition ability to antigens via immunoreactions. In general, antibodies are large protein molecules with Y-shape structures. The antigen binding site is located at each of the upper ends of the Y-shape structure. Compared with enzymes, antibodies are more stable.[34] Unlike proteins, nucleic acids (DNA/RNA) are robust molecules, which can be used over a board range of conditions. The hybridization properties allow DNA/RNA to respond to the target sequence in the presence of non-complementary strands.[35] Bacteriophage is another important biorecognition agent, which is bacteria-specific virus. The phage can bind to specific bacteria through its tail, inject its DNAs into the bacteria, replicate themselves, and destroy the host.[36] Due to the nature of biorecognition agent, enzymes, antibodies, and DNA/RNAs are typically used in paper-based detection systems, while bacteriophages are mainly used in paper-based bacteria killing products. **Table 2** summarizes some examples of using different biomolecules, as biorecognition agents, in paper-based biosensors.

Table 2: Examples of biomolecules used for paper-based biosensors

Biomolecule	Detected Sample
Enzyme	Heavy Metals (Hg(II), Ag(I), Cu(II), Cd(II), Pb(II), Cr(VI), Ni(II))[37], Pesticides (paraoxon, aflatoxin B1, Neostigmine)[10, 31, 38], E.coli BL21[23], Ecoli O157[30, 39], Salmonella spp.[39], Listeria monocytogenes[39]
Antibodies	Tumor Marker Screening(α-fetoprotein, carcinoembryonic antigen[40], nitrated ceruloplasmin[41]), Syphilis Screening[42], Virus (M13 Bacteriophage)[43], C-reactive protein[44], Blood Typing[45], Troponin I[46]
DNA/RNAs	Thrombin[47-48], ATP[32, 47], DNase I[9], adenosine[9, 49], C-jun protein[50], Ramos cells[51]
Bateriophages	E.coli K12[52], E. coli B (ATCC 11303)[53], E.coli O157[33]

1.1.3 The Immobilization of Biorecognition Agent

1.1.3.1 Physical immobilization

Physical immobilization, also known as physical adsorption, is a simple and easy method to immobilize bioreagent onto substrates. Such method heavily relies on the physical forces, such as electrostatic interaction, hydrophobic interaction, and Van der Waals force, between the bioreagent and the paper surface. A number of studies have reported on the use of physical immobilization to bind biomolecules, such as protein, antibody, DNA, and bacteriophage onto cellulose-based surfaces.

Halder et al.[54] conducted a systematic study of different types of protein adsorption on cellulose powder under various conditions. It was found that the protein adsorption ability of the cellulose powder is in the following order: gelatin > β-lactoglobulin > Lysozyme > BSA. Karra-Châabouni et al.[55] studied the physical adsorption of Rhizopus oryzae lipase (ROL) onto oxidized cellulose fibers and found that the adsorption ability improved with increasing carboxyl groups of cellulose. The result implied that the interaction between lipase and cellulose were mainly driven by electrostatic force. Irelma et al.[56] studied the physical adsorption of human immunoglobulin G (hIgG) and Bovine Serum Albumin (BSA) on carboxymethyl cellulose (CMC) or chitosan modified cellulose. The research concluded that both modified cellulose surfaces increase the attachment of biomolecules through electrostatic interaction. Ning Yan's group[57] also investigated the adsorption and inactivation of horseradish peroxidise (HRP) on cellulose fiber surfaces. However, they discovered that hydrophobic interactions play a more important role than electrostatic interaction in HRP adsorption. Hydrophobic surfaces can also significantly improve protein binding affinity. The results also revealed no clear evidence that hydrophobic treatment would inactivate enzyme. Our interfacial technologies research group also reported the antibody adsorption onto filter paper, treated with cationic paper wet-strength resin (PAE). It was found that low loading of PAE can improve the antibody adsorption, without interfering antibody activity.[15]

Physical adsorption of DNA onto cellulose was also being studied extensively. Halder et al.[54] reported that DNA can adsorb onto cellulose at pH 4, but not at pH 6 or 8. Su et al.[58] studied low-molecular weight DNA, also known as DNA aptamer, and found that the physical adsorption of DNA aptamer is very weak and unstable. Further study showed that cellulose surface, modified with cationic polymer, can stimulate DNA-aptamer adsorption, but the bound DNA-aptamer may lost functionality.[32]

Bacteriophages can have a negatively charged "head" and positively charged "tail". Due to the electrostatic charge on phage, the immobilization of phage onto cellulose becomes desirable through, surface modification of cellulose to become positively charged. In this way, the phage head is bound to the cellulose substrate, while the phage tail is made available to capture bacteria. Anany et al.[33] successfully showed significant improvement on phage infection with positively charged phage-bound substrate over the native phage-bound substrate.

In summary, as much as physical immobilization is known for its simplistic steps and low cost, such immobilization technique is not considered as a sophisticated strategy for biosensor immobilization, because it lacks in strength, robustness and stability.

1.1.3.2 Chemical immobilization

To overcome the weaknesses inherited in physical immobilization, chemical-based techniques have been explored and developed as an alternative to physical immobilization. Chemical immobilization, also known as covalent coupling, relies on the formation of chemical bonds between the functional groups of cellulose substrate and bioreagent. Pure cellulose is not a reactive substrate as it contains only few functional groups. Although cellulose contains relatively abundant hydroxyl group on backbone, the groups are generally not active in mild conditions. The only active functional groups found in cellulose are the carboxyl groups by oxidizing C-6 hydroxyls and cellulose end chains. However, the existing amount of these groups is very low.[2] Therefore, modification of pure cellulose is necessary prior to bioconjugation.

Orelma et al.[59] reported an effective approach to covalently immobilize antibodies onto cellulose. In this approach, the cellulose film was first modified by pre-adsorbing CMC at high ionic strength. Then, the antibody was covalently conjugated onto the surface via the EDC/NHS chemistry between carboxyl groups of the CMC and amine groups of the antibody. Besides the option of polymer pre-adsorption, cellulose can also be activated directly by different chemistry, mainly through hydroxyl groups. Kong's group[60] reported the use to epichlorohydrin with NaOH on cellulose to yield epoxy groups for DNA immobilization. Su et al.[58] oxidized the hydroxyl groups of cellulose to aldehyde groups by periodate for the conjugation of DNA aptamers. The formed aldehyde group of cellulose can couple with the terminal amino group of DNA-aptamer using a Schiff Base reaction and reduction with a resulting conjugation efficiency of 25%. Another method using photo-reactive modification on cellulose membrane for antibody conjugation was developed by Bora et al.[61]. Such modified membrane was proven to be successfully applied in enzyme-linked immunosorbent assays (ELISA). In this photo treatment process,

the hydroxyl group of the cellulose membrane was first activated by the 1-fluoro-2-nitro-4 azidobenzen (FNAB) in alkaline medium. The activation step was followed by UV light exposure on the membrane to convert the azido-group to highly reactive nitrene, which can bind proteins.

In short, chemical conjugation is an effective strategy to create strong, stable, specific, and efficient bioreagent conjugation on cellulose substrate. Due to the elaborative chemical reactions, this process generally involves multiple treatment steps and uses expensive reagents. Furthermore, the introduction of reagents into the process may also cause detriment on biosensor activity and release of some toxic substances.[62]

1.1.3.3 Bioaffinity immobilization

Apart from physical and chemical-based immobilization, bioaffinity conjugation is also considered as one of the viable approaches for bioreagent immobilization onto cellulose surface. A typical example of bioaffinity-based reagent which binds to cellulose is cellulose-binding modules (CBM). CBMs were first discovered in Trichoderma reesei and cellulomonas fimi, and they can spontaneously bind to cellulose with very high affinity and low desorption rate.[63] Ideally, CBMs could be coupled to antibodies, enzymes, bacteriophages, DNAs, or cells for immobilization on cellulose via genetic engineering approaches.[2] Cao et al.[64] developed a CBM fusion protein containing the protein A sequence as the linkage for antibody immobilization on magnetic cellulose microspheres. Protein A can specifically bind onto the Fc domain of immunoglobulin gamma (IgG) without interfering IgG functionality, while CBMs have high affinity to cellulose. As such, this linker can be widely used for antibody-cellulose conjugation. Mackenzie's group[65] has engineered a biospecific pentamer single domain antibody. Five CBMs and five single domain antibodies (sdAbs) were linked via verotoxin B subunit (VTBs). They had successfully proven that the complex antibody can spontaneously bind to the cellulose substrate through CBMs and capture antigen through sdAbs. DNA and RNA aptamers were also reported to be modified with CBMs to specifically bind to cellulose by Boese et al.[66-67] These CBM-DNA/RNA aptamers showed robust binding characteristic to cellulose powder and paper. Sato et al. [68] further investigated the adsorption of the CBM-DNA aptamer onto model cellulose surfaces using the quartz crystal microbalance with dissipation technique (QCM-D). They confirmed that the CBM-DNA aptamers adsorbed more onto cellulosed compared to other nonspecific oligonucleotide. They also demonstrated the use of CBD-DNA aptamers to promote the binding of anionic polyacrylamide onto cellulose at high ionic strength condition where the electrostatic interaction could not be applied. Griffiths's group[53] developed genetically modified T4 bacteriophages with CBM on their heads to be immobilized on cellulose. However, the immobilization of bacteriophages suffered an infectivity reduction compared to free bacteriophages.

1.1.3.4 Polymeric entrapment or attachment on particles

As illustrated in **Figure 4**, biomolecules can be physically entrapped within a sol-gel derived material and be used as biosensor. It is well known that the sol-gel matrix can prevent leaching of the biomolecules and retain biomolecular functionality for a long time period. Therefore, deposition of sol-gel derived materials laden with a biocomponent onto the cellulose surface is an effective strategy.[69] The sol and biomolecules can be coated or printed onto paper in liquid form, followed by gel formation on the paper. Brennan's group has used this method to successfully develop bioactive paper sensors for pesticide, heavy metals, and E.coli detection.[10, 30-31, 37] All of the reagents used for constructing the sensors, including silica sol and biomolecule solutions, were formulated and printed using a piezoelectric inkjet printer. Savolainen et al.[70] also reported the printing of polymer microcapsules for enzyme immobilization on paper. They found that the enzyme maintained above 40% of the original activity in the microcapsule for more than 8 weeks. The printing process did not affect the functionality of enzyme microcapsules. However, the only downside of this method is the incapability to capture targets, which are larger than the analyte entrapped within the network. The pore size of the sol-gel matrix is made smaller than the size of entrapped molecules to prevent leaching, while diffusion limitations of large targets is severely compromised.[7]
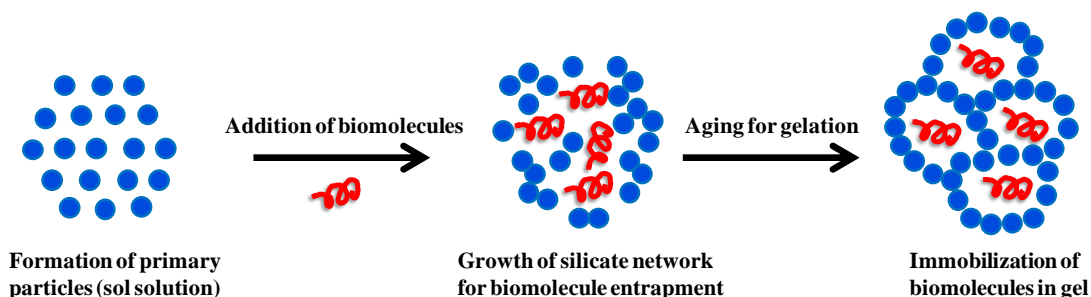

Figure 4: Entrapment of biomolecules by sol-gel process

An alternate solution is to immobilize biomolecules on a particle via covalent bonding and then deposit them onto the paper. Su et al.[32] reported the immobilization of DNA aptamers or antibodies onto poly (N-isopropylacrylamide) (PNIPAM) microgels. In this method, PNIPAM microgels were coupled with streptavidin, while aptamers or antibodies were biotinylated. The aptamers or antibodies were subsequently attached to the microgels, via the biotin-streptavidin reaction. The immobilized aptamers or antibodies retained their activity on the microgel and printed onto the paper surface. The microgels also served as a barrier to isolate the biomolecules from the paper surface and prevent the deactivation of biomolecules by the paper surface chemistry.

1.1.4 The Deposition of Biorecognition Agent

The selection of reagent deposition method in fabricating paper-based biosensor is a critical process, as different techniques can be applied depending on the type of production scale and the desired characteristics or properties of biosensor. On a lab scale,

most of the research work is carried out by pipeting the reagents onto the paper surface. Such technique becomes infeasible and uneconomically justified, when transferred to large scale production.

In order to scale up the production of paper-based biosensors, highly advanced and rapid deposition systems should be considered. Conventionally, paper enhancing materials, such as additives and fillers, are added into the paper pulp, during making process. This technique is proven to be a quick and effective solution to achieve uniform blending of the materials with pulp.[35] However, deposition of bioreagent via this method is both unviable and unattractive, due to the high costing associated to bioreagent and the potential waste issue that can occur throughout the process. Additionally, pH of the process medium, additives, process temperature, and mechanical shear force can significantly affect the functionality of bioreagents.

Printing techniques, on the other hand, can provide better precision and reliable deposition of bioreagents onto the paper. So far, there are several types of printing techniques made available commercially, as shown in **Figure 5**. These are primarily flexographic, gravure printing, lithography/offset printing, screen printing, and inkjet printing.
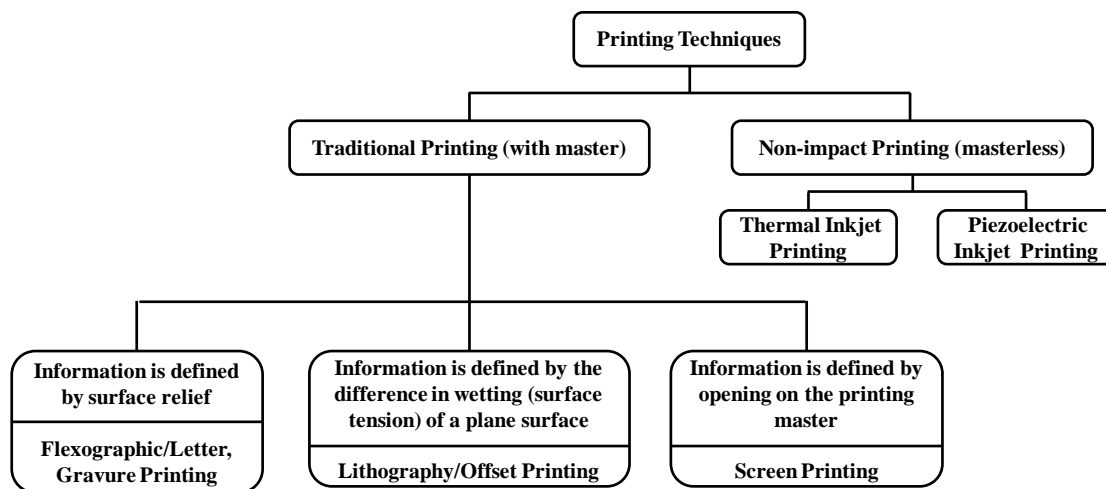

Figure 5: Overview of printing techniques (redrawn from Kipphan) [71]

Despite all the available printing technologies, this work will primarily focus on inkjet printing as the only printing technique for bioreagent deposition. Being a non-impact printing technique, inkjet printing can eject minute amounts of reagents with flexible control, non-contact operation, high speed, and precise localization.[35] There are two types of inkjet printing technologies, namely thermal inkjet and piezoelectic inkjet printing. As shown in **Figure 6**, the drops produced from thermo inkjet, also known as bubble jet, are ejected by direct heating and rapid localized vaporization of the ink to form bubbles and create high pressure in the chamber. Unlike, thermo inkjet concept, piezoelectric inkjet printing generates the drops by mechanically deforming the jet chamber, which is

composed of piezoelectric material. When the electronic signal is applied, the chamber wall changes its shape and ejects an ink drop.[71]
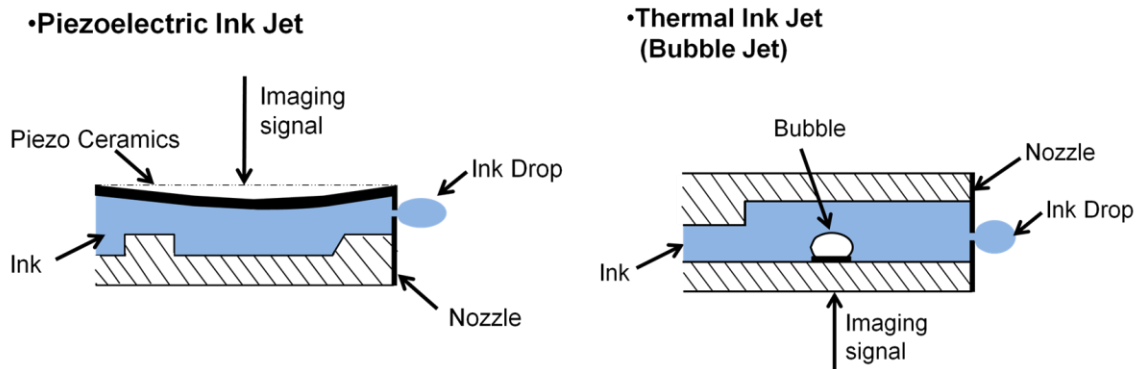

Figure 6: The schematic diagram of two inkjet printing technologies (Adapted from Kipphan)[71]

In order to make inkjet printing to work, ink formulation is one of the most crucial steps. Specifically, ink viscosity and surface tension are two important parameters in ink formulation. Due to the difference in printing techniques, ink property requirements must be different from one technique to another to achieve the desirable printing outcome. For instance, thermal inkjet printing requires low viscosity ink (1-1.5cP) to work properly, while piezoelectric inkjet printing requires higher viscosity ink (5-10cP) to achieve desirable printing effect. The ink viscosity can be adjusted typically using polyhydric alcohols, such as glycol.[35] The surface tension of the ink can be modified by addition of surfactants. The ink surface tension should not be below 35 mN/m, otherwise droplets cannot be ejected.[72-73]

1.1.5 The Reporting System

1.1.5.1 Colorimetric method

Among all the available reporting systems, colorimetric detection is the most popular, simple and straightforward method for producing signals on paper-based biosensors, due to specific enzymatic or chemical interaction. Whitesides's group demonstrated colorimetric detection of glucose and protein on patterned filter paper.[8] The change of color from colorless to brown indicated the presence of glucose, via the enzymatic oxidation of iodide, while the colour change of tetrabromophenol blue from yellow to blue indicated positive detection of BSA. Later on, Brennan's group from McMaster University successfully reported a series of paper-based biosensors.[10, 30-31, 37, 74] In one of their inventions, they had developed a paper-based colorimetric sensor for neurotoxin detection.[31] This assay relied on detecting acetylcholinesterase (AChE) activity, according to the developed colour intensity, using the well-known Ellman colorimetric assay. When the neurotoxin is present, it inhibits the AChE and reduces the change in color intensity from colourless to light yellow. However, if there is no neurotoxin, the AChE reacts with the substrate and produces a full yellow colour. This sensor provides

rapid detection (less than 5 min) and excellent detection limits (aflatoxin B1,~30 nM; paraoxon, ~100 nM).

1.1.5.2 Electrochemical methods

Electrochemical detection methods rely on (bio)chemical reactions, from which electrons are generated or consumed. The electrochemical sensor typically contains a reference electrode, a working electrode and a counter electrode. Compared with the colorimetric method, electrochemical detection can provide faster response and higher sensitivity. Another advantage of this method is that the reporting system is not interfered by ambient light and colour of paper.[75] In order to fabricate paper-based electrochemical sensors, conductive inks need to be deposited onto the paper, such as carbon inks (working electrode) and silver/silver chloride inks (counter electrodes).[75] Dungchai et al.[76] created electrochemical paper-based microfluidic devices for detecting glucose, lactate, and uric acids in biological samples using corresponding oxidase enzymes. These sensors rely on the detection of current changes, caused by hydrogen peroxide, formed from the catalyzed reaction of enzymes with their respective oxidase enzymes. The resulting current was measured by chronoamperometry. The detection limits for glucose, lactate, and uric acids are 0.21 mM, 0.36 mM and 1.38 mM respectively using the sensor they developed. Subsequently, Nie et al.[77] from the same group used the same concept to develop an upgraded version of paper-based electrochemical microfluidics which can be integrated with a commercial hand-held glucometer, allowing instant value reading. Liu et al.[78] also reported an interesting paper-based sensor for use in glucose detection. The significant feature of the paper-based sensor is the integration of metal-air battery, which drives electrochromic display and sensing chemistry. The sensor is made by sandwiching a piece of paper between two indium-doped tin oxide (ITO) electrodes. Wax was applied to divide the paper into sensor and metal-air battery region. The paper was also preloaded with glucose oxidase and $Fe(CN)_6^{3-}$. When the glucose was applied onto the paper, glucose oxidase oxidized the glucose and the reaction led to reduction of $Fe(CN)_6^{3-}$ to $Fe(CN)_6^{4-}$ at the bottom electrode. As a result, the $Fe(CN)_6^{4-}$ was re-oxidized back to $Fe(CN)_6^{3-}$,which converted the electrochromic Prussian blue to colorless Prussian white (PW). Therefore, blue color indication signified the absence of glucose and no color represented the presence of glucose. Besides biomolecule detection, paper-based electrochemical sensors are also widely used in detecting neurotransmitters[79], drugs[80], DNA[81], metals[82], and gaseous samples[83].

1.1.5.3 Fluorescence

Besides colorimetric and electrochemical method, fluorescence-generated signals can also be introduced onto paper as reporting signal. Fluorescence signal is an attractive option as it provides more sensitive analysis than colorimetric methods. Funes-Huacca et al. [84] developed a portable device for bacteria growth detection on paper. The growth of bacteria can be quantified with a fluorescent mCherry reporter. Ali et al.[85] demonstrated paper strips for DNA quantitative analysis using fluorescence signal. Allen et al.[86] described the detection of nucleic acids on paper using DNA circuits as amplifiers. The DNA circuits contained non-enzymatic amplifier and transduction to a fluorescent report,

which enhanced signal amplification and detection. A paper-based 96- or 384-microzone plate for quantitative fluorescence measurements was reported by Whitesides's group.[87] These papers offer several superior advantages compared to conventional plastic multiwall plates. The paper-based plate uses very thin papers, and requires small sample amounts and can be recycled. In general, there are two typical concerns associated with the use of paper-based fluorescence. Firstly, an additional instrument is required for fluorescent signal detection, which adds to capital cost and complexity of detection. Secondly, commercial paper content is not created uniformly across the sheet. As a result, some papers can produce high background signals, due to the non-uniform distribution of additives in papermaking.[88] Therefore, the choice of the paper and the strategy to prevent false signals are critical.

1.1.5.4 Chemiluminescence and Electrochemiluminescence

Chemiluminescence is the generation of light (in the ultraviolet, visible or infrared region) occurring, as a result of a chemical reaction. It is typically known to be more sensitive than fluorescence and chromogenic reactions.[89] Several groups have used the mechanism of chemiluminescence to generate detection signals on papers. Yu et al. [90-91] first developed a chemiluminescence paper microfluidics biosensor for uric acid and glucose detections. The glucose and uric acid react with glucose oxidase and urate oxidase, respectively, to produce hydrogen peroxide, which could react with rhodanine derivative and generate a chemiluminescence signal. Wang et al.[92-93] also successfully developed Chemiluminescence –ELISA (enzyme linked immunoassay) to detect different tumor markers on paper according to Yu's protocol as previously described.

Electrochemiluminescence is a method of combining the advantages of chemiluminescence and electrochemistry to yield high sensitivity within a wide dynamic concentration response range.[94] It emits luminescence via a trigger electrochemical reaction. Shen's group[95] reported the first electrochemiluminescence paper-based biosensor to detect 2-(dibutylamino)-ethanol (DBAE) and nicotinamide adenine dinucleotide (NADH). These analytes can react with a tris(2,20-bipyridyl)ruthenium(II) ($Ru(bpy)_3^{2+}$) trigger by the application of positive potential (1.25 V), resulting in the generation of orange luminescence signals, which can be detected by a modified mobile camera.

1.1.5.5 Smell detection

Apart from visual-based detection method, smell can also be used as a reporting signal for developing a biosensor. Although it has not been widely explored, smell can be detected easily by human nose without any expensive instrument, knowledgeable operator, or complicated handling. The first and only paper-based smell-generating biosensor was developed and reported by Xu et al.[96] They initially developed a smell generating enzymatic system for ATP detection, through the odor of indole or methyl mercaptan, using a bienzyme system combining tryptophanase and pyridoxal kinase. Then, they studied the immobilization of this bienzymatic smell generating system on paper. The enzymes were first immobilized onto microgels via EDC/NHS coupling. Then the

enzyme coupled microgel was applied onto paper. The results showed that the microgel helped the retention of enzymes on the paper and the enzymes remained active on the paper to detect targets and generate smells.

1.2 Objectives

Paper-supported biosensors are emerging as competent technologies. Before this work was initiated, there was very little literature information relating paper surface chemistry to the activity of biomacromolecules, particularly antibody molecules, immobilized on paper surfaces. Besides paper surface chemistry, environmental condition, such as temperature and relative humidity, also plays equally important role in biomolecule stability. In order to obtain useful information for designing paper-based biosensors, it is important to understand the effect of paper surface chemistry and environmental condition on biomolecule stability.

In addition to the investigation of biomolecule stability, paper surface characterization is another important aspect in biosensor design. Several paper-based biosensors have been developed based on ink-jet printing of silica sol-gel materials onto paper to entrap enzyme molecules. However, the nature of silica material on the paper has not been fully characterized. There is a need to develop characterization techniques for bio-silica material on paper surface. Besides enzyme entrapment, inkjet printable sol-gel materials can also potentially be used to create barrier for paper-based microfluidics based on hydrophobic sol–gel derived methylsilsesquioxane(MSQ).

The overall objective of this thesis is to investigate and explore paper-based biosensors in various perspectives as described above. The specific goals of this work are summarised below:

1. To investigate the paper surface chemistry and biomacromolecule interactions. The results can provide paper industries information about the optimum addition of paper wet-strength resin/sizing agent for antibody immobilization on paper.

2. To study the influence of temperature and relative humidity (RH) on stability of paper-immobilized antibodies on both untreated and PAE-treated papers, and understand how printing and different storage conditions affect antibody functionality.

3. To explore characterization approaches for silica sol-gel based paper biosensors. Through this work, we are aiming to understand what we can produce with sol-gel bioinks and how the printing affects the paper properties. In addition to conducting fundamental study, this work will pave the way for other paper-based biosensor development using sol-gel derived material.

4. To develop superior ink-jet printable barrier for paper-based microfluidics using sol-gel derived material ─ methylsilsesquioxane (MSQ), based on creating hydrophobic/hydrophilic contrast or direct printing hydrophobic barrier on paper.

14

1.3   Thesis Outline

Chapter 1: Introduction. This chapter presents a thorough background of this project, including the relevant literature and research objectives. The thesis outline is also given in this chapter.

Chapter 2: Effects of Temperature and Relative Humidity on the Stability of Paper-Immobilized Antibodies. This chapter studies the activity of paper-immobilized antibodies under various temperature (40−140 °C) and relative humidity (RH, 30−90%) conditions. PAE-impregnated and untreated papers were used as supports for comparison. Empirical equations are established from the results of this study to correlate the deactivation rate constant with respect to temperature and water content. The equation can also be used to estimate and evaluate printing and coating operation influences on antibody stability. This work has been published in *Biomacromolecules*.[97]

Chapter 3: Influence of A Paper Sizing Agent on Paper-immobilized Biosensing Antibodies. This chapter evaluates the effect of paper sizing agent (AKD specifically) on antibody adsorption and inactivation using membrane chromatography and paper-based immunoassay, respectively. The study also shows that the sizing agent used in the paper making process does not have an significant effect on antibody deactivation. Therefore, papers containing sizing agents, such as packaging cardboards, can be used as a substrate for antibody immobilization. This work has been submitted to *J-FOR (The Journal of Science and Technology for Forest Products and Processes).*

Chapter 4: MSQ-based channel patterning strategies for paper-based microfluidics. This chapter reports two strategies for creating patterns on paper, utilizing hydrophobic MSQ material derived from sol-gel process. The first strategy involves introduction of hydrophilic channels by printing a highly basic solution onto hydrophobic MSQ coated paper to dissolve MSQ and etch open the surface to reveal the original paper material. The second technique relies on direct printing of MSQ to outline the hydrophobic walls bordering the hydrophilic channels. The barriers were examined relative to wax and AKD barriers for containment of surfactant and organic solutions, and are shown to be amenable to an *E. coli* assay that requires the use of a bacteria lysing reagent. This work has been published in *Lab on a Chip*.[98]

Chapter 5: Morphology and Entrapped Enzyme Performance in Inkjet Printed Sol-Gel Coatings on Paper. This chapter described the characterization of sol-gel bioinks printing on paper using various methods. Protease test was developed to test enzyme entrapment within sol-gel network. It was found that the entrapment of enzyme molecules was improved with the increasing amount of the sol-gel derived material printed on paper. Moreover, the top layer of printed sol-gel material played the most important role in enzyme entrapment. Through the confocal microscopic results, we confirmed the uniform printing of polymer, sol-gel and biomolecule inks. SEM and TEM images further confirmed the formation of a stable silica thin layer on the fibers without completely filling the paper pores. This work has been published in *Chemistry of Materials*.[99]

Chapter 6: Concluding remarks. This chapter summarizes the major contributions of this study.

1.4   References

1.   Martinez, A. W.; Phillips, S. T.; Whitesides, G. M.; Carrilho, E., Diagnostics for the Developing World: Microfluidic Paper-Based Analytical Devices. *Anal. Chem.* **2009,** *82* (1), 3-10.

2.   Pelton, R., Bioactive paper provides a low-cost platform for diagnostics. *TrAC, Trends Anal. Chem.* **2009,** *28* (8), 925-942.

3.   Sicard, C.; Brennan, J. D., Bioactive Paper: Biomolecule Immobilization Methods And Applications In Environmental Monitoring *MRS Bull.* **2013,** *38* (4).

4.   Martin, A. J.; Synge, R. L., A new form of chromatogram employing two liquid phases: A theory of chromatography. 2. Application to the micro-determination of the higher monoamino-acids in proteins. *Biochem. J.* **1941,** *35* (12), 1358-1368.

5.   Free, A. H.; Adams, E. C.; Kercher, M. L.; Free, H. M.; Cook, M. H., Simple Specific Test for Urine Glucose. *Clin. Chem.* **1957,** *3* (3), 163-168.

6.   Mabey, D.; Peeling, R. W.; Ustianowski, A.; Perkins, M. D., Tropical infectious diseases: Diagnostics for the developing world. *Nature Rev. Microbiol.* **2004,** *2* (3), 231-240.

7.   Kong, F.; Hu, Y., Biomolecule immobilization techniques for bioactive paper fabrication. *Anal. Bioanal. Chem.* **2012,** *403* (1), 7-13.

8.   Martinez, A. W.; Phillips, S. T.; Butte, M. J.; Whitesides, G. M., Patterned Paper as a Platform for Inexpensive, Low-Volume, Portable Bioassays. *Angew. Chem. Int. Ed.* **2007,** *46* (8), 1318-1320.

9.   Zhao, W.; Ali, M. M.; Aguirre, S. D.; Brook, M. A.; Li, Y., Paper-Based Bioassays Using Gold Nanoparticle Colorimetric Probes. *Anal. Chem.* **2008,** *80* (22), 8431-8437.

10.   Hossain, S. M. Z.; Luckham, R. E.; McFadden, M. J.; Brennan, J. D., Reagentless Bidirectional Lateral Flow Bioactive Paper Sensors for Detection of Pesticides in Beverage and Food Samples. *Anal. Chem.* **2009,** *81*, 9055–9064.

11.   Wise, L. E.; Lauer, K. H., cellulose and the Hemicelluloses. In *Pulp and Paper Science and Technology*, Libby, C. E., Ed. McGRAW-Hill New York, 1962; Vol. 1.

12.   Bates, R.; Beijer, P.; Podd, B., Wet Stregnthening of Paper. In *Papermaking chemistry*, Neimo, L., Ed. Fapet Oy: Jyväskylä, 1999; pp 289-301.

13.   Obokata, T.; Yanagisawa, M.; Isogai, A., Characterization of polyamideamine-epichlorohydrin (PAE) resin: Roles of azetidinium groups and molecular mass of PAE in wet strength development of paper prepared with PAE. *J. Appl. Polym. Sci.* **2005,** *97* (6), 2249-2255.

14.   Obokata, T.; Isogai, A., The mechanism of wet-strength development of cellulose sheets prepared with polyamideamine-epichlorohydrin (PAE) resin. *Colloids Surf., A* **2007,** *302* (1–3), 525-531.

15.   Wang, J.; Pelton, R. H.; Veldhuis, L. J.; MacKenzie, R. C.; Hall, C. J.; Filipe, C. D., Wet-strength Resins and Surface Properties Affect Paper-based Antibody Assays. *Appita J.* **2010,** *63* (1), 32-36.

16.   Roberts, J. C., Neutral and alkaline sizing. In *Paper Chemistry*, Roberts, J. C., Ed. Blackie Academic & Professional Glasgow, 1996; pp 140-159.

17.   Isogai, A., Mechanism of Paper Sizing by Alkylketene Dimers. *J. Pulp Pap. Sci.* **1999,** *26*, 251-256.

18.   Lindström, T.; Larsson, P. T., Alkyl Ketene Dimer (AKD) sizing – a review. *Nord. Pulp Pap. Res. J.* **2008,** *23*, 202-208.

19.   Whatman http://www.whatman.com/References/Cellulose_Filter_Typical_Properties_pg12.pdf (accessed October 21st).

20.   GmbH, S. O. http://www.spo-gmbh.de/downloads/Specification_glassine.pdf (accessed Octorber 21st).

21.   http://dorena.diytrade.com/sdp/1699520/4/pd-6369817/10045240.html (accessed October 21st).

22.   Martinez, A. W.; Phillips, S. T.; Wiley, B. J.; Gupta, M.; Whitesides, G. M., FLASH: A rapid method for prototyping paper-based microfluidic devices. *Lab on a Chip* **2008,** *8* (12), 2146-2150.

23.   Li, X.; Tian, J.; Garnier, G.; Shen, W., Fabrication of paper-based microfluidic sensors by printing. *Colloids Surf., B* **2010,** *76* (2), 564-570.

24.   Olkkonen, J.; Lehtinen, K.; Erho, T., Flexographically Printed Fluidic Structures in Paper. *Anal. Chem.* **2010,** *82* (24), 10246-10250.

25.   Bruzewicz, D. A.; Reches, M.; Whitesides, G. M., Low-Cost Printing of Poly(dimethylsiloxane) Barriers To Define Microchannels in Paper. *Anal. Chem.* **2008,** *80* (9), 3387-3392.

26.   Carrilho, E.; Martinez, A. W.; Whitesides, G. M., Understanding Wax Printing: A Simple Micropatterning Process for Paper-Based Microfluidics. *Anal. Chem.* **2009,** *81* (16), 7091-7095.

27.   Abe, K.; Suzuki, K.; Citterio, D., Inkjet-Printed Microfluidic Multianalyte Chemical Sensing Paper. *Anal. Chem.* **2008,** *80* (18), 6928-6934.

28.   Li, X.; Tian, J.; Nguyen, T.; Shen, W., Paper-Based Microfluidic Devices by Plasma Treatment. *Anal. Chem.* **2008,** *80* (23), 9131-9134.

29.   Chitnis, G.; Ding, Z.; Chang, C.-L.; Savran, C. A.; Ziaie, B., Laser-treated hydrophobic paper: an inexpensive microfluidic platform. *Lab on a Chip* **2011,** *11* (6), 1161-1165.

30.   Hossain, S.; Ozimok, C.; Sicard, C.; Aguirre, S.; Ali, M.; Li, Y.; Brennan, J., Multiplexed paper test strip for quantitative bacterial detection. *Anal. Bioanal. Chem.* **2012,** *403* (6), 1567-1576.

31.   Hossain, S. M. Z.; Luckham, R. E.; Smith, A. M.; Lebert, J. M.; Davies, L. M.; Pelton, R. H.; Filipe, C. D. M.; Brennan, J. D., Development of a Bioactive Paper Sensor for Detection of Neurotoxins Using Piezoelectric Inkjet Printing of Sol-Gel-Derived Bioinks. *Anal. Chem.* **2009,** *81* (13), 5474-5483.

32.   Su, S.; Ali, M. M.; Filipe, C. D. M.; Li, Y.; Pelton, R., Microgel-Based Inks for Paper-Supported Biosensing Applications. *Biomacromolecules* **2008,** *9* (3), 935-941.

33.   Anany, H.; Chen, W.; Pelton, R.; Griffiths, M. W., Biocontrol of Listeria monocytogenes and Escherichia coli O157:H7 in Meat by Using Phages Immobilized on Modified Cellulose Membranes. *Appl. Environ. Microbiol.* **2011,** *77* (18), 6379-6387.
34.   Wang, W.; Singh, S.; Zeng, D. L.; King, K.; Nema, S., Antibody structure, instability, and formulation. *J. Pharm. Sci.* **2007,** *96* (1), 1-26.
35.   Di Risio, S.; Yan, N., Bioactive Paper Through Inkjet Printing. *J. Adhes. Sci. Technol.* **2010,** *24* (3), 661-684.
36.   Jabrane, T.; Jeaidi, J.; Dubé, M.; Mangin, P. J., Gravure Printing of Enzymes and Phages. *Advances in Printing and Media Technology* **2008,** *35*, 279-288.
37.   Hossain, S. M. Z.; Brennan, J. D., β-Galactosidase-Based Colorimetric Paper Sensor for Determination of Heavy Metals. *Anal. Chem.* **2011,** *83* (22), 8772-8778.
38.   Pohanka, M., Acetylcholinesterase Based Dipsticks with Indoxylacetate as a Substrate for Assay of Organophosphates and Carbamates. *Anal. Lett.* **2012,** *45* (4), 367-374.
39.   Jokerst, J. C.; Adkins, J. A.; Bisha, B.; Mentele, M. M.; Goodridge, L. D.; Henry, C. S., Development of a Paper-Based Analytical Device for Colorimetric Detection of Select Foodborne Pathogens. *Anal. Chem.* **2012,** *84* (6), 2900-2907.
40.   Ge, S.; Ge, L.; Yan, M.; Song, X.; Yu, J.; Huang, J., A disposable paper-based electrochemical sensor with an addressable electrode array for cancer screening. *Chem. Commun.* **2012,** *48* (75), 9397-9399.
41.   Li, Z.; Wang, Y.; Wang, J.; Tang, Z.; Pounds, J. G.; Lin, Y., Rapid and Sensitive Detection of Protein Biomarker Using a Portable Fluorescence Biosensor Based on Quantum Dots and a Lateral Flow Test Strip. *Anal. Chem.* **2010,** *82* (16), 7008-7014.
42.   Yang, D.; Ma, J.; Zhang, Q.; Li, N.; Yang, J.; Raju, P. A.; Peng, M.; Luo, Y.; Hui, W.; Chen, C.; Cui, Y., Polyelectrolyte-Coated Gold Magnetic Nanoparticles for Immunoassay Development: Toward Point of Care Diagnostics for Syphilis Screening. *Anal. Chem.* **2013,** *85* (14), 6688-6695.
43.   Larsson, P. A.; G. Puttaswamaiah, S.; Ly, C.; Vanerek, A.; Christopher Hall, J.; Drolet, F., Filtration, adsorption and immunodetection of virus using polyelectrolyte multilayer-modified paper. *Colloids Surf., B* **2013,** *101* (0), 205-209.
44.   Oh, Y. K.; Joung, H.-A.; Kim, S.; Kim, M.-G., Vertical flow immunoassay (VFA) biosensor for a rapid one-step immunoassay. *Lab on a Chip* **2013,** *13* (5), 768-772.
45.   Al-Tamimi, M.; Shen, W.; Zeineddine, R.; Tran, H.; Garnier, G., Validation of Paper-Based Assay for Rapid Blood Typing. *Anal. Chem.* **2011,** *84* (3), 1661-1668.
46.   Choi, D. H.; Lee, S. K.; Oh, Y. K.; Bae, B. W.; Lee, S. D.; Kim, S.; Shin, Y.-B.; Kim, M.-G., A dual gold nanoparticle conjugate-based lateral flow assay (LFA) method for the analysis of troponin I. *Biosens. Bioelectron.* **2010,** *25* (8), 1999-2002.
47.   Chen, J.; Fang, Z.; Lie, P.; Zeng, L., Computational Lateral Flow Biosensor for Proteins and Small Molecules: A New Class of Strip Logic Gates. *Anal. Chem.* **2012,** *84* (15), 6321-6325.
48.   Xu, H.; Mao, X.; Zeng, Q.; Wang, S.; Kawde, A.-N.; Liu, G., Aptamer-Functionalized Gold Nanoparticles as Probes in a Dry-Reagent Strip Biosensor for Protein Analysis. *Anal. Chem.* **2008,** *81* (2), 669-675.

49.   Liu, H.; Xiang, Y.; Lu, Y.; Crooks, R. M., Aptamer-Based Origami Paper Analytical Device for Electrochemical Detection of Adenosine. *Angew. Chem.* **2012,** *124* (28), 7031-7034.
50.   Fang, Z.; Ge, C.; Zhang, W.; Lie, P.; Zeng, L., A lateral flow biosensor for rapid detection of DNA-binding protein c-jun. *Biosens. Bioelectron.* **2011,** *27* (1), 192-196.
51.   Liu, G.; Mao, X.; Phillips, J. A.; Xu, H.; Tan, W.; Zeng, L., Aptamer−Nanoparticle Strip Biosensor for Sensitive Detection of Cancer Cells. *Anal. Chem.* **2009,** *81* (24), 10013-10018.
52.   Derda, R.; Lockett, M. R.; Tang, S. K. Y.; Fuller, R. C.; Maxwell, E. J.; Breiten, B.; Cuddemi, C. A.; Ozdogan, A.; Whitesides, G. M., Filter-Based Assay for Escherichia coli in Aqueous Samples Using Bacteriophage-Based Amplification. *Anal. Chem.* **2013,** *85* (15), 7213-7220.
53.   Minikh, O.; Tolba, M.; Brovko, L. Y.; Griffiths, M. W., Bacteriophage-based biosorbents coupled with bioluminescent ATP assay for rapid concentration and detection of Escherichia coli. *J. Microbiol. Methods* **2010,** *82* (2), 177-183.
54.   Halder, E.; Chattoraj, D. K.; Das, K. P., Adsorption of biopolymers at hydrophilic cellulose–water interface. *Biopolymers* **2005,** *77* (5), 286-295.
55.   Karra-Châabouni, M.; Bouaziz, I.; Boufi, S.; Botelho do Rego, A. M.; Gargouri, Y., Physical immobilization of Rhizopus oryzae lipase onto cellulose substrate: Activity and stability studies. *Colloids Surf., B* **2008,** *66* (2), 168-177.
56.   Orelma, H.; Filpponen, I.; Johansson, L.-S.; Laine, J.; Rojas, O. J., Modification of Cellulose Films by Adsorption of CMC and Chitosan for Controlled Attachment of Biomolecules. *Biomacromolecules* **2011,** *12* (12), 4311-4318.
57.   Di Risio, S.; Yan, N., Adsorption and inactivation behavior of horseradish peroxidase on cellulosic fiber surfaces. *J. Colloid Interface Sci.* **2009,** *338* (2), 410-419.
58.   Su, S.; Nutiu, R.; Filipe, C. D. M.; Li, Y.; Pelton, R., Adsorption and Covalent Coupling of ATP-Binding DNA Aptamers onto Cellulose. *Langmuir* **2006,** *23* (3), 1300-1302.
59.   Orelma, H.; Teerinen, T.; Johansson, L.-S.; Holappa, S.; Laine, J., CMC-Modified Cellulose Biointerface for Antibody Conjugation. *Biomacromolecules* **2012,** *13* (4), 1051-1058.
60.   Kong, D.; Schuett, W.; Dai, J.; Kunkel, S.; Holtz, M.; Yamada, R.; Yu, Y.; Klinkmann, H., Development of Cellulose-DNA Immunoadsorbent. *Artif. Organs* **2002,** *26* (2), 200-208.
61.   Bora, U.; Sharma, P.; Kannan, K.; Nahar, P., Photoreactive cellulose membrane—A novel matrix for covalent immobilization of biomolecules. *J. Biotechnol.* **2006,** *126* (2), 220-229.
62.   Shpigel, E.; Goldlust, A.; Efroni, G.; Avraham, A.; Eshel, A.; Dekel, M.; Shoseyov, O., Immobilization of recombinant heparinase I fused to cellulose-binding domain. *Biotechnol. Bioeng.* **1999,** *65* (1), 17-23.
63.   Shoseyov, O.; Shani, Z.; Levy, I., Carbohydrate Binding Modules: Biochemical Properties and Novel Applications. *Microbiol. Mol. Biol. Rev.* **2006,** *70* (2), 283-295.

64.   Cao, Y.; Zhang, Q.; Wang, C.; Zhu, Y.; Bai, G., Preparation of novel immunomagnetic cellulose microspheres via cellulose binding domain-protein A linkage and its use for the isolation of interferon α-2b. *J. Chromatogr. A* **2007,** *1149* (2), 228-235.

65.   Hussack, G.; Luo, Y.; Veldhuis, L.; Hall, J. C.; Tanha, J.; MacKenzie, R., Multivalent Anchoring and Oriented Display of Single-Domain Antibodies on Cellulose. *Sensors* **2009,** *9* (7), 5351-5367.

66.   Boese, B. J.; Breaker, R. R., In vitro selection and characterization of cellulose-binding DNA aptamers. *Nucleic Acids Res.* **2007,** *35* (19), 6378-6388.

67.   Boese, B. J.; Corbino, K.; Breaker, R. R., In Vitro Selection and Characterization of Cellulose-Binding RNA Aptamers Using isothermal Amplification. *Nucleosides Nucleotides Nucleic Acids* **2008,** *27* (8), 949-966.

68.   Sato, T.; Ali, M. M.; Pelton, R.; Cranston, E. D., DNA Stickers Promote Polymer Adsorption onto Cellulose. *Biomacromolecules* **2012,** *13* (10), 3173-3180.

69.   Jin, W.; Brennan, J. D., Properties and applications of proteins encapsulated within sol–gel derived materials. *Anal. Chim. Acta* **2002,** *461* (1), 1-36.

70.   Savolainen, A.; Zhang, Y.; Rochefort, D.; Holopainen, U.; Erho, T.; Virtanen, J.; Smolander, M., Printing of Polymer Microcapsules for Enzyme Immobilization on Paper Substrate. *Biomacromolecules* **2011,** *12* (6), 2008-2015.

71.   Kipphan, H., *Handbook of print media: technologies and production methods*. 2001.

72.   Calvert, P., Inkjet Printing for Materials and Devices. *Chem. Mater.* **2001,** *13* (10), 3299-3305.

73.   Krebs, F. C., Fabrication and processing of polymer solar cells: A review of printing and coating techniques. *Sol. Energy Mater. Sol. Cells* **2009,** *93* (4), 394-412.

74.   Luckham, R. E.; Brennan, J. D., Bioactive paper dipstick sensors for acetylcholinesterase inhibitors based on sol-gel/enzyme/gold nanoparticle composites. *Analyst* **2010,** *135* (8), 2028-2035.

75.   Liana, D. D.; Raguse, B.; Gooding, J. J.; Chow, E., Recent Advances in Paper-Based Sensors. *Sensors* **2012,** *12* (9), 11505-11526.

76.   Dungchai, W.; Chailapakul, O.; Henry, C. S., Electrochemical Detection for Paper-Based Microfluidics. *Anal. Chem.* **2009,** *81* (14), 5821-5826.

77.   Nie, Z.; Deiss, F.; Liu, X.; Akbulut, O.; Whitesides, G. M., Integration of paper-based microfluidic devices with commercial electrochemical readers. *Lab on a Chip* **2010,** *10* (22), 3163-3169.

78.   Liu, H.; Crooks, R. M., Paper-Based Electrochemical Sensing Platform with Integral Battery and Electrochromic Read-Out. *Anal. Chem.* **2012,** *84* (5), 2528-2532.

79.   Shih, W.-C.; Yang, M.-C.; Lin, M. S., Development of disposable lipid biosensor for the determination of total cholesterol. *Biosens. Bioelectron.* **2009,** *24* (6), 1679-1684.

80.   Shiroma, L. Y.; Santhiago, M.; Gobbi, A. L.; Kubota, L. T., Separation and electrochemical detection of paracetamol and 4-aminophenol in a paper-based microfluidic device. *Anal. Chim. Acta* **2012,** *725* (0), 44-50.

81.   Wang, P.; Ge, L.; Yan, M.; Song, X.; Ge, S.; Yu, J., Paper-based three-dimensional electrochemical immunodevice based on multi-walled carbon nanotubes

functionalized paper for sensitive point-of-care testing. *Biosens. Bioelectron.* **2012,** *32* (1), 238-243.

82.   Nie, Z.; Nijhuis, C. A.; Gong, J.; Chen, X.; Kumachev, A.; Martinez, A. W.; Narovlyansky, M.; Whitesides, G. M., Electrochemical sensing in paper-based microfluidic devices. *Lab on a Chip* **2010,** *10* (4), 477-483.

83.   Dossi, N.; Toniolo, R.; Pizzariello, A.; Carrilho, E.; Piccin, E.; Battiston, S.; Bontempelli, G., An electrochemical gas sensor based on paper supported room temperature ionic liquids. *Lab on a Chip* **2012,** *12* (1), 153-158.

84.   Funes-Huacca, M.; Wu, A.; Szepesvari, E.; Rajendran, P.; Kwan-Wong, N.; Razgulin, A.; Shen, Y.; Kagira, J.; Campbell, R.; Derda, R., Portable self-contained cultures for phage and bacteria made of paper and tape. *Lab on a Chip* **2012,** *12* (21), 4269-4278.

85.   Ali, M. M.; Aguirre, S. D.; Xu, Y.; Filipe, C. D. M.; Pelton, R.; Li, Y., Detection of DNA using bioactive paper strips. *Chem. Commun.* **2009,** (43), 6640-6642.

86.   Allen, P. B.; Arshad, S. A.; Li, B.; Chen, X.; Ellington, A. D., DNA circuits as amplifiers for the detection of nucleic acids on a paperfluidic platform. *Lab on a Chip* **2012,** *12* (16), 2951-2958.

87.   Carrilho, E.; Phillips, S. T.; Vella, S. J.; Martinez, A. W.; Whitesides, G. M., Paper Microzone Plates. *Anal. Chem.* **2009,** *81* (15), 5990-5998.

88.   Nery, E.; Kubota, L., Sensing approaches on paper-based devices: a review. *Anal. Bioanal. Chem.* **2013,** *405* (24), 7573-7595.

89.   Kobayashi, S.-I.; Sekino, J.; Honda, K.; Imai, K., Application of high-performance liquid chromatography with a chemiluminescence detection system to determine catecholamines in urine. *Anal. Biochem.* **1981,** *112* (1), 99-104.

90.   Yu, J.; Ge, L.; Huang, J.; Wang, S.; Ge, S., Microfluidic paper-based chemiluminescence biosensor for simultaneous determination of glucose and uric acid. *Lab on a Chip* **2011,** *11* (7), 1286-1291.

91.   Yu, J.; Wang, S.; Ge, L.; Ge, S., A novel chemiluminescence paper microfluidic biosensor based on enzymatic reaction for uric acid determination. *Biosens. Bioelectron.* **2011,** *26* (7), 3284-3289.

92.   Ge, L.; Wang, S.; Song, X.; Ge, S.; Yu, J., 3D Origami-based multifunction-integrated immunodevice: low-cost and multiplexed sandwich chemiluminescence immunoassay on microfluidic paper-based analytical device. *Lab on a Chip* **2012,** *12* (17), 3150-3158.

93.   Wang, S.; Ge, L.; Song, X.; Yu, J.; Ge, S.; Huang, J.; Zeng, F., Paper-based chemiluminescence ELISA: Lab-on-paper based on chitosan modified paper device and wax-screen-printing. *Biosens. Bioelectron.* **2012,** *31* (1), 212-218.

94.   Ge, L.; Yan, J.; Song, X.; Yan, M.; Ge, S.; Yu, J., Three-dimensional paper-based electrochemiluminescence immunodevice for multiplexed measurement of biomarkers and point-of-care testing. *Biomaterials* **2012,** *33* (4), 1024-1031.

95.   Delaney, J. L.; Hogan, C. F.; Tian, J.; Shen, W., Electrogenerated Chemiluminescence Detection in Paper-Based Microfluidic Sensors. *Anal. Chem.* **2011,** *83* (4), 1300-1306.

96.   Xu, Y. A Generic Smell Generating Enzymatic Biosensor. PhD Thesis, McMaster University, Hamilton 2011.

97.   Wang, J.; Yiu, B.; Obermeyer, J.; Filipe, C. D. M.; Brennan, J. D.; Pelton, R., Effects of Temperature and Relative Humidity on the Stability of Paper-Immobilized Antibodies. *Biomacromolecules* **2012,** *13* (2), 559-564.

98.   Wang, J.; Monton, M. R. N.; Zhang, X.; Filipe, C. D. M.; Pelton, R.; Brennan, J. D., Hydrophobic sol-gel channel patterning strategies for paper-based microfluidics. *Lab on a Chip* **2014,** *14* (4), 691-695.

99.   Wang, J.; Bowie, D.; Zhang, X.; Filipe, C.; Pelton, R.; Brennan, J. D., Morphology and Entrapped Enzyme Performance in Inkjet-Printed Sol–Gel Coatings on Paper. *Chem. Mater.* **2014,** *26* (5), 1941-1947.

Chapter 2 Effects of Temperature and Relative Humidity on the Stability of Paper-immobilized Antibodies

In chapter 2, all experiments were conducted by myself with assistance from two undergraduate students: Brian Yiu and Jaclyn Obermeyer. Dr. Pelton aided in the modelling of antibody deactivation and Dr. Brennan suggested the measurement of antibody melting point. The paper was initially drafted by myself, and edited later to final version by Dr. Pelton, Dr. Brennan and Dr. Filipe. This chapter has been published in *Biomacromolecules*, 2012, 13 (2), pp 559–564. Copyright © 2012 American Chemical Society

Effects of Temperature and Relative Humidity on the Stability of Paper-Immobilized Antibodies

Jingyun Wang,[†] Brian Yiu,[‡] Jaclyn Obermeyer,[†] Carlos D. M. Filipe,[†] John D. Brennan,[§] and Robert Pelton*,[†]

[†]Department of Chemical Engineering, McMaster University, 1280 Main Street West, Hamilton, Ontario, Canada L8S 4L7
[‡]Department of Chemical Engineering, University of Waterloo, 200 University Avenue West, Waterloo, Ontario, Canada N2L 3G1
[§]Department of Chemistry and Chemical Biology, McMaster University, 1280 Main Street West, Hamilton, Ontario, Canada L8S 4M1

Ⓢ *Supporting Information*

ABSTRACT: The stability of a paper-immobilized antibody was investigated over a range of temperatures (40−140 °C) and relative humidities (RH, 30−90%) using both unmodified filter paper and the same paper impregnated with polyamide-epichlorohydrin (PAE) as supports. Antibody stability decreased with increasing temperature, as expected, but also decreased with increasing RH. At 40 °C, the half-life was more than 10 days, with little dependence on RH. However, at 80 °C, the half-life varied from ∼3 days at low RH to less than half an hour at 90% RH, demonstrating that hydration of the antibody promotes unfolding. Antibody stability was not influenced by the PAE paper surface treatment. This work shows that antibodies are good candidates for development of bioactive paper as they have sufficient stability at high temperature to withstand printing and other roll-to-roll processing steps, and sufficient low temperature stability to allow long-term storage of bioactive paper materials.
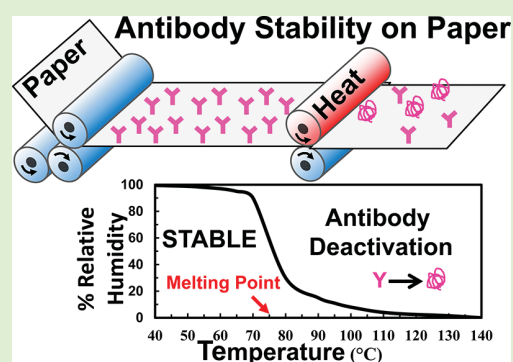
INTRODUCTION

In the past five years there has been a significant research effort focused to the development of inexpensive paper-based sensors that can detect a range of analytes rapidly in resource-limited settings.[1−7] As a biosensor support, paper offers many advantages including low cost, established printing and coating technologies for manufacture, and the potential integration of sensors in packaging. Unlike plastic films, paper can provide functional roles such as prefiltration, capillary driven lateral flow for multistep sequences or chromatographic separation, and the potential for paper-based microfluidic assays, which is currently a very active research area.

A critical biosensor component is the biorecognition agent, which specifically binds to or reacts with the target analyte. The recognition agents are usually of biological origin including enzymes,[1,4,7] antibodies,[8] DNA aptamers,[9] or bacteriophage,[10] which are bacteria-specific viruses. Of these, antibodies are the most versatile in terms of range of analytes and have been the most widely used for biosensor development, in particular for assays that utilize lateral flow devices. Antibodies (Immunoglobulins or Igs) are glycoprotein assemblies of two identical heavy chains and two identical light chains arranged in Y-shape configuration. There are five distinctive classes of antibodies (IgA, IgD, IgE, IgG, and IgM) in terms of different Ig units and functionalities. IgG is the most abundant immunoglobulin of all

the classes. IgG consists of two identical F_{ab} fragments on top of the Y-shape antibody, which contain IgG's antigen binding sites on the far ends, and one F_c fragment as the tail region.[11,12] Because most of the IgG structure is the same for all IgG antibodies, it is reasonable to propose that all IgG antibodies display similar stabilities.

One of the challenges related to incorporating biosensors into packaging and other consumer products is that the biorecognition agent must survive the manufacturing process and have a useful shelf life. Proteins are particularly sensitive, losing function with heating, dehydration, and shearing.[12−15] Denaturation is most often due to a loss of the tertiary or secondary structure (correct three-dimensional folding), though loss of function can also occur through protein aggregation, oxidation, methylation, or other modifications.[11,12,16,17] Antibodies tend to be more stable than many other types of proteins[12] as a result of their relatively rigid three-dimensional structures. For example, bovine IgG has been reported to show no loss in binding capacity after 30-min incubation at 63 °C, just below the unfolding temperature of the protein. However, up to 50% of the binding capacity was

lost after heating at 70 °C for 2 min and the protein was fully deactivated in 2 min at 80 °C, suggesting that, once unfolded, the antibody does not properly refold.[18,19]

At present there are no literature reports on protein deactivation during high speed printing, and, in particular, on the effects of high temperature drying associated with roll-to-roll printing operations. There is also little data available on the best conditions for storage of bioactive paper products, though there is some data on the long-term stability of lateral flow immunoassay strips that use nitrocellulose as a support.[20−22] The performance of paper-supported antibodies has previously been reported for different types of paper supports. In a preliminary publication, we compared cellulosic and synthetic filter papers as supports for antibody-based assays employing either a generic antibody, or an antibody that was genetically engineered to include cellulose binding domains to promote adhesion to cellulose.[23] The cellulosic filters were superior to synthetic filters as the supportive substrate for antibody assays to give high quality color indications.

Evengard et al. reported the temperature dependence of anti-HIV antibody activity when the antibody was dried on filter paper and used for detection of HIV antibodies in blood samples that were spotted onto the paper.[24] They found that the antibody could maintain its activity under heat treatment at 56 or 70 °C for 1 h, while the activity decreased significantly after 18 h at these temperatures. In a related study, Behets et al. evaluated the stability of paper-immobilized anti-HIV antibody for detection of HIV in blood when stored under different conditions.[25] They found that the samples generated positive signals over the first 6 weeks under all the conditions, followed by a gradual decline in detection ability when stored at elevated temperatures (up to 44 °C) and high humidity. However, they suggested that the use of gas-impermeable bags with desiccant for the storage of paper strips would help maintain antibody activity, especially in harsh tropical environments.

Perhaps the most relevant work is a series of papers from Boyd's group in which they reported the aging properties of antibody-coated polyester cloth.[26,27] They found that rabbit IgG and rabbit antihorseradish peroxidase antibody adsorbed onto polyester cloth could retain full immunoactivity at 32 °C for up to 70 days of storage.

There have also been a few reports on the stability of paper-supported enzymes by both Yan's[28] group in Toronto and the Garnier's group in Australia.[4,29] Yan's group studied the effect of hydrophobic and electrostatic interactions on enzyme adsorption and activity. Garnier's group studied thermal stability of enzymes on polymer-modified filter papers, followed by modeling the deactivation process. They concluded that paper-supported enzymes deactivated on two time scales, a short-term rapid decline and a longer term much slower decline. Enzyme deactivation rates were observed to increase with temperature. However, in this study, the role of relative humidity during storage was not evaluated.

Herein we report results of a detailed study on the influence of temperature and relative humidity on the deactivation rate of antibodies immobilized on paper, with the goal of understanding how printing processes and different storage conditions would affect antibody stability. Because Ig antibodies share similar structures and stabilities (see above), we chose commercially available antirabbit IgG as a model analyte. Our results were fit to an empirical equation and we demonstrate the use of this model to predict the extent of antibody deactivation when the antibody is printed and dried with a commercial printing operation, and when the antibody is stored at different temperatures and humidity levels.

■ EXPERIMENTAL SECTION

Materials. A-55 filter paper (Ahlstrom Corporation) was cut into 15 cm diameter disks. The acid-hardened filter paper is made with cotton fibers with a basis weight of 82 g/m^2, a caliper of 0.19 mm, and had an ash content <0.012%. Polyamide-epichlorohydrin (PAE) resin (Kymene 624) was provided by Hercules Inc. Anti-Rabbit IgG (AR-Ab) produced in goat was provided by Sigma-Aldrich. Skim milk powder was purchased from Becton Dickinson and Company. Tween 20 was provided by Fisher Scientific Inc. Rabbit IgG-HRP (horseradish peroxidase) was purchased from Santa Cruz Biotechnology, Inc. 3,3′,5,5′-Tetramethylbenzidine (TMB) Microwell Peroxidase Substrate System was purchased from Kirkegaard and Perry Laboratories, Inc. Sulfuric acid was obtained from Sigma-Aldrich. All buffers and protein solutions were prepared using Type 1 water (Barnstead Nanopure Diamond system).

Methods. *Paper Treatment.* Preconditioned (23 ± 0.5 °C and 50 ± 1% RH) Ahlstrom A-55 filter papers were submerged in a PAE solution (1 wt %) and soaked at room temperature for 30 min. Excess PAE was removed by blotting, and the paper samples were dried at room temperature, followed by heating on a speed dryer at 120 °C for 10 min to initiate a chemical reaction between PAE and paper fibers. The PAE content was determined by change in paper mass after drying. The PAE content of the treated papers was found to be ∼1.2 wt %. Paper samples were then used in the same manner as untreated filter paper for immunoassays and stability testing.

Antibody Unfolding Temperature. The unfolding temperature of the antibody was measured in buffered solution at pH 7.4. A solution of 0.12 mg/mL of AR-Ab was prepared and tryptophan (Trp) fluorescence was measured at an excitation wavelength of 295 nm and an emission wavelength of 344 nm using a Varian Cary Eclipse spectrometer with excitation and emission bandpasses of 10 nm. The temperature-dependent unfolding behavior of the antibody was monitored continuously as the temperature was increasing from 20 to 100 °C at a rate of 1 °C/min. The fluorescence data were not corrected for temperature dependent fluorescence quenching, and the unfolding temperature was estimated from the point where Trp fluorescence underwent the largest change in emission intensity.

Antibody Adsorption. Untreated papers or PAE-treated papers were hole-punched to create 6 mm diameter discs and placed onto a 96-well Bio-Dot microfiltration apparatus (Bio-Rad Laboratories Canada Ltd.). A total of 10 μL of AR-Ab solution (0.12 mg/mL) was applied to the paper sample in each well of the Bio-Dot apparatus, followed by a 30 min incubation at room temperature. Unoccupied wells were covered by Parafilm to facilitate vacuum filtration. A vacuum was applied subsequently to filter the excess solution, followed by washing the paper discs with 500 μL of PBST (10 mM PBS containing 0.5 vol% Tween 20, pH 7.4) 10 times and rinsing with 500 μL of PBS 3 times. After the final rinse, the paper dots were dried in a stream of air.

Temperature and Humidity Treatment of Paper Immobilized with Antibody. Two types of aging studies were done to assess the stability of antibody-treated paper samples: controlled temperature or controlled temperature and humidity aging. For controlled temperature aging, the paper samples were aged in a speed dryer (SD36D, Labtech Instruments Inc.) from 40 to 140 °C for 5 min to 24 h incubation, whereas the humidity + temperature control experiments were conducted with a constant temperature and humidity chamber (Platinous Sterling Series, ESL-2CA, ESPEC North America) at 30, 50, 70, and 90% RH at 40, 60, or 80 °C from 5 min to 24 h incubation.

Antibody Binding Activity Measurement. After thermal treatment, paper discs were inserted into the Bio-Dot instrument, followed by addition of 500 μL of 5% skim milk protein solution to the paper disk in each well at room temperature for 30 min. The skim milk solution was removed by applying a vacuum to the samples, which were then washed again with 500 μL of PBST ten times and rinsed with 500 μL

of PBS three times. A total of 10 μL of rabbit IgG-HRP solution (1:3000 dilution) was applied to the paper discs and incubated for 30 min at room temperature to allow the rabbit IgG-HRP to bind to active AR antibodies on the filter paper. The samples were then washed again with 500 μL of PBST 10 times, rinsed with 500 μL of PBS 3 times, and dried by applying a vacuum. After the antibody–antigen binding was complete, the paper discs were removed from the Bio-Dot apparatus and placed in a 96-well microtiter plate. A total of 150 μL of TMB substrate was added to each well to react with the bound rabbit IgG-HRP, followed by color development. The samples were incubated in the dark for 15−20 min and the solution in each well was mixed gently by pipetting every 5 min. The reaction between HRP and TMB substrate was terminated by adding 150 μL of 10% H_2SO_4 to each sample. The reacted solutions were then transferred into a new microtiter plate. Finally, the plate was placed in a microplate reader (Bio-Rad Laboratories Canada Ltd., Model 680 XR Microplate Reader) and absorbance was measured at 450 nm. Control experiments, in which no antibody was applied, were also conducted in a similar fashion to investigate if the passive binding of rabbit IgG-HRP on blocked paper would give a false signal. Antibody activities were expressed as relative activities by dividing each point by the initial absorbance value at time zero.

Antibody Adsorption Quantification. Adsorption of AR-Ab to the paper sample was quantified using a AKTA Prime Liquid Chromatography System (GE Healthcare Biosciences) fitted with a custom-designed module to hold the paper samples. Details of the apparatus have been described elsewhere.[30]

Each paper sample was cut into 8 mm diameter discs and a stack of three paper disks was housed within the module. The module was connected to the AKTA System downstream of the pump but before the UV measuring cell. All experiments were carried out at room temperature at a flow rate of 1 mL/min. The chromatography system was first equilibrated with PBS until UV readings at 280 nm and pressure in the system were constant. The experiment was started by injecting AR-Ab into the AKTA system using a 100 μL loop, after which the PBS buffer was continuously fed into the module to wash away any unbound antibody. The experiment was complete when the UV absorbance returned to the baseline. These AR-Ab samples were obtained by diluting the original antibody stocks (0.12 mg/mL) with PBS 1:4 v/v. UV absorbance at 280 nm, pH, and conductivity were continuously measured and logged into a computer using Prime View software (GE Healthcare Biosciences).

The correlation between absorbance and antibody amount was determined by injecting a known amount of antibody (100 μL of a 0.03 mg/mL solution) into the module without paper disks. Numerical integration of the area under the curve of the UV intensity (280 nm) as a function of time was done using Prime View for experiments where paper samples were not present in the module (no binding) and where paper samples were used in the module. The percentage of AR-Ab added that was able to bind to the paper disks was computed by calculating the difference in the areas under the UV-time curves for the control experiments (no paper disks) and the experiments where paper disks were used in the module.

■ RESULTS AND DISCUSSION

Two types of paper surfaces were investigated as antibody supports in this study, untreated cellulosic filter paper and the same paper impregnated with cationic PAE wet strength resin, a polymer commonly used in the papermaking industry to increase the mechanical strength of wet paper. The chemical structure of PAE and its reaction products are shown in Figure 1. PAE treatment gives a cross-linked cationic network polymer on the fiber surfaces, which is designed to facilitate cellulose fiber–fiber adhesion in the presence of water. We anticipated that PAE treatment would have two potential impacts on our results. First, the cationic surface is expected to promote antibody (antibody pI = 7.0) adsorption as the protein is slightly anionic in pH 7.4 buffer.[31] Second, by filling in pores in
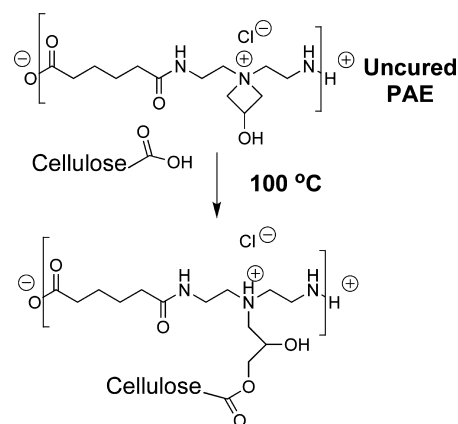

Figure 1. Interaction of PAE wet strength resin with paper.

the paper structure, PAE impregnation will lower the available surface area for antibody adsorption.

Adsorption experiments were performed to determine the capacity of the filter paper to adsorb antibodies. Approximately half of the added AR-Ab (54 ± 6%) was adsorbed by the untreated paper, whereas the PAE-treated paper gave slightly higher antibody binding (59 ± 5%), though the differences were statistically insignificant. This level of adsorption corresponded to a total mass of 1.62 mg of antibody that remained on the filter paper. Based on the adsorption data, known paper properties (thickness 155 μm, basis weight 82 g/m^2) and an assumed specific surface area of 9.5 m^2/g,[2] we estimate that the antibody density on our filter paper surfaces is ∼14 mg/m^2. Because a monolayer of most proteins falls between 0.1 and 1 mg/m^2, our surfaces clearly have a multilayer coating of deposited antibodies. This behavior suggests that significant nonspecific binding occurs on both treated and untreated paper, which may be the result of a relatively high concentration of the antibody solution that was used in the adsorption studies.

The equilibrium water content of the paper was measured gravimetrically as a function of temperature and relative humidity, and the results are shown in Tables 1 and 2 in the Supporting Information. PAE treatment had little influence on the equilibrium water content of paper, suggesting that this coating was not acting as a hygroscopic layer.

AR-Ab was adsorbed onto paper surfaces under ambient temperature and humidity conditions, and these protein-coated paper samples were then aged at constant temperature (see Figure 2) without control of relative humidity; such a method is similar to that used in the majority of studies describing the effect of temperature on antibody activity. After aging, the residual antibody activity was measured by first blocking with milk protein and then incubating with normal-rabbit IgG-HRP. The concentration of HRP immobilized on the paper was determined by the addition of TMB substrate, and the corresponding antibody binding activity was quantified by measuring the color intensity.

Figure 2 shows the influence of temperature and aging time on the antibody relative activity in both untreated and PAE-treated papers. At these high temperatures we were unable to control relative humidity. The main observations are (1) antibodies are stable at 80 °C and lower temperatures; (2) although antibodies are completely deactivated at 140 °C, the process is slow, taking more than 100 min; (3) antibody
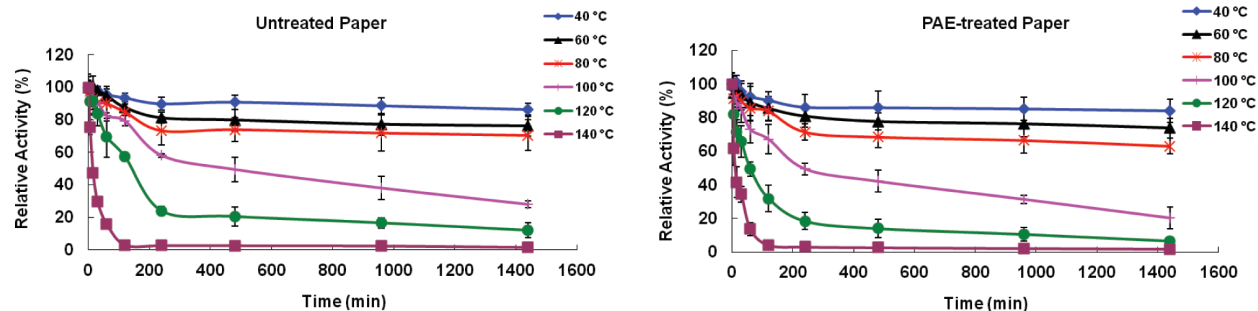
Figure 2. Influence of temperature and aging time on the activity of paper-immobilized antibodies. The error bars give the standard deviations of triplicates.
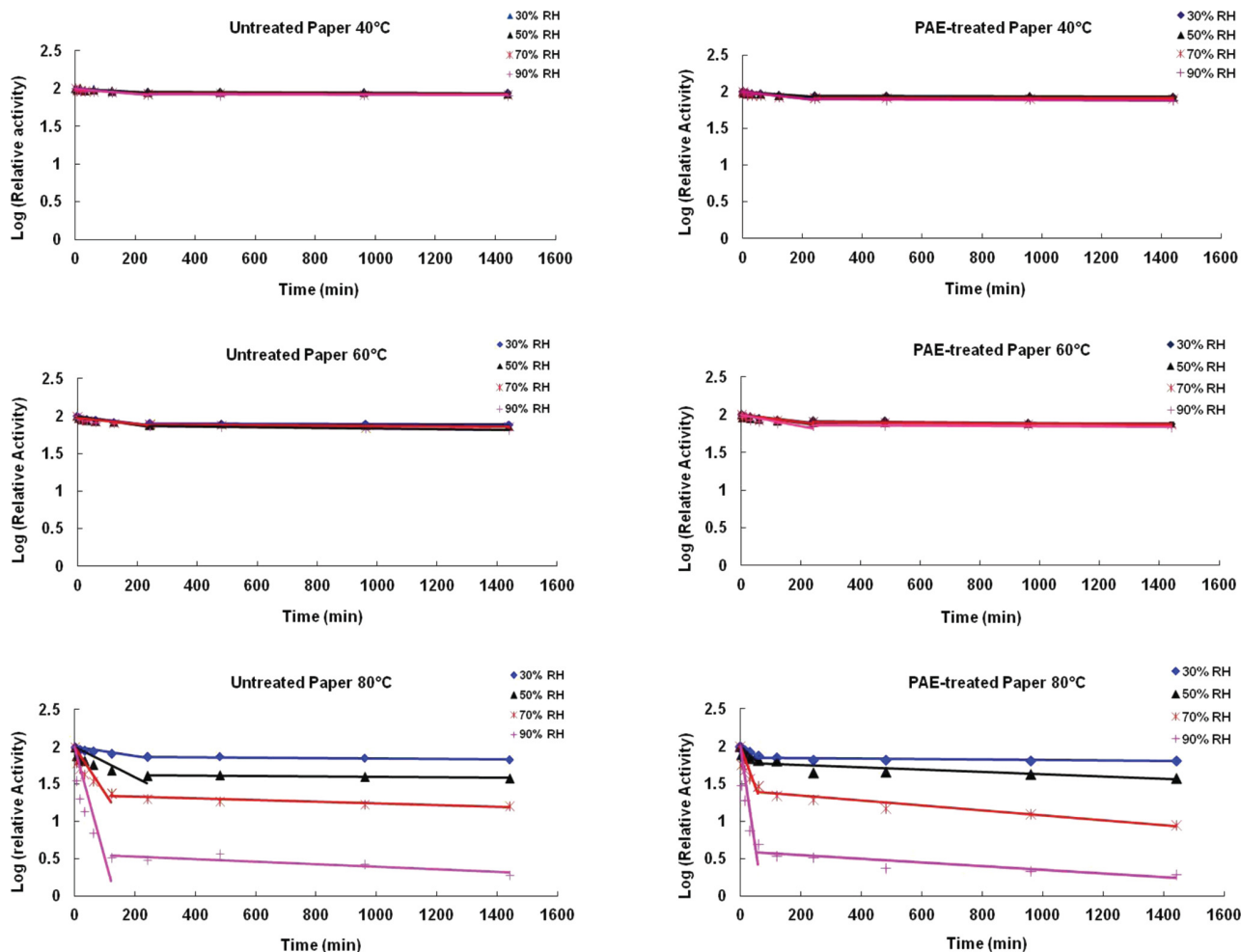

Figure 3. Logarithmic plot of the relative activity of paper-immobilized antibodies under different relative humidities at respective temperatures.

deactivation was initially rapid but slowed down at longer times, and (4) there was no significant difference between untreated and PAE-treated filter paper. These results were consistent with the work of Evengard et al. in which they claimed that the activity of the HIV antibody in filter-paper extracts was not significantly affected by 1 h of heat treatment at 56 and 70 °C, while prolonged treatment at both temperatures for 18 h could reduce the activity significantly, though the loss in activity was not quantified.[24]

The influence of relative humidity on antibody-immobilized paper was evaluated at 30, 50, 70, and 90% RH at 40, 60, or 80

°C from 5 min to 24 h incubation. The results are summarized in Figure 3 as plots of the logarithm of the antibody activity as a function of time under different conditions. The semilog plots suggest that there are two kinetic processes, a rapid deactivation up to about 150 min, and a slow process at longer times under all conditions. Two-step deactivation behavior has been reported by Khan for the stability of paper-supported antibodies.[4,29]

At low temperature (40 and 60 °C), the rate and extent of antibody deactivation were low and not sensitive to RH. By contrast, antibody stability showed extreme RH dependency at

27

80 °C. The antibody unfolding temperature (T_{un}) in solution, measured by monitoring tryptophan intensity (see Figure 1 in the Supporting Information), was ~75 °C corresponding to the onset of RH sensitivity. Perhaps the role of high RH is to increase the quantity of water available to solvate the antibody and promote deactivation through unfolding. Similar findings on the role of water on protein stability have been reported by several groups,[32−36] where water content was modulated by the addition of osmolytes and resulted in higher protein stability as water activity was lowered.

The time dependence of the antibody deactivation was further investigated by modeling the antibody deactivation $[\lambda(t)]$ in a unimolecular reaction[37] to allow extraction of rate constants for deactivation. The corresponding rate expression follows, where [Ab] is the concentration of active antibody at any time:

$$\frac{d[Ab]}{dt} = - \sum_i k_{d,i}[Ab] \tag{1}$$

For each experiment, two rate constants were extracted, one corresponding to the initial fast process, k_{d1}, and one for the final slow process, k_{d2}; the rate constants are tabulated in the Supporting Information. The half-life values for antibodies immobilized on paper were calculated from the two deactivation rate constants according to the two equations[4] (see Supporting Information) and are summarized in Table 3 in Supporting Information. The half-lives ranged from more than 10 days at low temperature (independent of RH) to less than 30 min at high temperature and RH (80 °C and 90% RH). Note the low temperature half-lives were extrapolated values that far exceeded the times of experimental results.

One goal of our work was to develop a computational tool so that antibody deactivation during various printing or coating operations could be estimated. The rate constant data in Supporting Information, Table 3 for the initial deactivation process was fitted to the following empirical equation using Mathcad 14.

$$k_{d1} = \alpha \cdot \exp\left[\frac{-E_a}{RT}\right]\left[\frac{T}{K} \cdot w\right]^{\beta} \tag{2}$$

where k_{d1} is the faster antibody deactivation rate constant, E_a is the deactivation energy for untreated or PAE-treated papers, R is the gas constant (8.314 J/mol·K), T is the temperature (K), and w is the water content on the paper (wt %). The fitted parameters were the activation energy, E_a = 54.88 kJ/mol, α = 1012 s^{-1}, and β = 1.379 for untreated paper. Figure 4 compares the experimental results with the predictions of eq 2, showing that this equation overestimates the rate of antibody deactivation for most of the data; as such, it provides a conservative estimate of the effects of printing on antibody activity. We have applied this model to simulate the extent of deactivation during a drying step typical of what might occur during flexographic printing. Antibody deactivation was calculated by the following function where the $k_d(T,w)$ was given by eq 2.

$$\lambda(t) = \frac{[Ab]_t}{[Ab]_0} = \exp\left[- \int_0^t k_d(T, w) dt\right] \tag{3}$$

Equation 3 was solved numerically in MathCad. We assumed that temperature change and weight loss during drying were linear, giving the profiles shown in the top half of Figure 5.
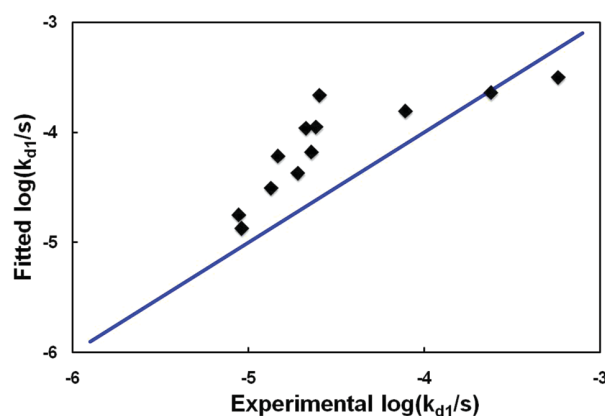

Figure 4. Comparison of the empirical fit, eq 2, with the experimental antibody deactivation rate constants.
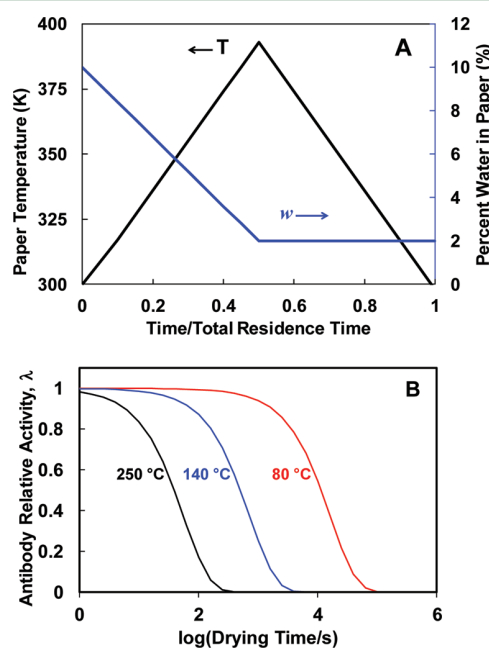

Figure 5. Simulating antibody deactivation during a commercial drying operation. (A) The assumed temperature and paper water content as functions of drying time; (B) the corresponding antibody activity, λ, as a function of drying time.

The bottom graph in Figure 5 shows the relative antibody activity, λ, as a function of residence time in the drier. Typical flexographic printer speeds are in the range of 120 to 150 m/min, giving residence times between milliseconds and seconds. For even the most extreme case of 250 °C heating, the results in Figure 5 suggest very little antibody deactivation on the 10 s time scale. In summary, our results suggest that antibody application on paper by conventional printing methods is feasible.

■ CONCLUSIONS

The stability of paper-supported antirabbit IgG depends on temperature and relative humidity. Between 40 and 60 °C (below T_{un}) there is a slow decline up to ~20% loss in activity, which is not dependent on RH, while at 80 °C (above T_{un}), slow deactivation occurs up to 50% relative humidity, with much faster deactivation occurring at higher RH. Temperatures

of 100−140 °C caused complete deactivation, owing to irreversible unfolding of the antibody. However, even at 140 °C, complete deactivation took 100 min and the half-life was about 23 min. Therefore, we conclude that antibodies can be applied by roll-to-roll printing or coating processes because the residence times in these processes are much shorter than the half-life of the antibody.

Paper treatment with PAE wet strength resin had no significant influence on antibody stability in our experiments, possibly because the antibodies were present in thick layers on the paper surfaces and were thus not interacting directly with the polymer coating. Further studies are needed to evaluate what effects, if any, the PAE resin would have when using lower antibody coverage.

The results of this study have been encapsulated in an empirical equation giving the deactivation rate constants as a function of temperature and water content, providing a tool to estimate the influence of printing and coating operations on antibody activity.

■ ASSOCIATED CONTENT

Ⓢ Supporting Information

AR-Ab thermal unfolding curve, moisture contents of untreated paper and PAE-treated paper, deactivation rate constants for the initial fast process, k_{d1}, and the final slow process, k_{d2}. Also given are the equations for calculating the half-life values. This material is available free of charge via the Internet at http://pubs.acs.org.

■ AUTHOR INFORMATION

Corresponding Author
*Tel.: +1-905-525-9140, ext. 27045. Fax: +1-905-528-5114. E-mail: peltonrh@mcmaster.ca.

Notes
The authors declare no competing financial interest.

■ ACKNOWLEDGMENTS

■ REFERENCES

(1) Hossain, S. M. Z.; Luckham, R. E.; Smith, A. M.; Lebert, J. M.; Davies, L. M.; Pelton, R. H.; Filipe, C. D. M.; Brennan, J. D. *Anal. Chem.* **2009**, *81*, 5474−5483.

(2) Pelton, R. *Trends Anal. Chem.* **2009**, *28*, 925−942.

(3) Martinez, A. W.; Phillips, S. T.; Butte, M. J.; Whitesides, G. M. *Angew. Chem., Int. Ed.* **2007**, *46*, 1318−1320.

(4) Khan, M. S.; Haniffa, S. B. M.; Slater, A.; Garnier, G. *Colloids Surf., B* **2010**, *79*, 88−96.

(5) Kinnunen, L. *Pap. Puu* **2006**, *88*, 84−86.

(6) Abe, K.; Suzuki, K.; Citterio, D. *Anal. Chem.* **2008**, *80*, 6928−6934.

(7) Hossain, S. M. Z.; Luckham, R. E.; McFadden, M. J.; Brennan, J. D. *Anal. Chem.* **2009**, *81*, 9055−9064.

(8) Su, S.; Ali, M. M.; Filipe, C. D. M.; Li, Y.; Pelton, R. *Biomacromolecules* **2008**, *9*, 935−941.

(9) Zhao, W.; Ali, M. M.; Aguirre, S. D.; Brook, M. A.; Li, Y. *Anal. Chem.* **2008**, *80*, 8431−8437.

(10) Tolba, M.; Minikh, O.; Brovko, L. Y.; Evoy, S.; Griffiths, M. W. *Appl. Environ. Microbiol.* **2010**, *76*, 528−535.

(11) Vermeer, A. W. P.; Norde, W. *Biophys. J.* **2000**, *78*, 394−404.

(12) Wang, W.; Singh, S.; Zeng, D. L.; King, K.; Nema, S. *J. Pharm. Sci.* **2007**, *96*, 1−26.

(13) Di Risio, S.; Yan, N. *Macromol. Rapid Commun.* **2007**, *28*, 1934−1940.

(14) Daniel, R. M.; Dines, M.; Petach, H. H. *Biochem. J.* **1996**, *317*, 1−11.

(15) Oobatake, M.; Ooi, T. *Prog. Biophys. Mol. Biol.* **1993**, *59*, 237−284.

(16) Davies, K. J. *J. Biol. Chem.* **1987**, *262*, 9895−9901.

(17) Egorova, K.; Olenkina, O.; Olenina, L. *Biochemistry (Moscow)* **2010**, *75*, 535−548.

(18) Li, S. Q.; Zhang, Q. H.; Lee, Y. Z.; Pham, T. V. *J. Food Sci.* **2003**, *68*, 1201−1207.

(19) Li-Chan, E.; Kummer, A.; Losso, J. N.; Kitts, D. D.; Nakai, S. *Food Res. Int.* **1995**, *28*, 9−16.

(20) Zhou, Y.; Li, Y.; Lu, S.; Ren, H.; Li, Z.; Zhang, Y.; Pan, F.; Liu, W.; Zhang, J.; Liu, Z. *Sens. Actuators, B* **2010**, *146*, 368−372.

(21) Blažková, M.; Rauch, P.; Fukal, L. *Biosens. Bioelectron.* **2010**, *25*, 2122−2128.

(22) Fung, K.-K.; Chan, C. P.-Y.; Renneberg, R. *Anal. Chim. Acta* **2009**, *634*, 89−95.

(23) Wang, J.; Pelton, R. H.; Veldhuis, L. J.; MacKenzie, R. C.; Hall, C. J.; Filipe, C. D. *Appita J.* **2010**, *63*, 32−36.

(24) Evengard, B.; Ehrnst, A.; von Sydow, M.; Pehrson, P. O.; Lundbergh, P.; Linder, E. *AIDS* **1989**, *3*, 591−596.

(25) Behets, F.; Kashamuka, M.; Pappaioanou, M.; Green, T. A.; Ryder, R. W.; Batter, V.; George, J. R.; Hannon, W. H.; Quinn, T. C. *J. Clin. Microbiol.* **1992**, *30*, 1179−1182.

(26) Boyd, S.; Yamazaki, H. *Biotechnol. Tech.* **1996**, *10*, 367−370.

(27) Boyd, S.; Yamazaki, H. *Immunol. Invest.* **1995**, *24*, 795−803.

(28) Di Risio, S.; Yan, N. *J. Colloid Interface Sci.* **2009**, *338*, 410−419.

(29) Khan, M. S.; Li, X.; Shen, W.; Garnier, G. *Colloids Surf., B* **2010**, *75*, 239−246.

(30) Ghosh, R. *J. Chromatogr., B* **2006**, *844*, 163−167.

(31) Hou, Y.; Tlili, C.; Jaffrezic-Renault, N.; Zhang, A.; Martelet, C.; Ponsonnet, L.; Errachid, A.; samitier, J.; Bausells, J. *Biosens. Bioelectron.* **2004**, *20*, 1126−1133.

(32) Guo, F.; Friedman, J. M. *J. Phys. Chem. B* **2009**, *113*, 16632−16642.

(33) Roche, C. J.; Guo, F.; Friedman, J. M. *J. Biol. Chem.* **2006**, *281*, 38757−38768.

(34) Rösgen, J.; Pettitt, B. M.; Bolen, D. W. *Biophys. J.* **2005**, *89*, 2988−2997.

(35) Eggers, D. K.; Valentine, J. S. *J. Mol. Biol.* **2001**, *314*, 911−922.

(36) Brennan, J. D.; Benjamin, D.; DiBattista, E.; Gulcev, M. D. *Chem. Mater.* **2003**, *15*, 737−745.

(37) Fukumoto, L. R.; Skura, B. J.; Nakai, S. *J. Food Sci.* **1994**, *59*, 757−759.

Appendix: Supporting Information for Chapter 2
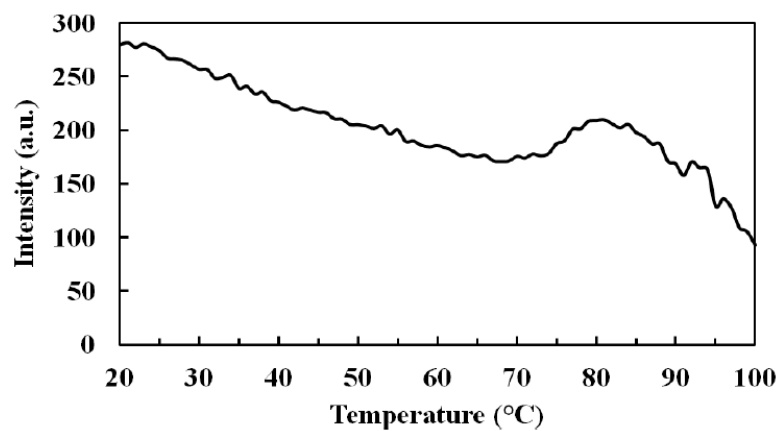
Supplementary Figure 1: AR-Ab thermal unfolding curve by monitoring tryptophan intensity change of AR-Ab solution.

Supplementary Table 1. The moisture content of untreated paper as function of relative humidity and temperature.

Temperature	Relative Humidity (%)			
	30	50	70	90
40 °C	2.70±0.56%	3.31±0.20%	4.97±0.22%	8.08±0.73%
60 °C	2.34±0.26%	3.22±0.32%	4.63±0.40%	7.64±0.99%
80 °C	1.97±0.1%	2.51±0.13%	3.13±0.11%	4.19±1.07%

Supplementary Table 2. The influence of temperature and relative humidity on the moisture content of PAE-treated papers.

Temperature	Relative Humidity (%)			
	30	50	70	90
40 °C	3.06±0.25%	3.97±0.06%	5.44±0.20%	8.44±1.25%
60 °C	2.69±0.07%	3.55±0.42%	4.89±0.12%	7.82±0.68%
80 °C	1.82±0.06%	2.55±0.20%	3.47±0.26%	4.63±1.25%

Supplementary Table 3. Deactivation rate constants for the initial fast process, k_{d1}, and one for the final slow process, k_{d2} on the untreated paper.

Temperature (°C)	Relative Humidity (%)	k_{d1} (min^{-1}×10^{-4})	k_{d2}(min^{-1}×10^{-5})	Half-life (min× 10^2)
40	30	5.48	2.80	211
40	50	5.27	3.70	161
40	70	8.06	2.80	198
40	90	8.82	2.10	247
60	30	11.5	2.30	205
60	50	13.7	3.50	128
60	70	12.7	6.90	66.0
60	90	15.2	9.90	41.3
80	30	14.6	7.60	53.6
80	50	46.8	6.00	1.48
80	70	143	25.8	0.48
80	90	346	39.8	0.2

Supplementary Equations: Calculations of the half-life values.

When half-life time is within range of the initial fast process: $t_{1/2} = \dfrac{0.693}{k_{d1}}$

When half-life time is within range of the initial fast process: $t_{1/2} = t_{fast} + \dfrac{\ln([Ab]_{t=t_{fast}} / [Ab]_{t=t_{1/2}})}{k_{d2}}$

(t_{fast} is the duration of the initial fast process of antibody deactivation)

The goal of this calculation is to fit experimental deactivation rate constant data

Experimental parameters: T is temperature, w is the mass fraction of water in paper, kdexp is the deactivation rate constant

$$\underset{\sim}{T} := \begin{pmatrix} 313.15 \\ 313.15 \\ 313.15 \\ 313.15 \\ 333.15 \\ 333.15 \\ 333.15 \\ 333.15 \\ 353.15 \\ 353.15 \\ 353.15 \\ 353.15 \end{pmatrix} K \qquad w := \begin{pmatrix} 8.08 \\ 4.97 \\ 3.31 \\ 2.7 \\ 7.64 \\ 4.63 \\ 3.22 \\ 2.34 \\ 4.19 \\ 3.31 \\ 2.51 \\ 1.97 \end{pmatrix} \cdot\% \qquad k_{dexp} := \begin{pmatrix} 0.00088189 \\ 0.000805905 \\ 0.000527292 \\ 0.000548015 \\ 0.001519706 \\ 0.00127333 \\ 0.001370038 \\ 0.001146687 \\ 0.034566407 \\ 0.0143405 \\ 0.004683458 \\ 0.001455234 \end{pmatrix} min^{-1} \qquad RH := \begin{pmatrix} 90 \\ 70 \\ 50 \\ 30 \\ 90 \\ 70 \\ 50 \\ 30 \\ 90 \\ 70 \\ 50 \\ 30 \end{pmatrix} \%$$

The model - entirely emperical

$$\underset{\sim}{R} := 8.314 \frac{J}{mol \cdot K}$$

Assume we know T, w - need to get best fits for α, β, and Ea

$$k_{dmod}(\alpha, Ea, T, w, \beta) := \alpha \cdot exp\left(\frac{-Ea}{R \cdot T}\right) \cdot \left(w \cdot \frac{T}{K}\right)^{\beta}$$

Initial guesses $\alpha := 200 min^{-1}$ $\beta := -1$ $Ea := 60063.48 \frac{J}{mol}$

$i := 0 .. 11$ array indices

$$SSE(\alpha, \beta, Ea) := \sum_{i} \left(k_{dexp_i} - k_{dmod}(\alpha, Ea, T_i, w_i, \beta)\right)^2 \qquad \text{sum of squares error}$$

$$SSE(\alpha, \beta, Ea) = 3.982 \times 10^{-7} \frac{1}{s^2}$$

Optimizing parameters

   Given

   $SSE(\alpha, \beta, Ea) = 0$

$$\begin{pmatrix} \alpha\alpha \\ \beta\beta \\ Eaa \end{pmatrix} := Find(\alpha, \beta, Ea)$$

$\dfrac{\alpha\alpha}{\alpha} = 303.457$ $\dfrac{\beta\beta}{\beta} = -1.379$ $\dfrac{Eaa}{Ea} = 0.914$

$SSE(\alpha\alpha, \beta\beta, Eaa) = 1.31 \times 10^{-7} \dfrac{1}{s^2}$

$\alpha\alpha = 1.012 \times 10^3 \dfrac{1}{s}$ $\beta\beta = 1.379$ $Eaa = 5.488 \times 10^4 \cdot \dfrac{joule}{mole}$

Comparing model to data

$Model_i := k_{dmod}(\alpha\alpha, Eaa, T_i, w_i, \beta\beta)$ $Ea = 6.006 \times 10^4 \dfrac{1}{mol} \cdot J$

$k_{dexp} =$

	0
0	1.47·10⁻⁵
1	1.343·10⁻⁵
2	8.788·10⁻⁶
3	9.134·10⁻⁶
4	2.533·10⁻⁵
5	2.122·10⁻⁵
6	2.283·10⁻⁵
7	1.911·10⁻⁵
8	5.761·10⁻⁴
9	2.39·10⁻⁴
10	7.806·10⁻⁵
11	2.425·10⁻⁵

$\dfrac{1}{s}$

$Model =$

	0
0	6.106·10⁻⁵
1	3.123·10⁻⁵
2	1.783·10⁻⁵
3	1.346·10⁻⁵
4	2.182·10⁻⁴
5	1.094·10⁻⁴
6	6.627·10⁻⁵
7	4.266·10⁻⁵
8	3.172·10⁻⁴
9	2.291·10⁻⁴
10	1.564·10⁻⁴
11	1.12·10⁻⁴

$\dfrac{1}{s}$
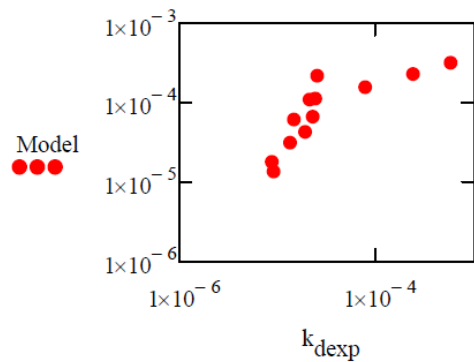
$$\alpha\alpha = 1.012 \times 10^3 \frac{1}{s}$$

$$\beta\beta = 1.379$$

$$Eaa = 5.488 \times 10^4 \frac{1}{mol} \cdot joule$$

Chapter 3 Influence of A Paper Sizing Agent on Paper-immobilized Biosensing Antibodies

In chapter 3, all experiments were conducted by myself. The chapter was first drafted by myself. The final version of the paper was edited by Dr. Pelton, Dr. Brennan and Dr. Filipe.

Influence of A Paper Sizing Agent on Paper-immobilized Biosensing Antibodies

Jingyun Wang,[1] Carlos D. M. Filipe,[1] John D. Brennan,[2] and Robert Pelton[1,*]

[1] Department of Chemical Engineering, McMaster University, 1280 Main Street West, Hamilton, ON, Canada L8S 4L7

[2] Biointerfaces Institute and Department of Chemistry & Chemical Biology, McMaster University, 1280 Main Street West, Hamilton, ON, L8S 4L8

*Author to whom correspondence should be addressed

Fax: +1-905-528-5114.

Tel: +1-905-525-9140 ext. 27045.

E-mail: peltonrh@mcmaster.ca

Abstract

The effects of AKD, a paper-sizing agent, on antibody adsorption and inactivation were evaluated. The results showed that paper treated with reasonable content of AKD solution (below 0.092%) actually helped antibody uptake by paper, possibly due to hydrophobic interactions. Further increases in the AKD content, however, suppressed antibody adsorption through the reduction of paper porosity. These results show that antibody-based assays can function on sized paper supports typical of packaging materials.

Key Words

Bioactive paper, Paper Sizing, Antibody stability, ELISA

3.1 Introduction

In the last few years there has been an exponential growth in scientific publications describing paper-based tests for small molecules, protein-based biomarkers and bacterial pathogens [1-8]. In most cases, the biosensors are supported on pure cellulose filter paper (usually Whatman 1). Furthermore, most of the existing literature focuses on small test kits for point-of-care diagnostics. However, we believe that biosensors have potential applications in packaging, such as detecting pathogenic contamination of food or beverages. Surface contamination sensors could be as inexpensive and as pervasive as bar codes, appearing on virtually all packages.

The heart of every biosensor is a recognition agent to which the target of the assay binds. In a second reporting step, the target binding is followed by the generation of a color or some other signal the human user can detect [4, 9]. Antibodies are the most common recognition agents. These are proteins, generated by the immune system, that specifically bind to a target [4, 10-12]. In a typical biosensor scheme, antibodies are attached to the paper surface, and when the paper is exposed to the test solution, specific targets bind to the antibodies, immobilizing the targets on the surface. Subsequent chemical treatments generate a color indicating the presence of the bound target [11, 13-16].

There are two major issues in converting a typical test strip assay to something useful on a package surface. The first is that most assays on filter papers employ lateral flow strategies, much like pregnancy tests. With lateral flow, the test fluid can undergo sequential chemical reactions as fluid moves along the filter paper by capillary driven flow. However, for biosensors printed on packaging, conventional lateral flow sequences cannot be implemented.   The packaging supported sensors must function as a result of simple contact with water, much like pH paper. The second is that antibodies and/or enzymes can be fragile – they are usually stored in sealed packages in freezers or refrigerators, and can denature rapidly if left at room temperature for extended periods of time. Thus the activity and stability of antibodies and proteins on packaging paper surfaces is an important issue.

From a paper science perspective, Whatman 1 and similar filter papers are outliers. Filter paper is hydrophilic, very porous, with low chemical reactivity [4]. By contrast, non-coated packaging paper is usually treated with sizing chemicals to inhibit water penetration, and possibly with wet-strength resin to withstand strength loss in humid environments [17-20]. Coated paper and paperboard are at the other extreme, with smooth, more hydrophobic surfaces, and low porosity. The work summarized herein addresses the influence of paper surface chemistry on antibody adsorption and stability.

In the first phase of this work we reported the influence of wet strength resins on the activity of antibodies printed on paper surfaces [21-22]. Since wet strength resins generate fiber surfaces that are much more reactive than cellulose, we anticipated that a high percentage of the added antibodies would be denatured on such surfaces. This was not the case. If anything, wet strength resin improved the antibody-based biosensors. Herein

we report the influence of AKD paper sizing on the activity of antibodies printed onto paper surfaces.

3.2 Experimental

Materials
Filter paper (A-55 Grade) was provided by Ahlstrom Corporation. Alkylketene Dimer (AKD, Hydrores 366MB) was received from Kemira Chemicals Canada Inc. Skim milk powder was purchased from BD (Becton, Dickinson and Company). Tween 20 was provided by Fisher Scientific Inc. TMB, (3,3',5,5'- tetramethylbenzidine) microwell peroxidase substrate system was purchased from KPL (Kirkegaard & Perry Laboratories, Inc.). Anti-Rabbit IgG (produced in goat), anti-Mouse IgG (produced in goat) and sulfuric acid were supplied by Sigma-Aldrich. Rabbit IgG-HRP (horseradish peroxidase) was obtained from Santa Cruz Biotechnology. All buffers and protein solutions were prepared by using Type 1 water (Barnstead Nanopure Diamond system).

Paper Impregnation with Sizing Agent
Prior to sizing treatment, the papers were conditioned at 23 ± 0.5 °C and $50 \pm 1.0\%$ relative humidity (RH) in a constant temperature and humidity (CTH) room, followed by measuring the original weight. Papers were submerged in AKD solution of various concentrations (0.001 wt%, 0.005 wt%, 0.01 wt%, 0.05 wt%, 0.1 wt%, 0.5 wt%, 1 wt%, 5 wt%, 10 wt%, 15 wt%) at room temperature. After half an hour, the weights of the wet papers were measured and the papers were cured on a speed dryer (SD36D, Labtech Instruments Inc.) at 105°C for 10 minutes followed by mass gain measurement. Finally, the treated papers were conditioned at the same temperature and relative humidity as described earlier before testing.

Scanning Electron Microscopy
The filter paper and AKD-treated paper were also examined using a Scanning Electron Microscope (SEM, JSM-7000F) to observe the change in morphology after paper treatment with different concentrations of paper sizing agent. Paper samples were cut into small pieces (0.5 x 0.5 mm) and coated with 4 nm of platinum before imaging.

Antibody Activity Measurement
Untreated and AKD-treated A-55 filter papers were punched into 6 mm diameter discs and placed onto a Bio-Dot apparatus (Bio-Rad). 10 µl of anti-rabbit IgG (0.12 mg/ml) was applied to the paper in each well and incubated at room temperature for 30 min, followed by applying the vacuum to remove excess solution, and washing 10 times with PBST (10 mM phosphate buffered saline containing 0.5% Tween 20, pH 7.5). 500 µl of a 5% skim milk solution was subsequently added into each well to prevent non-specific binding. After 30 minutes of incubation, the paper samples were washed again with PBST. 10 µl of Rabbit IgG-HRP solution (1:3000 dilution) was then added to each well for 30 minutes incubation, after which samples were washed 10 times with PBST buffer, and rinsed with PBS. The paper disks were finally removed from the Bio-Dot apparatus and transferred into a 96-well microtitre plate. 150 µl of TMB substrate solution was added

onto each paper sample in the well for color development in the dark and the solution was mixed gently every 5 min. After 20 minutes of incubation, the reaction, catalyzed by HRP, was stopped with 150 µl of 10% H_2SO_4, followed by transferring the solution into a new 96-well microtitre plate and reading the absorbance at 450 nm on a spectrometer (Bio-Rad Laboratories Canada Ltd., Model 680 XR Microplate Reader). For the negative and non-specific control, buffer solution and anti-mouse IgG solution were added, respectively, instead of anti-rabbit IgG solution in the study.

Antibody Adsorption Onto Filter Paper
A membrane chromatography system (AKTA Prime Liquid Chromatography System, GE Healthcare Biosciences) was used to quantify the adsorption of anti-Rabbit IgG onto paper samples. A stack of three 8 mm diameter paper samples was prepared and placed in a custom-designed membrane module, connected in between the pump and UV detector of the chromatography system. The UV detector was used to continuously record the absorbance of the effluent, leaving the membrane module at a wavelength of 280 nm. The adsorption experiment was conducted at room temperature using PBS buffer (10 mM, pH 7.5) at a constant flow rate of 1 ml/min. The system was initially equilibrated with PBS buffer until the UV absorbance and the pressure in the system were stable. Anti-rabbit IgG solution, diluted to 0.064 mg/ml concentration with PBS buffer, was injected into the system using a100 µl sample loop, followed by continuous feeding of PBS buffer to wash out any loosely bound antibodies. The experiment ended when the UV reading reached the baseline. The positive control was carried out without the paper samples in the membrane module. The adsorption percentage of added anti-rabbit IgG was determined by subtracting the area of UV-effluent volume curve from adsorption experiments from the positive control using Prime View Software.

3.3 Results and Discussion

A pure cellulose filter paper was impregnated with various concentrations of AKD and the papers were dried and heated to facilitate AKD grafting to fiber surfaces. The gravimetrically determined AKD contents are summarized in **Table 1** and SEM micrographs of the treated paper top surfaces are shown in **Fig. 1**. Micrographs for the three highest AKD loadings showed small white particles on the fiber surfaces.

The influence of AKD on the activity of antibody immobilized on treated filter paper was analyzed using the modified paper-based ELISA (Enzyme-linked immunosorbent assay). The essential features of the method are shown in **Fig. 2**. In this method, the anti-rabbit IgG antibody was physically adsorbed onto the paper surfaces, followed by exposure to milk proteins that adsorbed onto the fiber surfaces to prevent non-specific target adsorption. The targets in this work were antigens (rabbit IgG) that were coupled to HRP enzymes. The activity of adsorbed antibody was determined by reacting HRP enzymes with the TMB substrate to produce a colored solution. The intensity of solution color indicates the degree of antibody activity. Prior to the study, two sets of samples were prepared as controls. The first set of controls did not have anti-rabbit IgG added to paper samples, while the second set contained anti-mouse IgG, instead of anti-rabbit IgG, to

ensure that rabbit IgG did not have non-specific binding with anti-mouse IgG. The results of the control study concluded that the modified paper-based ELISA method did not yield false signals of antibody activity as a result of non-specific binding.

Fig. 3 shows the relative activity of antibodies as functions of the AKD content of the papers. The relative activity was the amount of color generated relative to the control filter paper with no AKD treatment. There was a slight increase in relative activity with AKD addition at the lower concentrations. However, at high AKD contents, antibody relative activity dropped. Interpreting these results is complicated because a drop in antibody activity can be caused either by decreasing the amount of antibody on the surface and/or by decreasing the binding efficiency of the enzyme. Changes in antibody orientation (i.e. active site facing the surface instead of facing the solution) and antibody protein denaturation will influence antigen binding efficiency.

To further understand the results in **Fig. 3**, the adsorption capacity of antibodies on AKD treated papers for antibody was measured and the results in **Table 2** show that antibody adsorption was enhanced by low AKD contents, but was diminished at higher AKD treatments. We believe that small levels of AKD make the surface more hydrophobic, which enhances antibody adsorption [23-25]. However, very high levels of AKD lower the available surface area, giving lower antibody contents.

We combined the antibody adsorption results in **Table 2** with activity results in **Fig. 3** to give specific activities, which is the activity per mass of bound antibody. The results in **Fig. 4** show that within error, AKD treatment does not influence antibody activity. In other words, an adsorbed antibody is just as active on an AKD coated surface as on a pristine cellulose surface. Similar conclusions have been made for the influence of AKD on the activity of adsorbed enzymes [26].

3.4 Conclusions

This work and the previous studies mentioned above all support the same conclusion – sizing and wet strength resins typically found on commercial packaging paper do not interfere with the activity of antibodies and enzymes sitting on the paper surfaces. Since these are arguably the two most important biomacromolecule types for biosensors, it is feasible to format biosensors on the surfaces of conventional packaging papers. Ongoing work is addressing the replacement of lateral flow as a mechanism for sequential reactions on paper surfaces.

Acknowledgements

3.5 References

1.   Liana, D. D.; Raguse, B.; Gooding, J. J.; Chow, E., Recent Advances in Paper-Based Sensors. *Sensors* **2012,** *12* (9), 11505-11526.
2.   Martinez, A. W.; Phillips, S. T.; Whitesides, G. M.; Carrilho, E., Diagnostics for the Developing World: Microfluidic Paper-Based Analytical Devices. *Anal. Chem.* **2009,** *82* (1), 3-10.
3.   Parolo, C.; Merkoci, A., Paper-based nanobiosensors for diagnostics. *Chem. Soc. Rev.* **2013,** *42* (2), 450-457.
4.   Pelton, R., Bioactive paper provides a low-cost platform for diagnostics. *TrAC Trends in Anal. Chem.* **2009,** *28* (8), 925-942.
5.   Sicard, C.; Brennan, J. D., Bioactive paper: Biomolecule immobilization methods and applications in environmental monitoring *MRS Bull.* **2013,** *38*, 331-334.
6.   Then Whui, L.; Garnier, G., Paper diagnostics in biomedicine. In *Reviews in Analytical Chemistry*, 2013; Vol. 32, p 269.
7.   Yetisen, A. K.; Akram, M. S.; Lowe, C. R., Paper-based microfluidic point-of-care diagnostic devices. *Lab on a Chip* **2013,** *13* (12), 2210-2251.
8.   Garnier, G.; Then, W. L., Paper Microfluidics: Appplications and Perspectives. *Transactions of the 15th Fundamental Research, Cambridge* **2013,** *2*, 541-583.
9.   Di Risio, S.; Yan, N., Bioactive Paper Through Inkjet Printing. *J. Adhes. Sci. Technol.* **2010,** *24* (3), 661-684.
10.   Saerens, D.; Huang, L.; Bonroy, K.; Muyldermans, S., Antibody Fragments as Probe in Biosensor Development. *Sensors* **2008,** *8* (8), 4669-4686.
11.   Wang, J.; Pelton, R. H.; Veldhuis, L. J.; MacKenzie, R. C.; Hall, C. J.; Filipe, C. D., Wet-strength Resins and Surface Properties Affect Paper-based Antibody Assays. *Appita J.* **2010,** *63* (1), 32-36.
12.   Wang, W.; Singh, S.; Zeng, D. L.; King, K.; Nema, S., Antibody structure, instability, and formulation. *J. Pharm. Sci.* **2007,** *96* (1), 1-26.
13.   Su, S.; Ali, M. M.; Filipe, C. D. M.; Li, Y.; Pelton, R., Microgel-Based Inks for Paper-Supported Biosensing Applications. *Biomacromolecules* **2008,** *9* (3), 935-941.
14.   Wang, J.; Yiu, B.; Obermeyer, J.; Filipe, C. D. M.; Brennan, J. D.; Pelton, R., Effects of Temperature and Relative Humidity on the Stability of Paper-Immobilized Antibodies. *Biomacromolecules* **2012,** *13* (2), 559-564.
15.   Lu, Y.; Shi, W.; Qin, J.; Lin, B., Fabrication and Characterization of Paper-Based Microfluidics Prepared in Nitrocellulose Membrane By Wax Printing. *Anal. Chem.* **2009,** *82* (1), 329-335.
16.   Cheng, C.-M.; Martinez, A. W.; Gong, J.; Mace, C. R.; Phillips, S. T.; Carrilho, E.; Mirica, K. A.; Whitesides, G. M., Paper-Based ELISA. *Angew. Chem. Int. Ed.* **2010,** *49* (28), 4771-4774.
17.   Hubbe, M. A., Paper's Resistance to Wetting-A Review of Internal Sizing Chemicals and Their effects. *Bioresources* **2006,** *2*, 106-145.
18.   Isogai, A., Mechanism of Paper Sizing by Alkylketene Dimers. *J. Pulp Pap. Sci.* **1999,** *26*, 251-256.

19.   Lindström, T.; Larsson, P. T., Alkyl Ketene Dimer (AKD) sizing – a review. *Nordic Pulp Paper Res. J.* **2008,** *23*, 202-208.

20.   Modaressi, H.; Garnier, G., Mechanism of Wetting and Absorption of Water Droplets on Sized Paper: Effects of Chemical and Physical Heterogeneity. *Langmuir* **2002,** *18* (3), 642-649.

21.   Wang, J.; Yiu, B.; Obermeyer, J.; Filipe, C.; Brennan, J. D.; Pelton, R., The Effects of Temperature and Relative Humidity on the Stability of Paper-immobilized Antibodies. *Biomacromolecules* **2012,** *13* (2), 559–564.

22.   Wang, J.; Pelton, R.; Veldhuis, L.; MacKenzie, C. R.; Hall, J. C.; Filipe, C. D. M., Wet-strength resins and surface properties affect paper-based antibody assays. *Appita J.* **2010,** *60* (1), 32-36.

23.   Yu, D.; Chen, X.; Pelton, R.; Ghosh, R., Paper-PEG-based membranes for hydrophobic interaction chromatography: Purification of monoclonal antibody. *Biotechnol. Bioeng.* **2008,** *99* (6), 1434-1442.

24.   Sun, X.; Yu, D.; Ghosh, R., Study of hydrophobic interaction based binding of immunoglobulin G on synthetic membranes. *J. Memb Sci.* **2009,** *344* (1–2), 165-171.

25.   Mah, K. Z.; Ghosh, R., Paper-based composite lyotropic salt-responsive membranes for chromatographic separation of proteins. *J. Memb Sci.* **2010,** *360* (1–2), 149-154.

26.   Di Risio, S.; Yan, N., Adsorption and inactivation behavior of horseradish peroxidase on cellulosic fiber surfaces. *J. Colloid Interface Sci.* **2009,** *338* (2), 410-419.

Table 1 -The AKD content on filter paper.

% AKD Concentration	Untreated Paper Dry Weight (g)	Treated Paper Wet Weight (g)	% AKD Content on paper
0.001	0.415	1.137	0.002
0.005	0.403	1.169	0.010
0.01	0.41	1.170	0.019
0.05	0.408	1.161	0.092
0.1	0.412	1.125	0.173
0.5	0.405	1.139	0.906
1	0.434	1.182	1.72
5	0.394	1.100	8.96
10	0.407	1.110	17.3
15	0.415	1.116	25.3
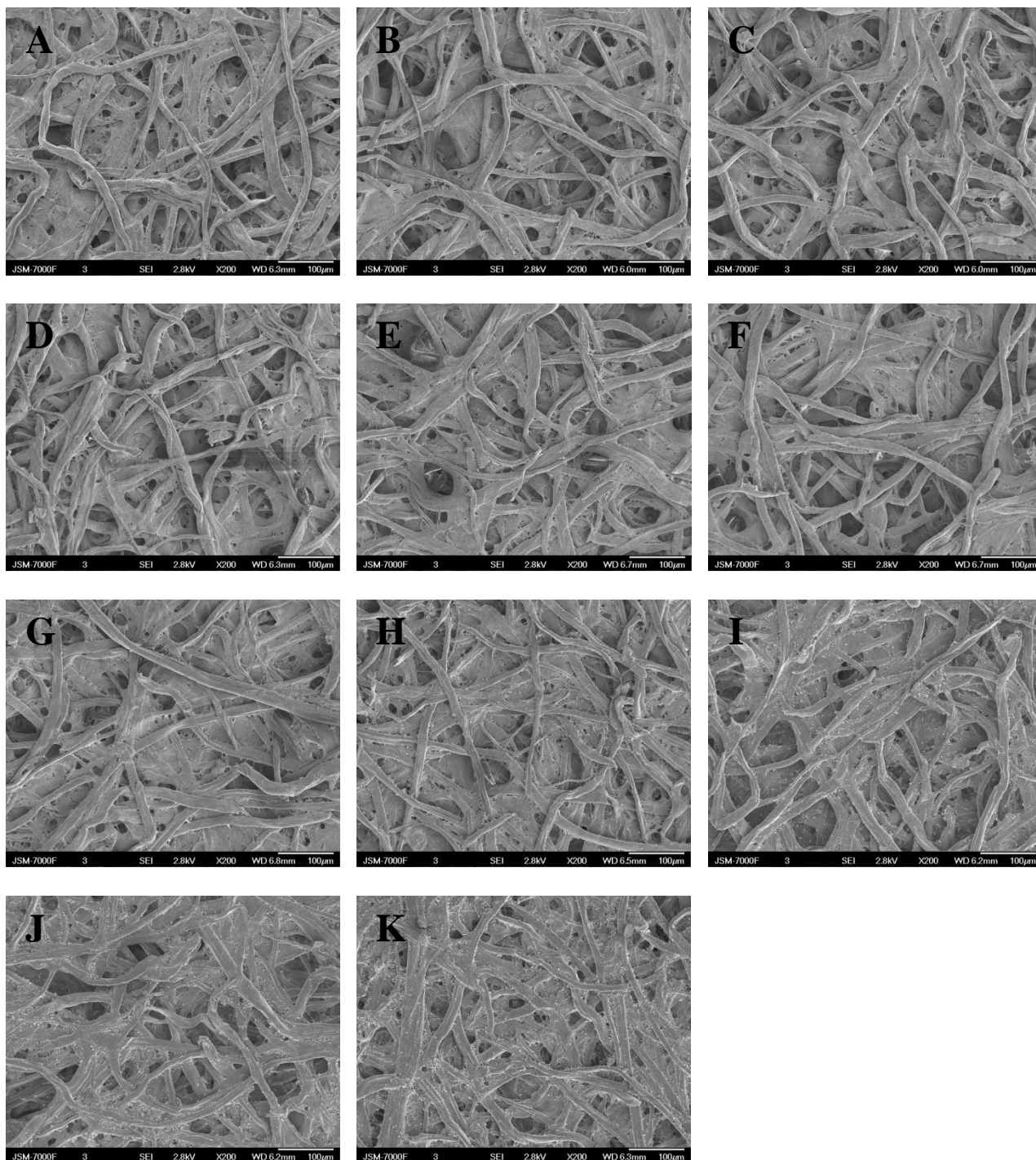
Fig. 1- SEM images of untreated paper and AKD-treated papers. (A) Untreated, (B)-(K): 0.002%, 0.010%, 0.019%, 0.092%, 0.173%, 0.906%, 1.72%, 8.96%, 17.3% and 25.3% AKD treated papers.
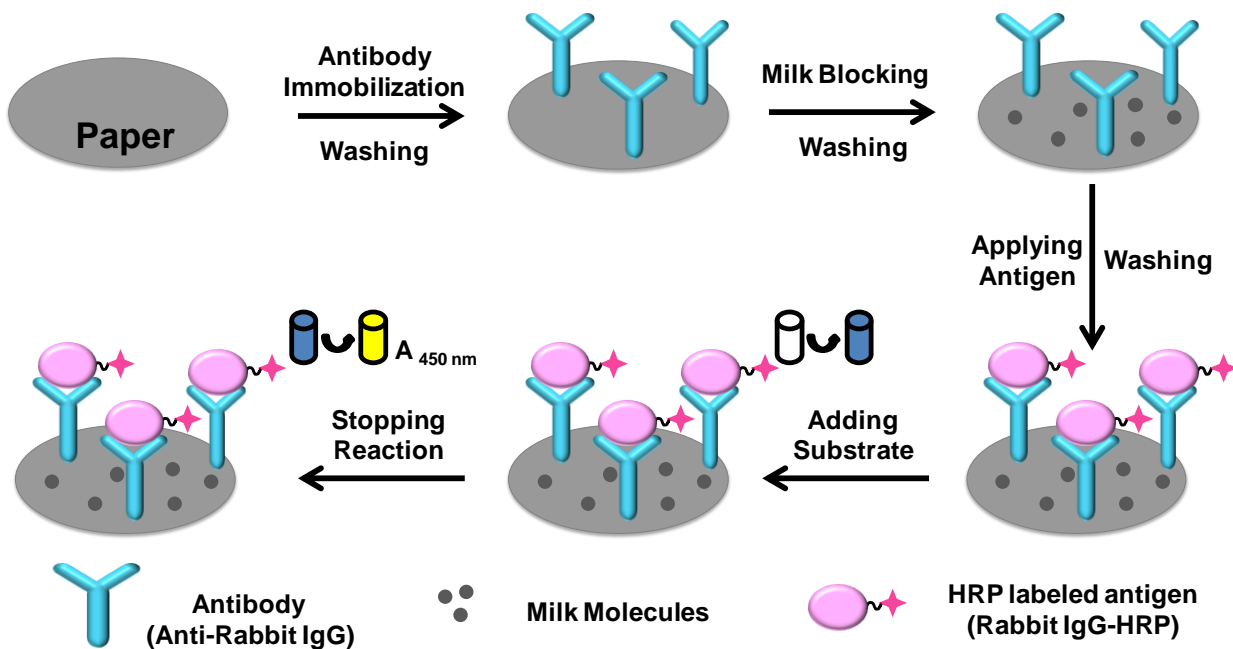
Fig. 2- Illustration of the modified paper-based ELISA assay.
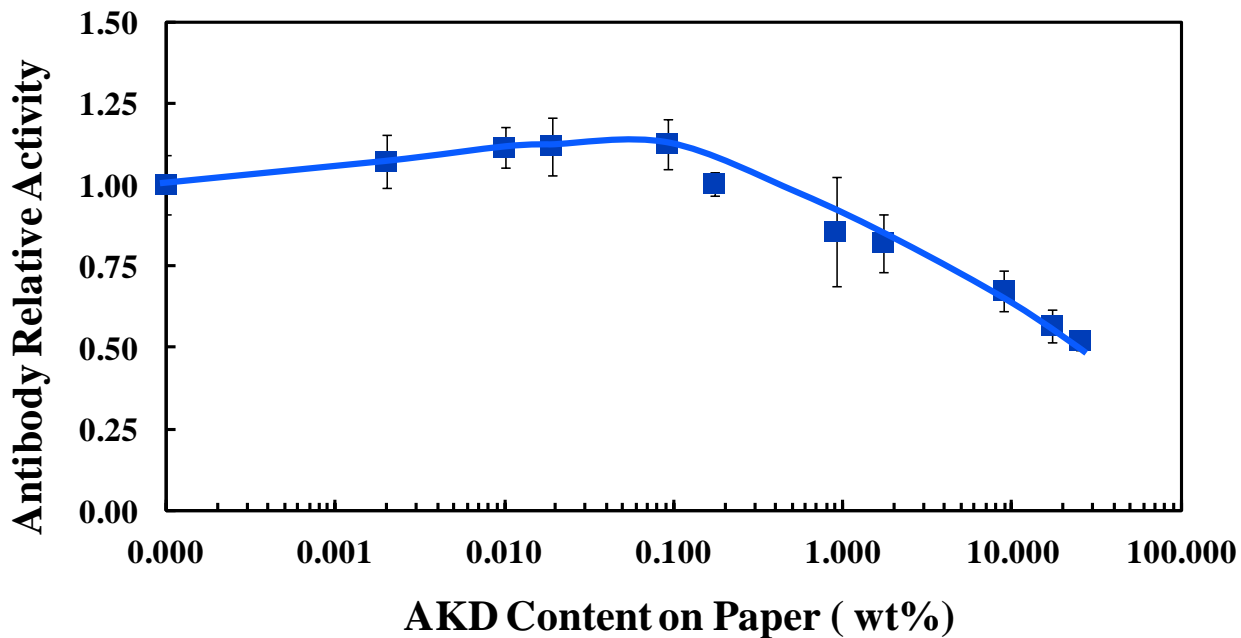
Fig. 3- Anti-rabbit IgG activity on untreated and different AKD-treated papers.

Table 2 - Adsorption of anti-rabbit IgG on the paper samples.

AKD Content (%)	Antibody Adsorption Percentage (%)
0.000	51± 4
0.002	56± 4
0.010	61± 3
0.019	64± 3
0.092	67± 3
0.173	45± 3
0.906	41± 5
1.73	39± 3
8.96	37± 3
17.3	35± 4
25.3	34± 6
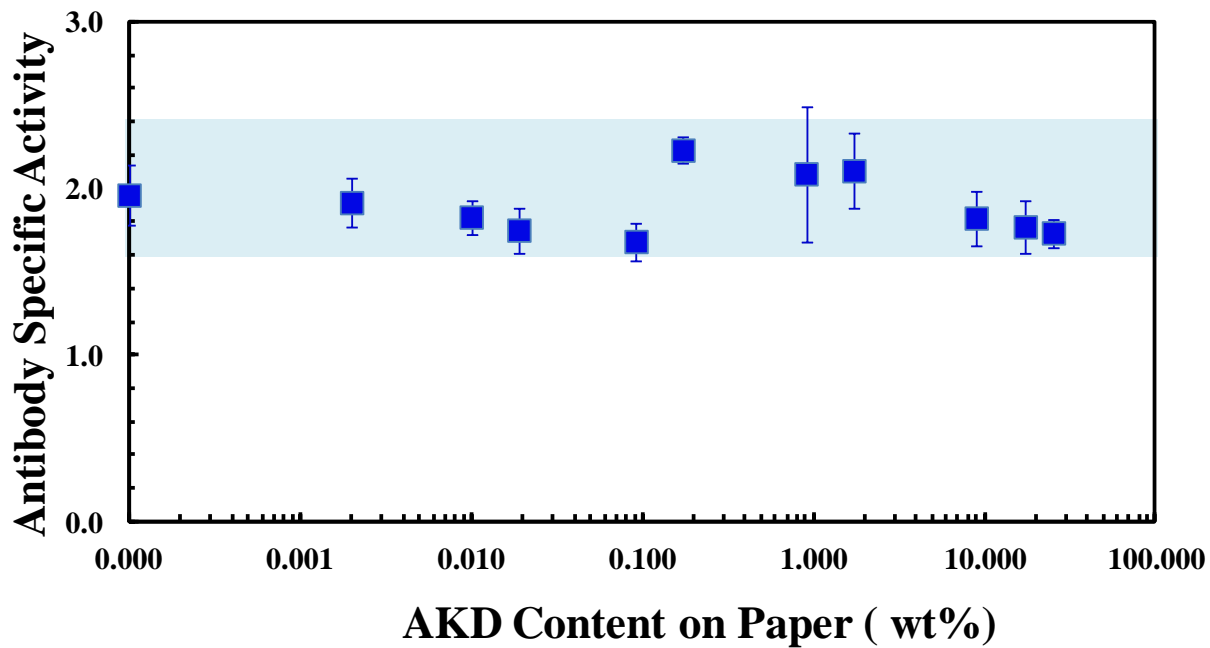
Fig. 4- The specific activity of anti-rabbit IgG on untreated and different AKD-treated papers.

Chapter 4 Hydrophobic Sol-gel Channel Patterning Strategies for Paper-based Microfluidics

In chapter 4, all experimental works were resulted from a joint effort from myself, Dr. Maria Rowena N. Monton and Xi Zhang. Dr. Monton initiated this project and contributed the idea of the NaOH-etching method. Zhang Xi, as a summer undergraduate student, worked with me to complete most of the experiments. Dr. Brennan gave many helpful suggestions on both experiments and data analysis. Dr. Pelton suggested the barrier testing, using different charges of surfactant solutions, and the barrier characterization, through pore volume calculation. Dr. Filipe helped a lot with the TOC graphic design. I initiated the first draft of the paper. Dr. Pelton, Dr. Brennan and Dr. Filipe helped in revising the draft to final version. This work has been published in Lab Chip, 2014, **14**, 691-695. It is produced by permission of The Royal Society of Chemistry.

Hydrophobic sol–gel channel patterning strategies for paper-based microfluidics†

Jingyun Wang,[a] Maria Rowena N. Monton,[b] Xi Zhang,[a] Carlos D. M. Filipe,[a] Robert Pelton*[a] and John D. Brennan*[b]

Hydrophobic sol–gel derived methylsilsesquioxane (MSQ) was compared to wax and alkylketene dimer (AKD) as barrier materials defining channels in paper-based microfluidic devices. While all three of the barrier types performed well with water, only the MSQ barriers were not breached by aggressive cell lysing solutions and surfactant solutions (SDS, CTAB, Triton X-100). The MSQ barriers also withstood glycerol, toluene and DMSO whereas all three barrier types were breached by alcohols. MSQ based devices could be prepared either by direct inkjet printing of the barriers or by base etching of MSQ impregnated paper. The functionality of MSQ based devices was demonstrated by formatting a colormetric sensor for *Escherichia coli*.

Introduction

Many recent publications describe paper-based microfluidic devices for chemical/biochemical/environmental analysis and point-of-care diagnostics.[1–7] In virtually all cases, flow channels in Whatman #1 filter paper are defined by the presence of hydrophobic barriers based on wax,[8–10] polystyrene,[11,12] alkyl ketene dimer (AKD),[13,14] polydimethylsiloxane[15] or fluorochemicals.[16,17] The barrier fabrication methods include photolithography,[18,19] various printing methods to form hydrophobic barriers[8,9,12,13,15] or the chemical,[11] plasma[14] or laser etching[20] of completely hydrophobized paper to regenerate hydrophilic channels. Of these, Whitesides' wax printing method appears to be the most popular because of its simplicity and compatibility with aqueous solutions.[8] However, when developing paper-based assays requiring cell lysing solutions, we found that both wax and AKD based barriers were breached by cell lysing detergents.

Herein we describe a new printable barrier based on acid-hydrolyzed methyltrimethoxysilane (MTMS) to produce a hydrophobic methylsilsesquioxane (MSQ). This material provides a hydrophobic, cross-linked siloxane network that is resistant to pH-induced hydrolysis between pH 2–12.[21–23] Compared to fluorochemicals[16,17] and other more exotic approaches, MSQ is inexpensive, safe and practical for device fabrication in the most challenging locations. Furthermore,

we demonstrate an *E. coli* assay on paper with MSQ barriers that uses a surfactant solution to lyse the bacterial cells prior to analysis.[24]

Experimental

Preparation of paper barriers

A MSQ precursor sol for impregnation was prepared as a mixture of MTMS (Sigma-Aldrich) and 0.1 M hydrochloric acid (HCl, LabChem Inc.) at a 4 : 1 v/v ratio that was sonicated in an ice bath for 1 h. Whatman #1 paper strips were immersed in the solution for ~15 min and air-dried overnight. Preliminary experiments identified 1.0 M sodium hydroxide (NaOH, LabChem Inc.) as a viable etching reagent. The corresponding etching ink, suitable for the Dimatix piezoelectric inkjet printer (DMP-2800), was 1.0 M NaOH (final concentration) in 30% glycerol (v/v, Sigma-Aldrich) and 0.1 wt% Triton X-100 (Sigma-Aldrich). Channels in MSQ impregnated paper were printed using 10 μm drop spacing. After 15 min, the etched paper strips were then immersed in 0.01 M HCl and water successively for 5 min. The treated strips were air-dried overnight.

Two inkjet printers were evaluated for printing MSQ barriers – a Canon PIXMA MP280 thermal inkjet printer operated in "high quality printing" mode, and a Dimatix piezoelectric inkjet printer. For the Canon printer, the first step required 3 printing passes of Tris buffer (pH 8.0, 100 mM). Then three layers of MSQ precursor ink (MTMS: 0.001 M HCl at 4 : 1 v/v) were printed. For the Dimatix piezoelectric printer both the Tris layer and the precursor sol ink were printed in a single pass. The Tris ink contained 30% glycerol (v/v) and 0.1 wt% Triton X-100, and was first printed in the desired pattern using a 20 μm

[a] Department of Chemical Engineering, McMaster University, 1280 Main Street West, Hamilton, Ontario, L8S 4L7, Canada
[b] Biointerfaces Institute & Department of Chemistry and Chemical Biology, McMaster University, 1280 Main Street West, Hamilton, ON, L8S 4M1, Canada. E-mail: brennanj@mcmaster.ca; Tel: +1 905 527 9950 (ext. 20682)

† Electronic supplementary information (ESI) available. See DOI: 10.1039/c3lc51313k

drop spacing. The precursor sol ink formulation was prepared by mixing MSQ sol (MTMS: 0.01 M HCl at 4:1 v/v) with hydroxypropyl cellulose (HPC, 8 wt%, 100 kDa, Sigma-Aldrich) at a 8:1 v/v ratio and the ink was printed using an 8 μm drop spacing. Initial results showed that the curing of inkjet printed sols required 6 h with Tris *vs.* >12 h without printing the Tris buffer layer (Fig. S1†).

Wax printing and AKD printing methods were also used to create hydrophobic channels. Wax-printed channels were made using a wax printer (Xerox Phaser 6580), followed by melting the wax in an oven at 120 °C for 2 min. To prepare the AKD hydrophobic channels, a 2 wt% AKD emulsion (Kemira Chemicals Canada Inc.) in water was printed onto the paper using the Canon printer. AKD was printed in two passes. The printed papers were then heated in an oven at 100 °C for 10 min.

Testing barrier performance

The resistance of the barriers to surfactants and organic solvents was tested by adding 40 μl of the test liquid into the channel (7.5 mm inner width and 30 mm inner length with 1.5 mm thick barrier) created using NaOH etched MSQ, printed MSQ, wax or AKD. The surfactant solutions tested were 1% (w/v) of Triton X-100, sodium dodecyl sulfate (SDS, Sigma-Aldrich) or hexadecyltrimethylammonium bromide (CTAB, Sigma-Aldrich) in water. Note that these solutions were just above the critical micelle concentration for each surfactant. The organic solvents tested included methanol, isopropanol, glycerol, dimethyl sulfoxide (DMSO) and toluene (Caledon Labs.). The surfactant solutions, methanol and isopropanol contained xylenol orange (Sigma-Aldrich) to aid in visualization. Glycerol contained phenol red (Sigma-Aldrich). DMSO and toluene contained nile red (Sigma-Aldrich).

Barrier characterization

The basis weight (bw = mass/superficial area of the top face) of barrier regions was determined by weighing oven-dried paper (105 °C for 2 h) and the thickness (τ) was measured using a digital micrometer (Testing Machine Inc.). The pore volume fractions (ϕ_{air}) of the barrier regions were estimated by eqn (1) where: bw_o is the basis weight of untreated paper, bw_p is the basis weight after printing; τ_p is the thickness of the printed paper; ρ_{cel} is the density of cellulose (1540 kg m^{-3}); and, ρ_{ink} is the density of pore-free hydrophobic material (AKD and wax: 930 kg m^{-3}, MSQ: 1340 kg m^{-3}).[5,25] The penetration of MSQ ink can be calculated using eqn (2) where: Γ_v is the volume of wet ink per unit area (cm^3 m^{-2}) and ϕ pore fraction for Whatman #1 paper (0.68). According to the printing setting, the transferred wet ink volume was 156 cm^3 m^{-2}.

$$\phi_{air} = 1 - \frac{bw_o}{\rho_{cel} \cdot \tau_p} - \frac{bw_p - bw_o}{\rho_{ink} \cdot \tau_p} \qquad (1)$$

$$\delta_p = \frac{\Gamma_v}{\phi} \qquad (2)$$

The MSQ barriers were characterized by Scanning Electron Microscopy (SEM, JSM-7000F, JEOL), water contact angle (FDS OCA35), optical microscopy (BX53, Olympus) and Fourier Transform Infrared Spectroscopy (FTIR, Vertex 70, Bruker).

Detection of *E. coli* using printed patterns

Circular barriers with a 12 mm outer diameter, 9 mm inner diameter (1.5 mm thick) were printed on paper using either MSQ, AKD or wax. The Canon printer was then used to print a 2 wt% poly-arginine solution (MW >70 kDa, Sigma-Aldrich) followed by a 9 mM chlorophenol red-β-D-galactopyranoside solution (CPRG, Sigma-Aldrich) as solid circles inside the barriers.

E. coli BL21 was cultured overnight in LB (Luria Bertani) media for 16 h (37 °C with a shaking rate of 250 rpm) to obtain a cell concentration of 10^7 cfu mL^{-1}. The *E. coli* sample was then lysed with B-PER® direct bacterial protein extraction reagent (Thermo Scientific) at a 9:1 culture: B-PER® volume ratio according to the supplier's protocol for 30 min. 15 μl of the lysed *E. coli* suspension was manually spotted into the circle sensors. Color changes were recorded with an iPhone 4S camera 5 min after addition of the *E. coli* suspension. Control experiments were conducted by using LB media without *E. coli*, but with the addition of an identical amount of the B-PER® lysing reagent.

Results and discussion

MSQ is a hydrophobic sol–gel derived material prepared by the hydrolysis of MTMS and treated papers were prepared either by dipping (impregnation) paper sheets into the sol or ink jet printing of the sol to generate specific patterns on chromatographic paper.

Preliminary experiments were conducted to determine the NaOH concentration required to etch channels in MSQ impregnated paper. Fig. 1A shows photographs of droplets of various NaOH concentrations sitting on MSQ impregnated papers. Only the 1.0 M NaOH solution seemed to completely penetrate the MSQ. Fig. 1B shows two examples after dyed water was spotted on the circular region and underwent capillary driven flow along the hydrophilic channels. The photograph of the channel cross-section (Fig. 1C) shows that the hydrophilic channel was mostly restricted to the top half of the paper, although some of the dye solution still penetrated to the bottom.

The direct inkjet printing of barriers and other biosensor components is an attractive approach to biosensor manufacture.[7] We evaluated a Canon thermal inkjet printer, and a Dimatix research-grade piezoelectric inkjet printer. The thermal inkjet printer is widely available, cost-effective and can
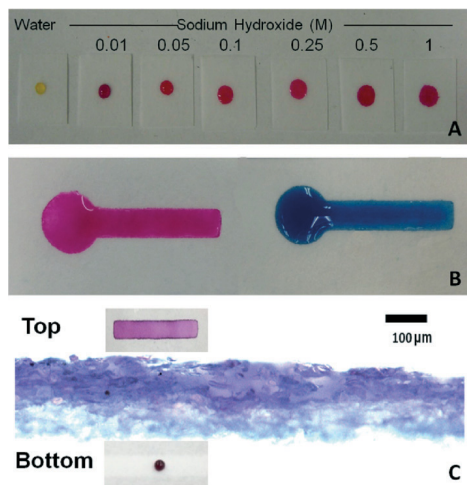
54

Fig. 1 (A) Penetration of NaOH dye solution on MSQ-derivatized paper, (B) dye solutions on the MSQ-derivatized paper etched with 1.0 M NaOH, (C) cross-sectional image of the etched hydrophilic channel; the purple region indicates the channel filled with aqueous dye.

print multiple pages rapidly using the built-in sheet feeder. In addition, no additives are required to modify the viscosity or surface tension of aqueous inks. However, the heating of the ink associated with the thermal inkjet technology made the hydrolyzed MTMS solution unstable, causing accelerated condensation of the MTMS sol, leading to clogging of cartridges.

The Dimatix printer is a single sheet, single head laboratory printer requiring inks with viscosities in the range 2–30 mPa s and surface tension in the range 30–38 mN m^{-1}.[26] Glycerol, polyvinyl alcohol, carboxymethyl cellulose, Pluronic L-61 and HPC were evaluated with the hydrolyzed MTMS sol to yield an ink solution with desirable printing characteristics. Among these additives, only Pluronic L-61 and HPC did not induce phase separation of the MTMS sol. However the resulting barrier with Pluronic L-61 based ink was not sufficiently hydrophobic, presumably because of surfactant contamination. By contrast, the HPC based ink performed well. Fig. 2 shows photographs of dyed water in MSQ, AKD

Fig. 2 Flow of dye solutions in various channels.

and wax channels – all three are able to contain the aqueous solution. However, differences occurred when using more challenging solvents (see below).

Table 1 summarizes the water contact angles, the densities and the estimated pore volume fraction of the MSQ, wax and AKD treated papers. All four treatments gave hydrophobic surfaces (i.e. water contact angle >90°). The MSQ printed surface had the lowest contact angle possibly because the MSQ printed surfaces were the smoothest (see below).

Microfluidic barriers can function either by transforming cellulose surfaces to being non-wetting or by filling the pores with an insoluble material. All four barrier types had significant pore volumes, however, the MSQ-printed barrier showed the lowest pore volume whereas AKD had the highest, suggesting at least partial filling of pores by MSQ.

Fig. 3 shows SEM micrographs of the four barrier types. MSQ impregnated paper (B), wax barrier (G), and AKD barrier (H) showed some porosity in agreement with the estimates in Table 1. By contrast, the inkjet printed MSQ barriers (E and F) were relatively smooth and appeared to have little macroscopic porosity on the exterior surfaces. We anticipate nanoscale porosity in the sol–gel materials but do not expect macropore formation under the hydrolysis and condensation conditions employed in this work.[21-23] We also noticed that the MSQ ink penetrated through the thickness of the paper since the calculated maximum penetration of the MSQ was about 230 μm. The FTIR result also confirmed that a larger amount of MSQ material was present on the MSQ-printed paper than on MSQ-impregnated paper (Fig. S2†).

The ability of directly printed and NaOH-etched MSQ barriers, as well as wax printed and AKD barriers, to contain surfactants without leakage is shown in Fig. 4. The wax-printed channels fail to function properly, regardless of the type of surfactant used, while AKD-printed channels retained only the 1% CTAB solution. The NaOH-etched MSQ channels could contain solutions with 1% SDS or CTAB, but not 1% Triton X-100. By contrast, MSQ materials printed with the Dimatix printer contained 1% solutions of all of the surfactants tested. Table 1 shows that the void fraction of the impregnated MSQ paper was substantially higher than the printed MSQ barriers, suggesting that low void volumes are important for MSQ barriers holding challenging solvents.

Fig. 5 shows the integrity of different types of barriers when exposed to various organic solvents. Interestingly, none of the barriers were compatible with alcohols, such as methanol and isopropanol. On the other hand, glycerol, which is often used as a protein stabilizer, could be used with all

Table 1 Typical properties of MSQ, wax and AKD-treated barriers

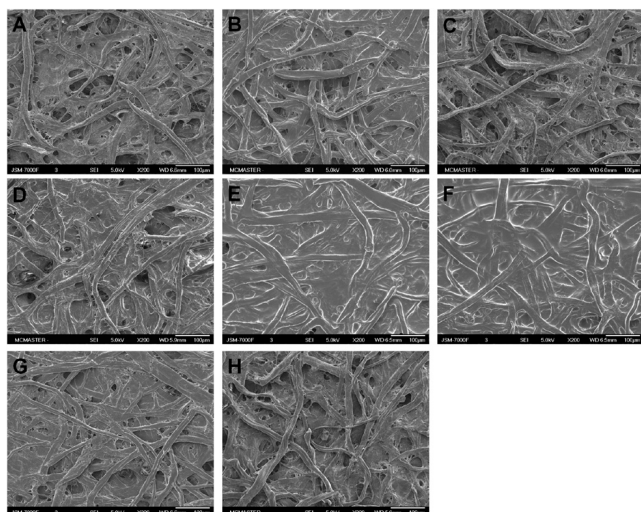|	Print coverage (g m^{-2})	Paper density (kg m^{-3})	Pore volume fraction	Water contact angle (degrees)
Whatman #1	N/A	494	0.68	N/A
MSQ impregnated	N/A	717	0.51	113 ± 1
MSQ printed	86	880	0.39	100 ± 3
Wax printed	12	638	0.55	133 ± 1
AKD printed	5	512	0.66	136 ± 1

55

Fig. 3 SEM images of (A) Whatman #1 paper, (B) paper impregnated with MSQ, (C) NaOH-etched MSQ paper – top side, (D) NaOH-etched MSQ paper – back side, (E) MSQ-printed paper using Dimatix printer – top side, (F) MSQ-printed paper using Dimatix printer – back side, (G) wax-printed paper – top side, and (H) AKD-printed paper – top side.
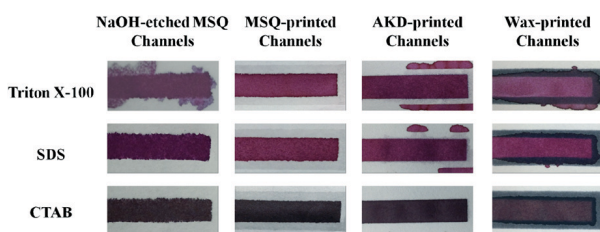

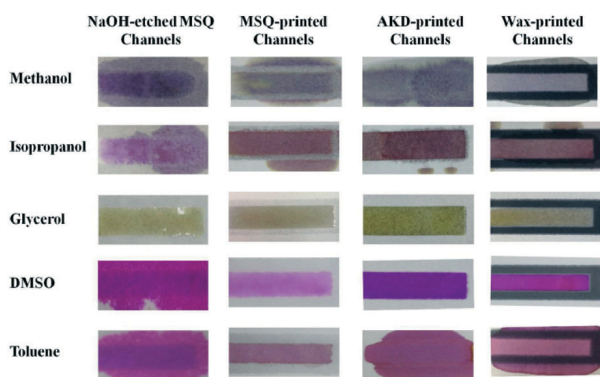**Fig. 4** Flow of dye solutions with surfactants on various channels.

Fig. 5 Flow of organic solvents through various channels.

barriers without wicking through the hydrophobic boundaries. DMSO, often used to solubilize small molecule libraries, could also flow within the defined hydrophilic area for each barrier type with the exception of NaOH-etched MSQ channels. Of all the barrier types, only the MSQ-printed barrier was found to be resistant to toluene.

A key goal in developing the MSQ barrier was to evaluate compatibility with B-PER® direct lysing reagent, which is used as part of a previously published assay for detection of
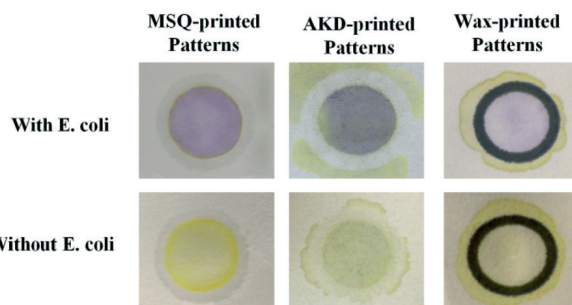
Fig. 6 Detection of lysed *E. coli* BL21 using various barriers.

E. coli on paper.[24] A key step in this assay is the lysing of an *E. coli* suspension by B-PER® direct lysing reagent to release the enzyme β-galactosidase (β-GAL). The released enzyme reacts with CPRG to produce a yellow-to-purple colour change. The results for the three barrier types are illustrated in Fig. 6. Only the MSQ barriers contained the assay without breaching the barriers.

Conclusions

For assays involving non-challenging aqueous solutions, both wax and AKD barriers are attractive. The wax process is simple and AKD is an inexpensive agent widely used in the paper industry to hydrophobize (size) paper. However, with surfactant-rich solutions typically used to lyse cells, the MSQ barriers showed superior performance, making these amenable to quantitative paper-based assays for *E. coli*. The MTMS/MSQ chemistry is inexpensive, safe and thus viable for devices manufactured in resource-limited situations. MSQ, wax and AKD barriers were all breached by alcohols. For very challenging liquids (MeOH), fluorochemical barriers may be required.[16,17]

Acknowledgements

Notes and references

1 C. D. Chin, V. Linder and S. K. Sia, *Lab Chip*, 2012, **12**, 2118–2134.
2 D. D. Liana, B. Raguse, J. J. Gooding and E. Chow, *Sensors*, 2012, **12**, 11505–11526.
3 A. W. Martinez, S. T. Phillips, G. M. Whitesides and E. Carrilho, *Anal. Chem.*, 2009, **82**, 3–10.
4 C. Parolo and A. Merkoci, *Chem. Soc. Rev.*, 2013, **42**, 450–457.
5 R. Pelton, *TrAC, Trends Anal. Chem.*, 2009, **28**, 925–942.

6   A. K. Yetisen, M. S. Akram and C. R. Lowe, *Lab Chip*, 2013, **13**, 2210–2251.

7   K. Maejima, S. Tomikawa, K. Suzuki and D. Citterio, *RSC Adv.*, 2013, **3**, 9258–9263.

8   E. Carrilho, A. W. Martinez and G. M. Whitesides, *Anal. Chem.*, 2009, **81**, 7091–7095.

9   W. Dungchai, O. Chailapakul and C. S. Henry, *Analyst*, 2011, **136**, 77–82.

10 T. Songjaroen, W. Dungchai, O. Chailapakul and W. Laiwattanapaisal, *Talanta*, 2011, **85**, 2587–2593.

11 K. Abe, K. Suzuki and D. Citterio, *Anal. Chem.*, 2008, **80**, 6928–6934.

12 J. Olkkonen, K. Lehtinen and T. Erho, *Anal. Chem.*, 2010, **82**, 10246–10250.

13 X. Li, J. Tian, G. Garnier and W. Shen, *Colloids Surf., B*, 2010, **76**, 564–570.

14 X. Li, J. Tian, T. Nguyen and W. Shen, *Anal. Chem.*, 2008, **80**, 9131–9134.

15 D. A. Bruzewicz, M. Reches and G. M. Whitesides, *Anal. Chem.*, 2008, **80**, 3387–3392.

16 X. Li, J. Tian and W. Shen, *Cellulose*, 2010, **17**, 649–659.

17 F. Deiss, A. Mazzeo, E. Hong, D. E. Ingber, R. Derda and G. M. Whitesides, *Anal. Chem.*, 2013, **85**, 8085–8094.

18 A. W. Martinez, S. T. Phillips, M. J. Butte and G. M. Whitesides, *Angew. Chem., Int. Ed.*, 2007, **46**, 1318–1320.

19 A. W. Martinez, S. T. Phillips, B. J. Wiley, M. Gupta and G. M. Whitesides, *Lab Chip*, 2008, **8**, 2146–2150.

20 G. Chitnis, Z. Ding, C.-L. Chang, C. A. Savran and B. Ziaie, *Lab Chip*, 2011, **11**, 1161–1165.

21 H. Dong and J. D. Brennan, *Chem. Mater.*, 2005, **18**, 541–546.

22 H. Dong, M. A. Brook and J. D. Brennan, *Chem. Mater.*, 2005, **17**, 2807–2816.

23 C. Carrasquilla, P. S. Lau, Y. Li and J. D. Brennan, *J. Am. Chem. Soc.*, 2012, **134**, 10998–11005.

24 S. Hossain, C. Ozimok, C. Sicard, S. Aguirre, M. Ali, Y. Li and J. Brennan, *Anal. Bioanal. Chem.*, 2012, **403**, 1567–1576.

25 H.-J. Lee, C. L. Soles, D.-W. Liu, B. J. Bauer, E. K. Lin, W.-L. Wu and M. Gallagher, *J. Appl. Phys.*, 2006, **100**, 064104.

26 S. M. Z. Hossain, R. E. Luckham, A. M. Smith, J. M. Lebert, L. M. Davies, R. H. Pelton, C. D. M. Filipe and J. D. Brennan, *Anal. Chem.*, 2009, **81**, 5474–5483.

Appendix: Supporting Information for Chapter 4

MSQ-printed Channels

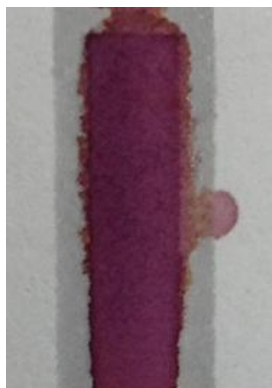**With Tris Buffer**   **Without Tris Buffer**

Fig. S1: Flow of dye solution on MSQ-printed channels with or without Tris buffer layer. The channels were tested 6 hr after printing. The line thickness set for the printing was 1.5 mm and the actually formed barrier was about 2 mm.
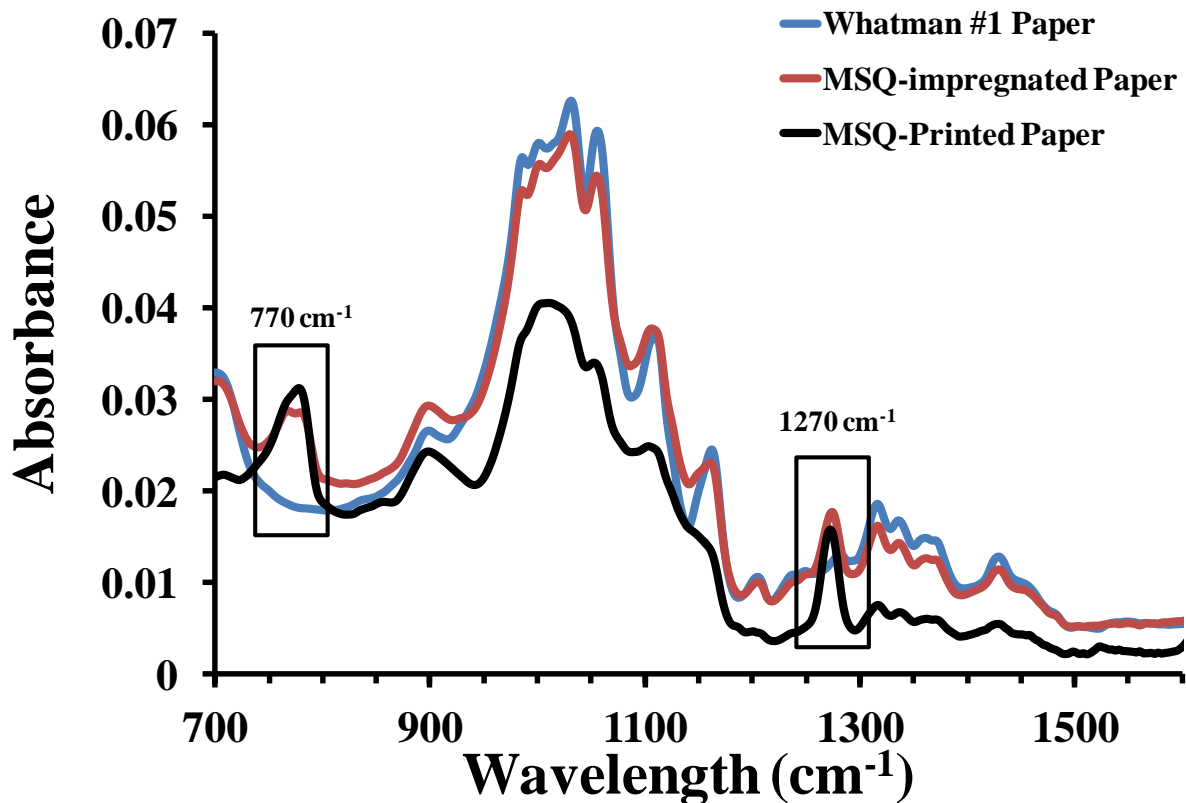
Fig. S2: FTIR spectra of whatman #1 paper, MSQ-impregnated and MSQ-printed paper. The sharp band at 1270 cm^{-1} and 770 cm^{-1} represented Si-CH$_3$ group.

The goal of this calculation is develop relationships for void volume on filled papers
Assume that the xy dimensions do not change with printing whereas thickness might

$$\rho_{cel} := 1540 \frac{kg}{m^3}$$

solid cellulose density

$$\rho_{ink} := \begin{pmatrix} 1340 & 0 & 0 & 0 \\ 0 & 1340 & 0 & 0 \\ 0 & 0 & 930 & 0 \\ 0 & 0 & 0 & 930 \end{pmatrix} \frac{kg}{m^3}$$

dried ink density

- MSQ impregnated
- MSQ printed
- Wax printed
- AKD printed

$$\tau_o := 168 \mu m$$

initial paper thickness

$$\tau_p := \begin{pmatrix} 166 \\ 192 \\ 149 \\ 172 \end{pmatrix} \mu m$$

printed paper thickness

- MSQ impregnated
- MSQ printed
- Wax printed
- AKD printed

$$bw_o := 83 \frac{gm}{m^2}$$

initial paper basis wt

$$bw_p := \begin{pmatrix} 119 \\ 169 \\ 95 \\ 88 \end{pmatrix} \frac{gm}{m^2}$$

printed paper basis wt

- MSQ impregnated
- MSQ printed
- Wax printed
- AKD printed

Initial filter paper

$$\rho_o := \frac{bw_o}{\tau_o} = 0.494 \cdot \frac{gm}{mL}$$

$$\phi_{cel} := \frac{\rho_o}{\rho_{cel}} = 0.3208$$

Printed filter paper

$$\rho_p := \frac{bw_p}{\tau_p} = \begin{pmatrix} 0.7169 \\ 0.8802 \\ 0.6376 \\ 0.5116 \end{pmatrix} \cdot \frac{gm}{mL}$$ Printed filter paper density

- MSQ impregnated
- MSQ printed
- Wax printed
- AKD printed

$$\phi_{cel} = \frac{Vcel}{V_p} = \frac{bw_o \cdot m^2}{m^2 \cdot \tau_p \cdot \rho_{cel}} = \frac{bw_o}{\tau_p \cdot \rho_{cel}} = \frac{\tau_o \cdot \rho_o}{\tau_p \cdot \rho_{cel}}$$

$$\phi_{ink} = \frac{Vink}{V_p} = \frac{(bw_p - bw_o) \cdot m^2}{m^2 \cdot \tau_p \cdot \rho_{ink}} = \frac{bw_p - bw_o}{\tau_p \cdot \rho_{ink}} = \frac{\rho_p \cdot \tau_p - \rho_o \cdot \tau_o}{\tau_p \cdot \rho_{ink}}$$

$$\phi_{air} = 1 - \phi_{cel} - \phi_{ink} = 1 - \frac{\tau_o \cdot \rho_o}{\tau_p \cdot \rho_{cel}} - \frac{\rho_p \cdot \tau_p - \rho_o \cdot \tau_o}{\tau_p \cdot \rho_{ink}} = 1 - \frac{bw_o}{\tau_p \cdot \rho_{cel}} - \frac{bw_p - bw_o}{\tau_p \cdot \rho_{ink}}$$

$$\phi_{air} := 1 - \frac{bw_o}{\tau_p \cdot \rho_{cel}} - \frac{bw_p - bw_o}{\rho_{ink} \cdot \tau_p} = \begin{pmatrix} 0.5135 \\ 0.385 \\ 0.5517 \\ 0.6554 \end{pmatrix}$$ Pore volume fraction

- MSQ impregnated
- MSQ printed
- Wax printed
- AKD printed

The goal of this calculation is to find out the average penetration depth of wet ink (δp) into paper

The drop-to-drop spacing (dp) $dp := 8\mu m$

$$\alpha := \frac{1m}{dp} \cdot \frac{1m}{dp} \cdot \frac{1}{m^2}$$ $\alpha = 1.563 \times 10^{10} \frac{1}{m^2}$ The drop number per m² (α)

$$\beta := 10^{-8} mL$$ The volume per drop (β, 10 pL)

$$\Gamma_v := \alpha \cdot \beta$$ Superfical ink volumetric coverage printed on paper

$$\Gamma_v = 156.25 \frac{cm^3}{m^2}$$

$$\phi := 0.68$$ Paper Pore Volume

$$\delta_p := \frac{\Gamma_v}{\phi}$$ Wet ink penetration thickness

$$\delta_p = 229.779 \mu m$$

62

Chapter 5 Morphology and Entrapped Enzyme Performance in Inkjet Printed Sol-Gel Coatings on Paper

In chapter 5, all of the experiments were conducted by myself, Devon Bowie and Xi Zhang. Devon assisted in the development of protease assay and the preparation of paper samples for microscope imaging. Xi Zhang conducted the protease assay for printed paper samples. Dr. Brennan proposed the idea of using proteolysis to examine enzyme entrapment. Dr. Pelton suggested the calculation of printed silica layer thickness and the layer characterization by SEM/TEM. Dr. Pelton and Dr. Filipe both contributed to the TOC graphic design. I initiated and completed the first draft of the paper. Dr. Pelton, Dr. Brennan and Dr. Filipe edited the first draft to the final version. This work has been published in *Chem. Mater.*, 2014, 26 (5), pp 1941–1947. Copyright © 2014 American Chemical Society

# Morphology and Entrapped Enzyme Performance in Inkjet-Printed Sol−Gel Coatings on Paper

Jingyun Wang,[†] Devon Bowie,[†] Xi Zhang,[†] Carlos Filipe,[†] Robert Pelton,[*,†] and John D. Brennan[*,‡]

[†]Department of Chemical Engineering, McMaster University, 1280 Main Street West, Hamilton, Ontario L8S 4L7, Canada
[‡]Biointerfaces Institute and Department of Chemistry and Chemical Biology, McMaster University, 1280 Main Street West, Hamilton, ON L8S 4L8, Canada

Ⓢ *Supporting Information*

ABSTRACT: We recently reported on the multilayer printing of sol−gel/enzyme bioinks onto porous filter paper to create bioactive paper test strips. The method involves printing of four inks: a polymer underlayer, a sol−gel-based silica layer, an acetylcholinesterase (AChE) enzyme layer, and finally a top layer of silica. To improve our understanding of the nature of these printed materials, filter paper printed with various ink components was characterized by activity assays (with and without protease treatment), confocal microscopy to assess the location and mixing of layers, and scanning electron microscopy of deposited inks to assess the morphology and ink location. Although the silica and enzyme solutions were printed sequentially, they formed a composite material within the porous paper network and coated only the fibers as a 35 ± 15 nm thin film without filling the macropores. The silica coating on the cellulose fibers was sufficiently flexible to allow bending of the paper substrate, unlike traditional silica thin films. The protease assay results showed that the AChE was more protected as the amount of sol−gel-derived silica printed on paper was increased. The top layer of sol−gel ink was found to play a critical role in protection against proteolysis, while the bottom layer of sol−gel ink was found to be necessary to prevent the potential inhibition of AChE by the cationic polymer (used as a capture agent for the product of the enzymatic reaction). Overall, the data show that inkjet-printed sol−gel materials form thin, protein-entrapping films that are suitable for the production of printed biosensors.
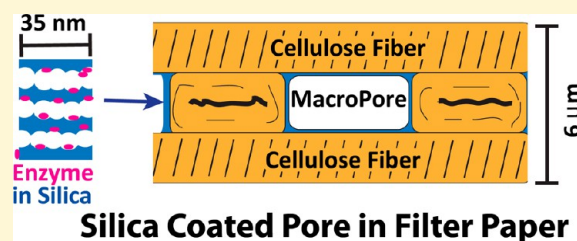
INTRODUCTION

Paper-based biosensors are emerging as a cost-effective technology for performing point-of-care (POC) analytical assays.[1−9] The core requirement for paper-based biosensors is that biological reagents be immobilized onto the paper surface by a simple and scaleable process in a manner that maintains their biological activity.[5,6,10] Recently, Hossain et al.[11−13] described biosensors based on enzymes trapped in paper-supported sol−gel-derived silica. The biosensors were prepared by sequential inkjet printing of four layers onto filter paper: (1) a poly-L-arginine layer, (2) a colloidally stable silica sol at pH 4, (3) an enzyme layer in Tris buffer (pH 8.0), and (4) a second layer of silica sol at pH 4. We proposed that following the printing, the two silica sol layers mixed with the enzyme at higher pH and the mixture cured to form a sol−gel-derived silica matrix that protected fragile enzymes but was sufficiently porous for substrate penetration.

The entrapment of biomolecules into printed sol−gel-derived silica offers a unique methodology for placing biomolecules onto paper, as it provides a simple, low-cost process[10,14−16] that is amenable to immobilization of a wide range of species such as enzymes,[16−23] antibodies,[24−29] DNA/RNA aptamers,[30−33] and living cells.[34−39] However, the specific location of the various printed layers on paper has not been characterized, and issues such as the amount of enzyme entrapped and the nature of the silica material (homogeneity, layer thickness, etc.) have not been characterized. Given that the development of paper-supported sol−gel biosensors is undergoing a transition from laboratory-scale prototypes to commercial-scale inkjet manufacturing, the need to better characterize the nature of the printed biomaterials has arisen.

The major goals of this study are to more fully characterize the material that is deposited onto paper surfaces upon inkjet printing of separate polymer, silica, and enzyme layers and to determine (1) the role each layer plays in maintaining enzyme activity, (2) how the individual layers interact with each other, (3) the nature of the material once deposited on porous filter paper (distribution and coating thickness), and (4) the fraction of enzyme that is entrapped. To address these issues, we have utilized activity assays with and without added protease to assess the degree of active enzyme entrapment, confocal microscopy to assess the location and mixing of fluorescently labeled ink components (polymer, silica, and enzyme) after printing, and scanning and transmission electron microscopy to assess the morphology and extent of ink coating on filter paper surfaces.

■ MATERIALS AND METHODS

Materials. Dowex 50WX8-100 ion exchange resin, acetylcholinesterase (AChE, from *Electrophorus electricus*, type VI-S), poly-L-arginine hydrochloride (>70 kDa), human serum albumin (HSA), 5,5′-dithiobis(2-nitrobenzoic acid) (DTNB), acetylthiocholine iodide (ATCh), protease type XIV from *Streptomyces griseus* (a mixture of at least three caseinolytic activities and one aminopeptidase activity), fluorescein 5(6)-isothiocyanate (FITC), rhodamine 6G (R6G), anhydrous glycerol, Triton X-100, dimethyl sulfoxide (DMSO), tris(2-carboxyethyl)phosphine (TCEP), tris(hydroxymethyl)-aminomethane, phosphate-buffered saline, and Fluoromount aqueous mounting medium were purchased from Sigma-Aldrich. The sodium silicate solution was obtained from Fisher Scientific. Cy5 maleimide monoreactive dye was purchased from GE Healthcare Life Science. Whatman #1 paper was obtained from VWR. All buffers and protein solutions were prepared using Type 1 water (Barnstead Nanopure Diamond system).

Printing of Sol–Gel Bioinks on Paper. To prepare sodium silicate (SS) sols, 2.59 g of the sodium silicate solution (pH ~13) was mixed with 10 mL of ddH$_2$O, followed by the addition of 5.5 g of Dowex cation exchange resin, which had previously been soaked in 0.1 M HCl for 1 h and then washed several times with water to charge the resin. The sol was stirred with the Dowex resin for 2 min to bring the final solution pH to 4, and the mixture was then vacuum-filtered through a Büchner funnel and filtered through a 0.25 μm membrane syringe filter to produce the final silica sol. Preparation of 2× sodium silicate sols used 5.18 g of sodium silicate and 11 g of Dowex exchange resin, and the resulting sol was mixed with 10 mL of ddH$_2$O.

Three different materials were printed on filter paper (Whatman #1) using a piezoelectric inkjet printer (model DMP-2800) from Fujifilm Dimatix, Inc.: (1) a polymer (poly-L-arginine, 2 wt %), (2) an enzyme (AChE, 500 units/mL, prepared by diluting the lyophilized enzyme with Tris buffer), and (3) the SS sol. Glycerol [30% (v/v)] and Triton X-100 (0.1 wt %) were added to each of the three materials to increase viscosity and lower surface tension and thus achieve optimal printing performance.[11] Materials containing the glycerol and Triton X-100 additives are termed "inks" in this study. The order of printing of the inks on paper was as follows: (1) polymer base layer (P), (2) silica sol bottom layer (S$_b$), (3) enzyme in Tris buffer solution (E), and (4) silica sol top layer (S$_t$). The samples were printed to a final amount of 25 cm^3/m^2 of each ink using a 20 μm drop-to-drop spacing, a nozzle voltage of 40 V, and a firing frequency of 5 kHz at room temperature and humidity. Layers were allowed to dry for 15 min prior to the printing of the next layer. Studies of enzyme activity and entrapment within the sol–gel material network involved different combinations of layers, including removal of the SS bottom or top layer, or removal of the polymer layer. In addition, the SS sol ink was printed using different drop-to-drop spacings to obtain varying amounts of silica deposition on filter paper to further examine the effect of the silica material on enzyme performance.

Monitoring Enzyme Entrapment and Activity. Prior to measuring the enzyme activity and degree of entrapment on filter paper, we first performed the assay and verified it in microwell plates. Volumes of μL each of SS sol (~1.5 mm), AChE (10 units/mL), and SS sol were sequentially added to the wells of a 96-well microwell plate, such that the enzyme was entrapped within two layers of sol–gel-derived material in a sandwich format. To accelerate the gelation of the sol–gel material, the SS sol layer was prepared by mixing 2× sodium silicate sol with Tris buffer (100 mM, pH 7.8) in a 1:1 ratio. The enzyme layer was added after 1 h, when the bottom layer had gelled (gelation time of ~15 min). As a comparison, 50 μL of AChE (10 units/mL) was added to a clean well without the sol–gel-derived material. As a negative control, sol–gel-derived material without AChE was also prepared. The microwell plate was subsequently stored at 4 °C overnight to allow aging. Afterward, 50 μL of a protease solution (5 mg/mL in Tris buffer) or Tris buffer (100 mM, pH 7.8) was added to each sample, and the samples were allowed to incubate for 60 min at room temperature. In the final step, 50 μL of a mixture of ATCh (2 mM) and DTNB (1 mM) was applied to the samples for color

development. After 5 min, an image was taken with an iPhone 4S camera with the flash turned off and processed as described below.

For testing the function of printed silica sol layers, paper samples printed with top, bottom, or both silica layers as described above were first punched to ~6 cm diameter disks and placed into the wells of a 96-well microwell plate. Ten microliters of the protease solution (5 mg/mL in Tris buffer) or Tris buffer alone was then added to each sample at room temperature for 1 h. The samples were subsequently removed from the wells for drying. The dried samples were then treated with 2 μL of substrate (mixture of 2 mM ATCh and 1 mM DTNB) for color development. A smaller volume was used to just wet the paper surface, and a higher concentration of the substrate was used to provide a higher color intensity for imaging. After 5 min, an image of the paper disk was taken with an iPhone 4S camera and analyzed using ImageJ. The image was first inverted, and then the color intensity was simply quantified using a 256-bit scale.

A second assay was performed to further quantify the percentage of active enzyme entrapped on paper surfaces printed either with or without a polymer base layer, in the presence or absence of different silica layers, and with or without protease added. Following a 1 h incubation, 200 μL of substrate (mixture of 300 μM ATCh and 500 μM DTNB) was added to the dry paper samples in the wells and gently mixed in the wells by pipetting every 5 min for color development. After incubation for 15 min, 100 μL of the reacted solution was then transferred to a new well, and the absorbance was measured at 415 nm using a Bio-Rad model 680 XR microplate reader. The background value from the substrate was subtracted for each reading.

Monitoring the Effect of the Cationic Polymer on Enzyme Activity. Forty microliters of AChE (1 unit/mL) in Tris buffer (100 mM, pH 7.8) was mixed with 40 μL of 2 wt % polyarginine in ddH$_2$O in a 96-well plate, and then 20 μL of a mixture of ATCh (300 μM) and DTNB (500 μM) was pipetted into each well. As a control, the activity was tested without polyarginine. The absorbance at 412 nm was recorded every 10 s over a 10 min period using a Tecan M1000 plate reader and plotted as a function of time. The relative enzyme activity was obtained using the initial rates of the reactions, which were determined from the slopes of the initial part of the absorbance–time curves.

Fluorescent Labeling of Ink Components. The ink components were labeled with fluorescent dyes to allow fluorescence imaging of ink location and mixing. The cationic polymer polyarginine was labeled covalently using FITC. The dye was first dissolved in DMSO to form a 1 mg/mL solution. Ten milliliters of 2 mg/mL poly-L-arginine in borate buffer (100 mM, pH 9.0) was added to 0.1 mL of the FITC solution. The mixture was then stirred using magnetic stirring for 2 h at room temperature in the dark. To remove unbound dye molecules, the mixture was washed several times with ddH$_2$O using a 30 kDa molecular mass cutoff centrifugal ultrafiltration device (spin column) until the filtrate did not contain any dye molecules as determined by measuring the fluorescence intensity of the filtrate.

Labeling of sodium silicate sols utilized a well-known ionic labeling reagent, R6G, which forms a very strong complex with silica particles.[40,41] R6G solutions were prepared in water to a final concentration of 10 μM and mixed with 2× SS sol at a 1:1 (v/v) ratio for 1 h. Time-resolved fluorescence anisotropy decay (TRFA) of the mixture was measured using an IBH 5000U time-correlated single-photon counting fluorimeter as described elsewhere.[40,41] The residual anisotropy (r_∞) was greater than 0.3, which confirmed that the majority of the R6G molecules (>90%) were bound to the silica particles. For confocal microscopy, AChE was replaced with HSA as preliminary experiments indicated that the AChE concentration was insufficient to produce a strong fluorescence signal. In this case, Cy5 maleimide monoreactive dye was used to label HSA. HSA was first dissolved at a concentration of 1 mg/mL in degassed PBS buffer (100 mM, pH 7.4) at room temperature. Then 10 μL of tris(2-carboxyethyl)phosphine (TCEP, 18 mg/mL in PBS per milligram of protein) was added to 1.0 mL of the HSA solution. After incubation for 10 min, 50 μL of the dye solution (prepared by adding 500 μL of anhydrous dimethylformamide to one pack of dye) was added to 1.01

mL of the protein solution containing TCEP. The reaction was first conducted at room temperature with gentle shaking, followed by incubation in the fridge overnight. The labeled proteins were then separated from the free dye molecules by ultrafiltration using a 30 kDa molecular mass cutoff centrifugal ultrafiltration device. The separation was stopped when no florescence signal was detected in the filtrate.

Confocal Laser Scanning Microscopy Characterization. Both surface and cross-sectional images of filter paper printed with labeled inks were obtained using a Zeiss LSM 510 confocal laser scanning microscope, with excitation wavelengths of 488, 543, and 633 nm for FITC, R6G, and Cy5, respectively. For surface imaging, 1 cm × 1 cm samples were cut and placed between a glass microscope slide and coverslip. The images were taken with a Plan-Neofluar 5×/0.25 objective. To prepare samples for cross-sectional imaging, paper samples were cut manually along the z direction with a blade under an optical microscope to produce a straight edge. The cut side was mounted on the cover glass using Fluoromount aqueous mounting medium, which is similar to gel mount, and left 30 min for drying, followed by imaging with a Plan-Neofluar 10×/0.3 objective.

The lateral movement of printed enzyme molecules on the paper was also examined via confocal microscopy. The paper strips (4 cm long × 1 cm wide) were printed with HSA-Cy5 ink in a 0.5 cm wide area across the paper strip and 1.5 cm from the bottom of the paper, with or without the presence of the polymer or silica sol. Then the bottom of the paper strip (0.5 cm) was dipped into ddH$_2$O to allow lateral flow. After the water level had reached the top edge, the paper samples were dried and imaged using the confocal microscope with a Plan-Neofluar 10×/0.3 objective. The enzyme retention level was determined by quantifying the fluorescence intensity remaining in the printed region using ImageJ (blue color). The fluorescence intensity of a paper sample that was not dipped into water was also examined, and the fluorescence intensity was used as the 100% value.

Scanning Electron Microscopy. The morphological differences between unprinted and printed papers were examined using scanning electron microscopy (SEM) (JEOL 7000F) in the secondary electron image (SEI) mode with a voltage of 1.5 kV. Paper samples were cut into small pieces (0.5 cm × 0.5 cm) and splutter-coated with 4 nm of platinum before being imaged. The images were obtained with magnifications of 200× and 3000×.

Transmission Electron Microscopy. The printed silica ink layer on paper (without a polymer underlayer) was also imaged using transmission electron microscopy (TEM) (JEOL 2010 FEG). The paper samples were embedded in Spurr's epoxy resin, using a BEEM mold, and cured at 60 °C overnight. Thin sections (~500 nm) were cut on a Leica UCT Ultramicrotome with a diamond knife and picked up onto Formvar-coated TEM copper grids. The sections were then characterized using a high-resolution transmission electron microscope, operating at an accelerating voltage of 200 keV. The images were acquired with a digital camera. Energy dispersive spectroscopy (EDS) line scans were obtained with an Oxford Instruments INCA detector.

RESULTS AND DISCUSSION

Activity Assays and Proteolysis Studies. The primary goals of this work were to characterize the sol–gel bioinks after printing on porous filter paper and to determine if the enzyme molecules were actually entrapped within the sol–gel network after multistage printing on filter paper. To achieve these objectives, a protease was used to degrade any non-entrapped enzyme, followed by assaying the activity of the remaining enzyme. As a proof of concept, the assay was first performed and verified using the enzyme present in microtiter plates. As shown in Figure S1 of the Supporting Information, the enzyme-entrapped sol–gel samples (S$_b$–E–S$_t$), which were incubated in two different buffers (protease and Tris), produced a strong yellow color, indicative of high enzyme activity and minimal proteolytic degradation. In contrast, yellow color was observed only in free enzyme (E) samples incubated in Tris buffer, but

not in protease buffer. This result confirmed that the protease degraded free AChE molecules in the solution and indicated that the failure of the protease to degrade AChE within the sol–gel-based material was the result of an inability to access the enzyme, confirming that the enzyme was entrapped.

Function of Printed Silica Layers. On the basis of the success of the protease assay in microwells, we extended the assay to printed layers on filter paper. The impact of the bottom and top silica layers printed on filter paper on enzyme activity and entrapment was first investigated using samples with S$_b$, S$_t$, S$_b$ and S$_t$, and no silica layers. Figure 1 shows images

	With Protease	Without Protease	ΔCI
P-S$_b$-E-S$_t$			18
P-E-S$_t$			14
P-S$_b$-E (dry)			50
P-S$_b$-E (wet)			28
P-E			44

Figure 1. Addition of protease to paper printed with different layers of materials (all samples were run in triplicate). Abbreviations: P, polyarginine; S$_b$, bottom printed layer of sol–gel material when dry (dry) or wet (wet); S$_t$, top printed layer of sol–gel material; E, AChE. ΔCI stands for the color intensity difference between the samples incubated with and without protease. The standard deviation is typically around ±10%. The printing coverage for each layer was 25 cm^3/m^2.

of each sample and indicates that samples containing the S$_t$ layer or the S$_b$ and S$_t$ layer showed only slight enzyme inactivation when treated with protease, with color intensity decreasing by 14−18 color intensity (CI) units, as compared to a decrease of 44−50 CI units for samples without a top silica layer. These observations were consistent with the finding of Hossain et al.,[11] who demonstrated that the top silica layer was critical for enzyme entrapment and protection. These data clearly show that printing the enzyme onto a preexisting silica layer (S$_b$) affords little or no protection from proteases and, thus, that the enzyme is not entrapped. However, printing of the enzyme on a S$_b$ layer that is still wet does afford some protection (ΔCI of 28), but this method cannot protect AChE as well as printing of a top silica layer. In general, the data suggest that a wet (nongelled) silica layer can mix with the enzyme layer to create a homogeneous layer that effectively entraps the enzyme. Hence, scaling up of the printing process should accommodate simultaneous printing of the silica and enzyme inks using inkjet printing with multiple printing heads to aid in the mixing of layers.

The other important contribution of the silica layer (particularly S$_b$) is to protect the enzyme from being inactivated by the cationic polymer layer due to strong electrostatic interactions between the polymer and enzyme.[11] As shown in Figure 1, the samples printed without a bottom layer of silica showed a lighter color compared with the samples with the bottom silica layer, even when samples were not exposed to the protease solution. The data suggest that the polyarginine layer

likely inactivates the enzyme. To confirm the influence of the cationic polymer on enzyme activity, the activity of AChE was measured in solution with and without polyarginine present. As shown in Figure S2 of the Supporting Information, the rate of turnover of the substrate was reduced by ∼15-fold when the cationic polymer was present. These results clearly indicate that the bottom silica layer is necessary to prevent inactivation of the enzyme by the capture polymer.

Effect of the Amount of Printed Silica. To quantitatively determine the percentage of active enzyme on paper, the absorbance of a substrate solution was measured after its reaction with paper-immobilized enzymes printed with different amounts of silica sol ink in each layer. Two series of samples were prepared and incubated with or without the protease solution. One set of samples was printed with the cationic polymer underneath layer ($P-S_b-E-S_t$), while the other set did not have the cationic layer (S_b-E-S_t). The print density of silica ink was varied (200, 139, 89, 69, 50, 32, and 13 cm^3/m^2) by varying the drop-to-drop spacing (10, 12, 15, 17, 20, 25, and 40 μm). Print densities (cubic centimeters per square meter) are expressed as wet ink volumes divided by the superficial area of the top surface of the filter paper. By comparing the $P-S_b-E-S_t$ and S_b-E-S_t samples without the protease solution, we observed that the absorbance of the S_b-E-S_t sample was always higher than that of the corresponding $P-S_b-E-S_t$ sample with the same amount of silica. This shows that even the largest amount of silica in the S_b layer does not fully protect the enzyme from the positively charged polymer, indicating some mixing of layers. As shown in Figure 2a, 90% of enzyme
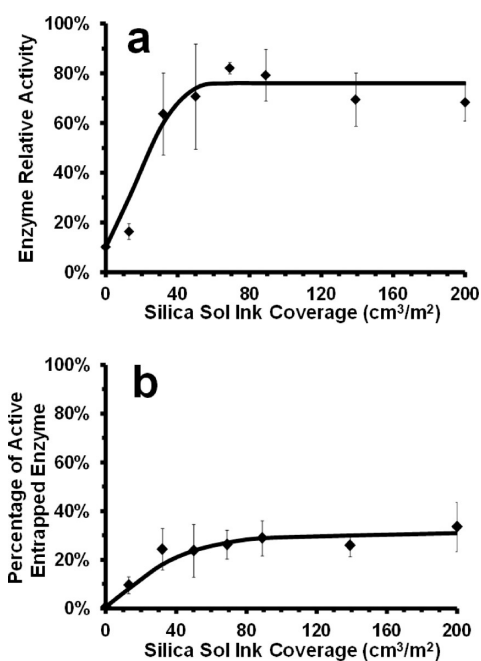
molecules were inactivated when the enzyme layer was printed directly on the polymer layer (no silica), while only 25% of the enzyme activity was lost when ≥50 cm^3/m^2 of silica sol (total for both layers) was printed. Hence, 50 cm^3/m^2 of silica is the minimal amount needed to maximize enzyme activity.

To further determine the extent of enzyme entrapment within the printed silica network, paper samples were incubated with the protease solution followed by measuring the absorbance of the overlying substrate solution. As expected, non-entrapped enzyme molecules were fully degraded by the protease and showed no measurable activity. The $P-S_b-E-S_t$ samples incubated in the protease solution were compared to those without a polymer layer incubated in Tris buffer (samples without polymer incubated in protease were not tested as we were interested in assessing enzyme activity under conditions that are used for actual test strips). As shown in Figure 2b, ∼25% of the active enzyme molecules were completely entrapped within the silica network when the amount of silica that was printed was >69 cm^3/m^2. We note that this amount of silica is also sufficient to protect the enzyme from inactivation by the polymer, and thus, the inactivation is due to leaching or degradation of enzyme that is sufficiently close to the silica surface to be accessed by the proteases.

Confocal Fluorescence Imaging of Inks Deposited on Paper. The homogeneity of printed materials on paper was examined by labeling each of the inks with fluorescent tags and imaging via confocal microscopy. The cationic polymer, silica sol, and enzyme solutions were labeled with FITC, R6G, and Cy5, respectively. As shown in the top row of Figure 3, all ink types were distributed uniformly on the paper. From the overlapping images (panels D and F), the various inks do not necessarily deposit in the same spot, because of the porous nature of filter paper. The cross-sectional images shown in the bottom row of Figure 3 show that all printed inks penetrated almost throughout the paper and were relatively homogeneous from the top to the bottom of the paper, though the polymer had a higher concentration near the bottom and the silica a higher concentration near the top of the paper. Importantly, the majority of the inks mixed to form a homogeneous composite inside the paper network and did not show distinctive separate layers with different labeling. Therefore, we can conclude that a composite biosilica material was created within the paper network.

To further probe the ability of the composite ink to keep the enzyme in the location where it was initially printed, the lateral movement of the enzyme after performing a lateral flow of water through the enzyme region was investigated using confocal microscopy and is shown in Figure 4. On paper printed with only the enzyme solution, the enzyme molecules smeared across the paper in the direction of lateral flow with only 1% of enzyme molecules remaining on the originally printed area based on color intensity. This clearly shows that biomolecules adsorbed onto cellulose are not immobilized but rather can dissolve in water and move freely along the paper. Paper with a polymer layer (P) or silica layers (S_b-E-S_t) retained the majority of enzyme molecules where they were printed (63 and 62%, respectively). The pI of AChE is ∼4.7,[42] and therefore, under the experimental condition, it would be expected to adsorb strongly to the cationic polymer but in doing so is inactivated. When the silica ink was printed on the paper, it also prevented lateral movement of the enzyme, showing that the enzyme remained entrapped within the silica network. The fact that >60% of the enzyme is retained while
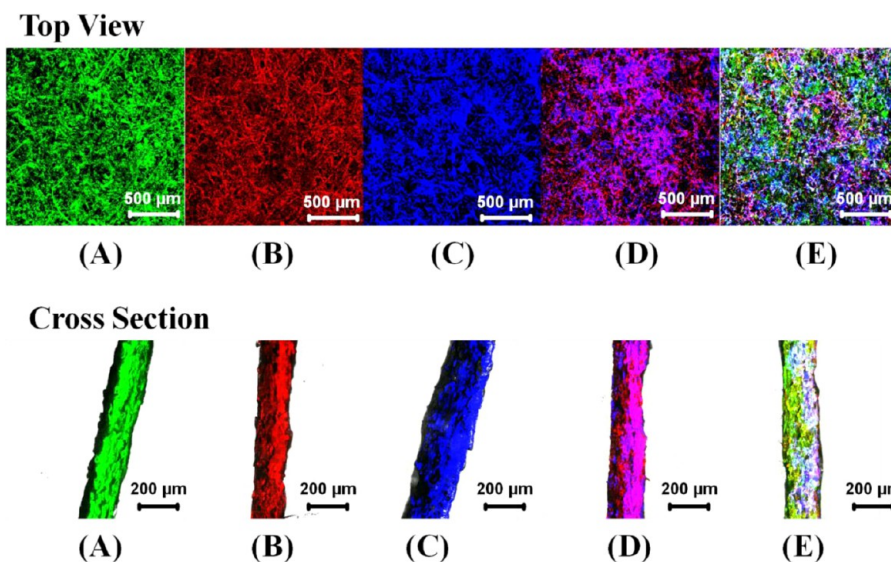

Figure 2. (a) Relative enzyme activity on paper using various amounts of printed silica, with the cationic polymer layer present, prior to protease treatment. The 100% value is obtained for a sample with no polymer underlayer (S_b-E-S_t) with the corresponding amount of silica. (b) Entrapment percentage of the active enzyme printed with polymer and two layers of silica in varying amounts after protease treatment. The 100% value is obtained for the sample with no polymer underlayer (S_b-E-S_t) without protease treatment. The ink coverage is expressed as the wet ink volume divided by the superficial top area of the printed paper.

Top View

(A)   (B)   (C)   (D)   (E)

Cross Section

(A)   (B)   (C)   (D)   (E)

Figure 3. Confocal images of paper printed with various fluorescent inks: (A) polymer−FITC, (B) SS−R6G, (C) HSA−Cy5, (D) HSA−Cy5 between two layers of SS−R6G, and (E) polymer−FITC first and then HSA−Cy5 between two layers of SS−R6G. In the cross-section image, the right-hand side is the top side of the paper.
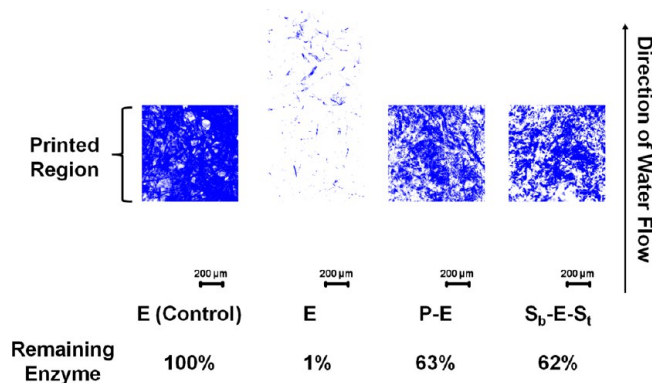

Figure 4. Lateral movement of HSA−Cy5 on papers printed with different materials.

only 25% survives proteolytic treatment indicates that much of the enzyme is present in a thin silica layer that partially exposes the enzyme to solution, making it susceptible to proteolytic degradation. This possibility is investigated further below.

Calculation of Ink Layer Thickness. Whatman #1 filter paper is made with hollow cellulose fibers, approximately 20 μm wide with 2 μm thick porous walls. The paper-making process causes the tubular fibers to collapse into ribbons. The overall pore volume fraction of Whatman #1 is ∼0.68 with large (∼10 μm) pores between the fibers and pore sizes down to 50 nm in fiber walls. The corresponding specific surface area (area per mass) of Whatman #1 is 9.5 m^2/g based on a protein probe.[43] When a water-based ink is deposited on filter paper, capillary forces pull the ink into the pores until the free solution disappears from the surface. When capillary flow stops, the fraction of pores filled depends upon the amount of added ink. Upon drying, the pigments in the ink will remain in the pores. Our silica sols were very dilute (4 wt % based on silica), and if all the pores in Whatman #1 where filled with silica sol, after drying the fiber surfaces will have an average silica coverage of 7 mg/m^2, which for pure, nonporous silica corresponds to an average layer thickness of 2.5 nm and for a porous silica material (generally 50% porous)[31] would be ∼5 nm thick per

silica layer, or 10 nm thick upon printing of two silica layers as was done in this work. However, this estimate is sensitive to the assumed specific surface area available to the silica sol. For example, if instead of 9.5 m^2/g, we assume a value of 5 m^2/g for the specific surface area, the corresponding porous silica layer is ∼20 nm thick (see the Supporting Information for calculations). These order-of-magnitude estimates provide a framework for interpreting the electron microscopy observations presented below.

SEM and TEM Analysis. SEM and TEM were used to characterize the nature of the printed silica layers, including the layer thickness, morphology, and stability of the silica layer on the paper. Two types of surfaces were examined and compared. One was nonporous glassine paper and the other Whatman #1 filter paper with a 10 μm pore size. As shown in panels C and D of Figure 5, SEM demonstrates that the silica material that interpenetrated the porous structure covered the individual fibers of the filter paper as a thin film without completely filling the pores between the fibers. An interesting finding was that the silica material was reinforced by the cellulose and showed very little cracking even when the paper was bent or folded (Figure 5E,F). When the same amount of silica material was printed on the nonporous glassine paper (Figure 5I,J), a thick layer of silica (∼2−3 μm thick) was formed on the surface of the paper, with extensive cracking of the material being observed. Hence, the thin film was stable on filter paper, while the thicker coating was susceptible to cracking when printed on nonporous glassine paper.

TEM was used to more accurately determine the thickness of the printed sol−gel layers. As shown in Figure 6A, a dark thin layer was formed on the surface of the fibers with a thickness of 35 ± 15 nm. This thin film was confirmed to be the silica using an EDS line scan. As a control, no silica was detected on the unprinted Whatman #1 filter paper (Figure 6B). The thickness of this silica layer is in general agreement with the calculated values presented above and has the desirable feature of being thin enough to be stable on the fibers without cracking and thick enough to entrap enzyme molecules.
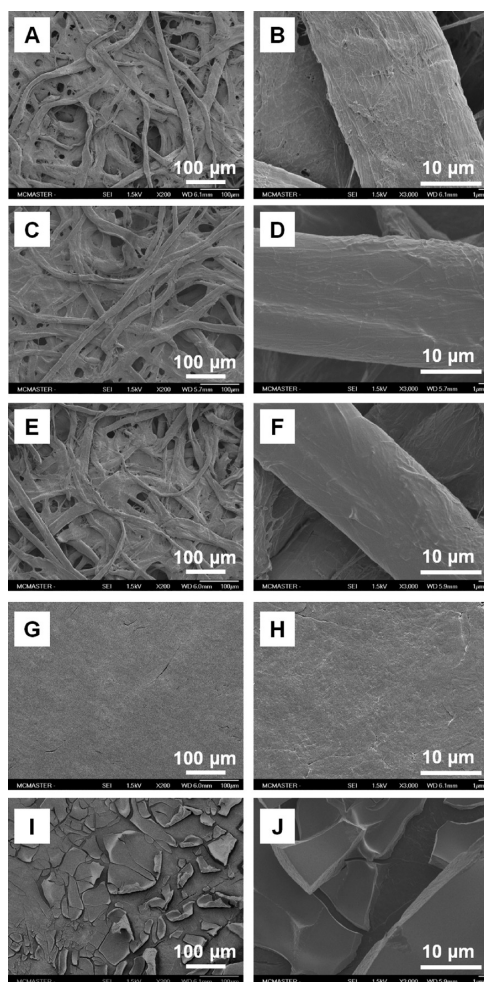
Figure 5. SEM images of papers: (A and B) Whatman #1 paper; (C and D) Whatman #1 paper printed with polymer, sol−gel material, and the enzyme solution; (E and F) Whatman #1 papers printed with polymer, sol−gel material, and the enzyme solution after being bent; (G and H) nonporous glassine papers; and (I and J) glassine papers printed with polymer, sol−gel material, and the enzyme solution.

Figure 6. TEM images of coated and uncoated paper: (A) Whatman #1 paper printed with sol−gel material and the enzyme solution and (B) uncoated Whatman #1 paper. EDS scans were conducted along the yellow lines shown in the images.

■ CONCLUSIONS

Multistep inkjet printing of sol−gel-based bioinks on filter paper was characterized via activity assays, proteolysis assays, confocal microscopy, SEM, and TEM. Our data show that both layers of silica are necessary for the protection of the enzyme. The bottom layer isolates the enzyme from the cationic capture polymer and at sufficient amounts can preserve up to 75% of enzyme activity. The top layer of silica is important for enzyme entrapment and also provides some protection from proteolysis. Overall, the printed enzyme retained ∼25% of the initial activity after exposure to a cocktail of proteases and closer to 75% of initial activity prior to the addition of proteases, provided that sufficient silica is printed in the top and bottom layers (∼69 cm^3 per superficial square meter of printed paper, giving a silica coating of ∼13 mg/m^2 on the fiber surfaces).

A second finding from this work is that a silica-entrapped protein, HSA, does not migrate during lateral flow while maintaining activity. Given that HSA is smaller that AChE and has a similar pI, we assume that the AChE would also be retained on paper. Filter paper coated with cationic polymer also immobilized HSA; however, studies using AChE showed
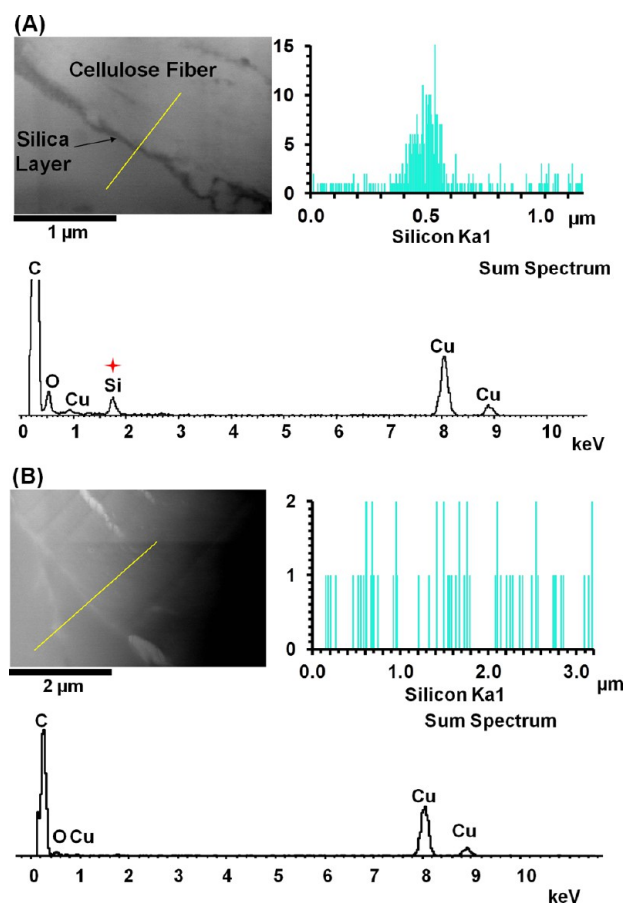
that the polymer degraded the catalytic activity of AChE. More robust enzymes or those with pI values that are more basic may not be adversely affected by polyarginine, and this issue will require further investigation.

Finally, confocal microscopy and SEM and TEM imaging studies showed that the final material on the paper was a uniform thin film that coated the fibers of the filter paper, indicating that the inks mix and conformally coat the paper fibers, producing a cellulose-reinforced film that was tens of nanometers thick. Such thin films promote rapid substrate transport and enhance mechanical stability. Indeed, our sensors resisted cracking, even when the paper was folded, showing that the cellulose−silica−enzyme composite provided a robust coating for the development of paper-based biosensors. Our previous work has demonstrated that the printed silica−AChE−silica film retains >95% activity after being stored for 2 months at 4 °C,[11,12] demonstrating the utility of sol−gel-derived inks for stabilizing enzymes on paper.

■ ASSOCIATED CONTENT

ⓢ Supporting Information

Solution-based protease tests, AChE assays in solution, and properties of silica sol inks. This material is available free of charge via the Internet at http://pubs.acs.org.

AUTHOR INFORMATION

Corresponding Authors
*E-mail: peltonrh@mcmaster.ca. Telephone: (905) 525-9140, ext. 27045.
*E-mail: brennanj@mcmaster.ca. Telephone: (905) 525-9140, ext. 20682.

### Notes
The authors declare no competing financial interest.

ACKNOWLEDGMENTS

REFERENCES

(1) Liana, D. D.; Raguse, B.; Gooding, J. J.; Chow, E. *Sensors* **2012**, *12*, 11505−11526.
(2) Then, W. L.; Garnier, G. *Rev. Anal. Chem.* **2013**, *32*, 269.
(3) Parolo, C.; Merkoci, A. *Chem. Soc. Rev.* **2013**, *42*, 450−457.
(4) Yetisen, A. K.; Akram, M. S.; Lowe, C. R. *Lab Chip* **2013**, *13*, 2210−2251.
(5) Pelton, R. *TrAC, Trends Anal. Chem.* **2009**, *28*, 925−942.
(6) Kong, F.; Hu, Y. *Anal. Bioanal. Chem.* **2012**, *403*, 7−13.
(7) Di Risio, S.; Yan, N. *J. Adhes. Sci. Technol.* **2010**, *24*, 661−684.
(8) Martinez, A. W.; Phillips, S. T.; Whitesides, G. M.; Carrilho, E. *Anal. Chem.* **2010**, *82*, 3−10.
(9) Maejima, K.; Tomikawa, S.; Suzuki, K.; Citterio, D. *RSC Adv.* **2013**, *3*, 9258−9263.
(10) Sicard, C.; Brennan, J. D. *MRS Bull.* **2013**, *38*.
(11) Hossain, S. M. Z.; Luckham, R. E.; Smith, A. M.; Lebert, J. M.; Davies, L. M.; Pelton, R. H.; Filipe, C. D. M.; Brennan, J. D. *Anal. Chem.* **2009**, *81*, 5474−5483.
(12) Hossain, S. M. Z.; Luckham, R. E.; McFadden, M. J.; Brennan, J. D. *Anal. Chem.* **2009**, *81*, 9055−9064.
(13) Hossain, S. M. Z.; Brennan, J. D. *Anal. Chem.* **2011**, *83*, 8772−8778.
(14) Ciriminna, R.; Fidalgo, A.; Pandarus, V.; Béland, F.; Ilharco, L. M.; Pagliaro, M. *Chem. Rev.* **2013**, *113*, 6592−6620.
(15) Gupta, R.; Chaudhury, N. K. *Biosens. Bioelectron.* **2007**, *22*, 2387−2399.
(16) Monton, M. R. N.; Lebert, J. M.; Little, J. R. L.; Nair, J. J.; McNulty, J.; Brennan, J. D. *Anal. Chem.* **2010**, *82*, 9365−9373.
(17) Avnir, D.; Braun, S.; Lev, O.; Ottolenghi, M. *Chem. Mater.* **1994**, *6*, 1605−1614.
(18) Escobar, S.; Bernal, C.; Mesa, M. *Biochem. Eng. J.* **2013**, *75*, 32−38.
(19) Helka, B. J.; Brennan, J. D. *Journal of visualized experiments: JoVE* **2013**.
(20) Shen, Y.; Mackey, G.; Rupcich, N.; Gloster, D.; Chiuman, W.; Li, Y.; Brennan, J. D. *Anal. Chem.* **2007**, *79*, 3494−3503.
(21) Frenkel-Mullerad, H.; Avnir, D. *J. Am. Chem. Soc.* **2005**, *127*, 8077−8081.
(22) Ge, X.; Lebert, J. M.; Monton, M. R. N.; Lautens, L. L.; Brennan, J. D. *Chem. Mater.* **2011**, *23*, 3685−3691.
(23) Mohidem, N.; Mat, H. *J. Sol-Gel Sci. Technol.* **2012**, *61*, 96−103.
(24) Sun, X.; Du, S.; Wang, X.; Zhao, W.; Li, Q. *Sensors* **2011**, *11*, 9520−9531.
(25) Lee, W.; Park, K.-S.; Kim, Y.-W.; Lee, W. H.; Choi, J.-W. *Biosens. Bioelectron.* **2005**, *20*, 2292−2299.
(26) Reiter, E. V.; Cichna-Markl, M.; Tansakul, N.; Shim, W.-B.; Chung, D.-H.; Zentek, J.; Razzazi-Fazeli, E. *J. Chromatogr., A* **2011**, *1218*, 7627−7633.
(27) Altstein, M.; Aziz, O. B.; Skalka, N.; Bronshtein, A.; Chuang, J. C.; Van Emon, J. M. *Anal. Chim. Acta* **2010**, *675*, 138−147.
(28) Bronshtein, A.; Aharonson, N.; Avnir, D.; Turniansky, A.; Altstein, M. *Chem. Mater.* **1997**, *9*, 2632−2639.
(29) Shalev, M.; Miriam, A. *Materials* **2011**, *4*, 469−486.
(30) Carrasquilla, C.; Brennan, J. D. *Methods* **2013**, *63*, 255−265.
(31) Carrasquilla, C.; Lau, P. S.; Li, Y.; Brennan, J. D. *J. Am. Chem. Soc.* **2012**, *134*, 10998−11005.
(32) Ahn, J.-Y.; Lee, S.; Jo, M.; Kang, J.; Kim, E.; Jeong, O. C.; Laurell, T.; Kim, S. *Anal. Chem.* **2012**, *84*, 2647−2653.
(33) Rupcich, N.; Nutiu, R.; Li, Y.; Brennan, J. D. *Anal. Chem.* **2005**, *77*, 4300−4307.
(34) Harper, J. C.; Lopez, D. M.; Larkin, E. C.; Economides, M. K.; McIntyre, S. K.; Alam, T. M.; Tartis, M. S.; Werner-Washburne, M.; Brinker, C. J.; Brozik, S. M.; Wheeler, D. R. *Chem. Mater.* **2011**, *23*, 2555−2564.
(35) Eleftheriou, N. M.; Ge, X.; Kolesnik, J.; Falconer, S. B.; Harris, R. J.; Khursigara, C.; Brown, E. D.; Brennan, J. D. *Chem. Mater.* **2013**, *25*, 4798−4805.
(36) Dickson, D.; Ely, R. *Appl. Microbiol. Biotechnol.* **2013**, *97*, 1809−1819.
(37) Depagne, C.; Masse, S.; Link, T.; Coradin, T. *J. Mater. Chem.* **2012**, *22*, 12457−12460.
(38) Ge, X.; Eleftheriou, N. M.; Dahoumane, S. A.; Brennan, J. D. *Anal. Chem.* **2013**, *85*, 12108−12117.
(39) Desimone, M. F.; De Marzi, M. C.; Alvarez, G. S.; Mathov, I.; Diaz, L. E.; Malchiodi, E. L. *J. Mater. Chem.* **2011**, *21*, 13865−13872.
(40) Tleugabulova, D.; Sui, J.; Ayers, P. W.; Brennan, J. D. *J. Phys. Chem. B* **2005**, *109*, 7850−7858.
(41) Tleugabulova, D.; Zhang, Z.; Brennan, J. D. *J. Phys. Chem. B* **2003**, *107*, 10127−10133.
(42) Vlasova, I. M.; Saletsky, A. M. *J. Appl. Spectrosc.* **2009**, *76*, 536−541.
(43) Hong, J.; Ye, X. H.; Zhang, Y. H. P. *Langmuir* **2007**, *23*, 12535−12540.

1947

dx.doi.org/10.1021/cm500206s | *Chem. Mater.* 2014, 26, 1941−1947

Appendix: Supporting Information for Chapter 5
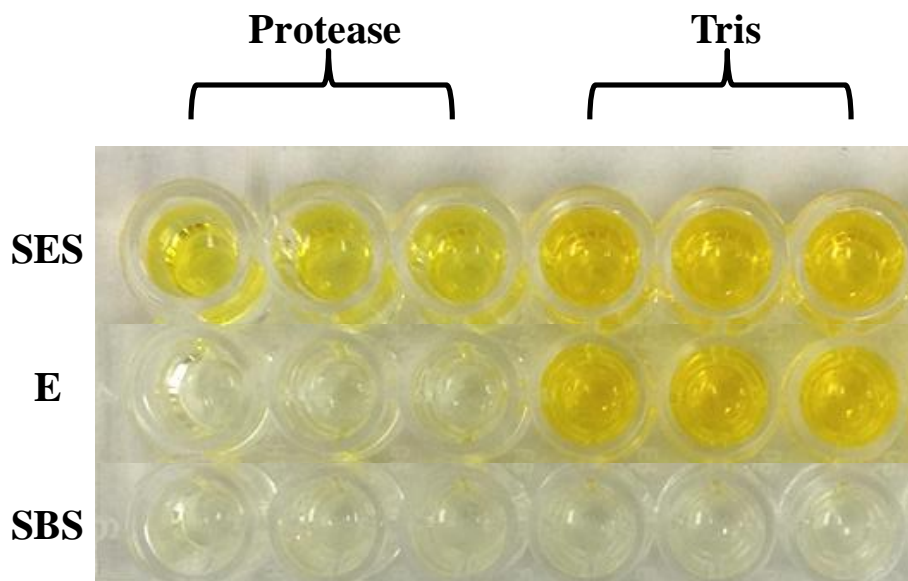
Supporting Figure 1: Protease test in solution with different samples. SES: enzyme entrapped between two layers of sol-gel materials; E: enzyme solution; and SBS: Tris buffer without enzyme entrapped between two layers of sol-gel materials
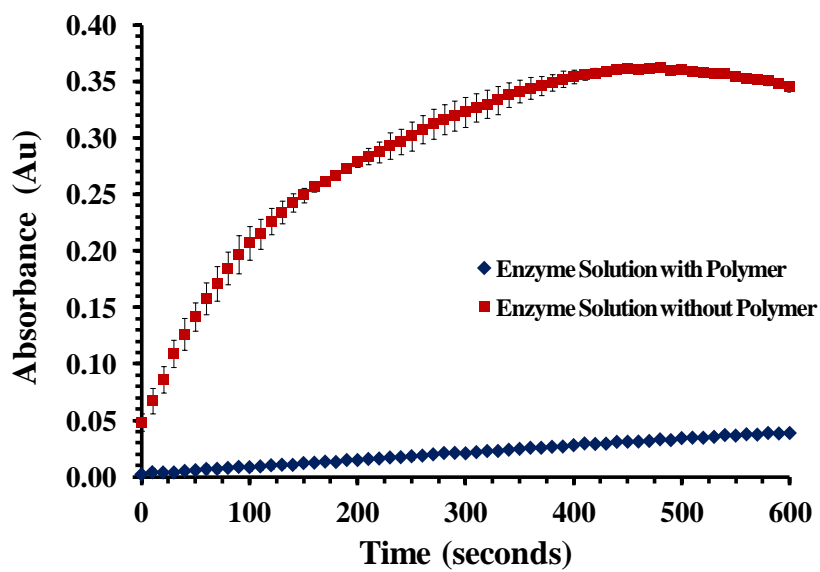
Supporting Figure 2: Kinetic reaction of AChE solution with or without cationic polymer after addition of substrate.

.

Supporting Table 1: The properties of silica sol ink.

Composite	Density	Theoretical Silica Content
Silica Sol (70% v/v) Glycerol (30% v/v) Triton X-100 (0.1 wt%)	1.122 g/mL	4.1 wt%

Silica Content in Sodium Silicate Sol Ink

To prepare sodium silicate sol

2.59 gm of Sodium Silicate + 10 mL of water

Sodium silicate contains <40% of sodium silicate and >60% of water according to product information (Fisher)

$$m_{ss} := 2.59 gm$$

$$\rho_{ss} := 1.4 \frac{gm}{mL} \qquad \text{Density of sodium silicate}$$

$$V_{ss} := \frac{m_{ss}}{\rho_{ss}} = 1.85 \cdot mL$$

$$V_{water} := 10mL \qquad m_{water} := 10gm$$

$$V_{sssol} := V_{ss} + V_{water} = 11.85 \cdot mL \qquad \text{Total volume of prepared sodium silicate sol}$$

$$m_{sssol} := m_{ss} + m_{water} = 12.59 \cdot gm \qquad \text{Total mass of prepared sodium silicate sol}$$

Sodium Silicate Mol Ratio(R.mol) is greater than 3.2 which means SiO2: Na2O is at least 3.2:1. Assume it is 3.2.

$$R_{mol} := 3.2$$

$$MW_{SiO2} := 60.08 \frac{gm}{mol}$$

$$MW_{Na2O} := 61.9789 \frac{gm}{mol}$$

$$R_W := R_{mol} \cdot \frac{MW_{SiO2}}{MW_{Na2O}} = 3.102$$

$$m_{SiO2} := m_{ss} \cdot 40\% \cdot \frac{R_W}{R_W + 1} = 0.783 \cdot gm \qquad \text{Assume sodium silicate contains 40\% of sodium silicate and 60\% of water}$$

To prepared sodium silicate ink

sodium silicate sol   70% volume

Glycerol   30% volume

$$V_{glycerol} := V_{sssol} \cdot \frac{3}{7}$$

$$\rho_{glycerol} := 1.26 \frac{gm}{mL} \qquad \text{Density of Glycerol}$$

$$m_{glycerol} := V_{glycerol} \cdot \rho_{glycerol} = 6.399 \cdot gm$$

$$\chi_{ink} := \frac{m_{SiO2}}{m_{sssol} + m_{glycerol}} = 0.041 \qquad \text{Mass fraction of solids in ink}$$

$$\rho_{wetink} := \frac{m_{sssol} + m_{glycerol}}{V_{sssol} + V_{glycerol}} = 1.122 \cdot \frac{gm}{mL}$$

$$\rho_{dryink} := 2.65 \frac{gm}{mL}$$

Whatman #1 paper

$$\phi_{porew1} := 0.68 \qquad\qquad \text{Pore Fraction}$$

$$bw := 87 \frac{gm}{m^2} \qquad\qquad \text{Basis Weight}$$

$$\rho_{cel} := 1540 \frac{kg}{m^3} \qquad\qquad \text{Density of dry cellulose}$$

$$ssa_{w1} := 9.5 \frac{m^2}{gm} \qquad\qquad \text{Specific Surface Area per gram}$$

$$\Gamma_v := 50 \frac{cm^3}{m^2} \qquad\qquad \text{Superficial ink volumetric coverage printed on paper}$$

$$\delta := \frac{\Gamma_v}{\phi_{porew1}} = 73.529 \cdot \mu m$$

Theoretical Ink Penetration Thickness

$$\Gamma_{inkonfiber} := \frac{\phi_{porew1} \cdot \rho_{wetink} \cdot \chi_{ink}}{(1 - \phi_{porew1}) \cdot \rho_{cel} \cdot ssa_{w1}} = 6.722 \cdot \frac{mg}{m^2}$$

$$\phi_{silicapv} := 0.51$$

Silica Porosity
According to C Carrasquilla and JD Brennan
2012 JACS Supporting Information

$$\tau sg := \frac{\Gamma_{inkonfiber}}{\rho_{dryink} \cdot (1 - \phi_{silicapv})} = 5.177 \cdot nm$$

For one layer of silica coating

$$\tau sg_2 := 2 \cdot \tau sg = 10.353 \cdot nm$$

For two layers of silica coating

$$\phi_{silicapv} := 0$$

Nonporous silica

$$\tau sg := \frac{\Gamma_{inkonfiber}}{\rho_{dryink} \cdot (1 - \phi_{silicapv})} = 2.537 \cdot nm$$

For one layer of silica coating

In the second case when the paper specific surface area was 5 m^2/gm instead of 9.5 m^2/g

$$ssa_{w1} := 5 \frac{m^2}{gm}$$

$$\Gamma_{inkonfiber} := \frac{\phi_{porew1} \cdot \rho_{wetink} \cdot \chi_{ink}}{(1 - \phi_{porew1}) \cdot \rho_{cel} \cdot ssa_{w1}} = 12.772 \cdot \frac{mg}{m^2}$$

$$\phi_{silicapv} := 0.51$$

Silica Porosity
According to C Carrasquilla and JD Brennan
2012 JACS Supporting Information

$$\tau sg := \frac{\Gamma_{inkonfiber}}{\rho_{dryink} \cdot \left(1 - \phi_{silicapv}\right)} = 9.836 \cdot nm \qquad \text{For one layer of silica coating}$$

$$\tau sg_2 := 2 \cdot \tau sg = 19.672 \cdot nm \qquad \text{For two layers of silica coating}$$

$$\phi_{silicapv} := 0 \qquad \text{Nonporous silica}$$

$$\tau sg := \frac{\Gamma_{inkonfiber}}{\rho_{dryink} \cdot \left(1 - \phi_{silicapv}\right)} = 4.82 \cdot nm \qquad \text{For one layer of silica coating}$$

Chapter 6 Concluding Remarks

This work focuses on the printing and characterization of paper-based biosensors. The results push the boundaries of the paper-based biosensor limitations and provide a better understanding of structure and mechanisms. The work has yielded many remarkable outcomes and innovative discoveries, paving the way for the commercialization of paper-based biosensors. The research objectives proposed in Chapter 1 were fully achieved and the major contributions of this work are given as follows:

1. Enzymes encapsulated between two layers of silica were prepared by multi-stage inkjet printing and the resulting biosensors were fully characterized for the first time by activity assays, confocal microscopy and SEM/TEM. The results confirmed that both layers of silica were necessary for protection of the enzyme. The bottom layer isolates the enzyme from the cationic capture polymer and the top layer of silica is important for enzyme entrapment and also provides some protection from proteolysis.

2. Although the silica and enzyme inks were printed sequentially, they formed a flexible and stable composite material within the porous paper network with little cracking, and coated on the fiber surfaces as a thin film. The film thickness was thin enough (less than 50 nm) to be mechanically stable and thick enough to partially entrap enzymes.

3. Two novel and simple techniques for patterning paper have been developed, based on deposition of a hydrophobic, cross-linked MSQ material, for spatial control of fluid transport on paper. Applying strong base to MSQ coated surfaces alters the hydrophilic/hydrophobic contrast of MSQ-treated paper, producing hydrophilic regions that can support fluid flow. The direct printing of MTMS-based "inks" using a piezoelectric ink-jet printer was done with a one-pass printing method to produce a strong barrier.

4. The ability of different types of barriers, including directly printed MSQ, NaOH-etched MSQ, wax printed and AKD printed barriers, to contain surfactant solutions was examined. Although all four barrier types performed well with water, only the MSQ printed barriers was found to be resistant to surfactant solutions. The functionality of MSQ based devices was further demonstrated using an assay for detection of *E. coli* on paper, which requires aggressive lysing reagent.

5. The integrity of various barriers was also evaluated when exposed to different types of organic solvents, including methanol, isopropanol, DMSO, glycerol and toluene. It was found that none of the channels contain the alcohols. Further efforts are needed to develop a stronger hydrophobic barrier which would resistant a wider range of organic solvents.

6. The stability of paper-supported antibodies was evaluated experimentally over a broad range of temperature and relative humidity (RH) conditions. It was found that the half-life of the antibody is much longer than the residence time in paper roll-to-roll printing

or coating processes. Therefore, I concluded that antibodies can be applied onto the paper in these processes.

7. An empirical equation was developed based on the experimental results of paper-supported antibody stability under various conditions, providing the antibody deactivation rate constants with respect to the changes of temperatures and water contents. This model can serve as a design tool for predicting antibody survival in specific coating or printing processes.

8. The effect of a paper sizing agent (AKD) on antibody adsorption and inactivation were investigated using both membrane chromatography and paper-based immunoassay analysis. The results showed that sizing agent used in paper making process does not promote antibody deactivation. Therefore, papers containing sizing agent, such as packaging cardboards, can be used as the substrate for antibody immobilization.